Paper I

BOREAS An international journal of Quaternary research

Active retreat of a Late Weichselian marine-terminating glacier: an example from Melasveit, western Iceland

THORBJÖRG SIGFÚSDÓTTIR, ÍVAR ÖRN BENEDIKTSSON AND EMRYS PHILLIPS

BOREAS

Sigfúsdóttir, T., Benediktsson, Í. Ö. & Phillips, E. 2018 (July): Active retreat of a Late Weichselian marine-terminating glacier: an example from Melasveit, western Iceland. *Boreas*, Vol. 47, pp. 813–836. https://doi.org/10.1111/bor.12306. ISSN 0300-9483.

Large and complete glaciotectonic sequences formed by marine-terminating glaciers are rarely observed on land, hampering our understanding of the behaviour of such glaciers and the processes operating at their margins. During the Late Weichselian in western Iceland, an actively retreating marine-terminating glacier resulted in the large-scale deformation of a sequence of glaciomarine sediments. Due to isostatic rebound since the deglaciation, these formations are now exposed in the coastal cliffs of Belgsholt and Melabakkar-Ásbakkar in the Melasveit district, and provide a detailed record of past glacier dynamics and the inter-relationships between glaciotectonic and sedimentary processes at the margin of this marine-terminating glacier. A comprehensive study of the sedimentology and glaciotectonic architecture of the coastal cliffs reveals a series of subaquatic moraines formed by a glacier advancing from Borgarfjörður to the north of the study area. Analyses of the style of deformation within each of the moraines demonstrate that they were primarily built up by ice-marginal/proglacial thrusting and folding of marine sediments, as well as deposition and subsequent deformation of ice-marginal subaquatic fans. The largest of the moraines exposed in the Melabakkar-Ásbakkar section is over 1.5 km wide and 30 m high and indicates the maximum extent of the Borgarfjörður glacier. Generally, the other moraines in the series become progressively younger towards the north, each designating an advance or stillstand position as the glacier oscillated during its overall northward retreat. During this active retreat, glaciomarine sediments rapidly accumulated in front of the glacier providing material for new moraines. As the glacier finally receded from the area, the depressions between the moraines were infilled by continued glaciomarine sedimentation. This study highlights the dynamics of marine-terminating glaciers and may have implications for the interpretation of their sedimentological and geomorphological records.

Thorbjörg Sigfúsdóttir (thorbjorg.sigfusdottir@geol.lu.se), Department of Geology, Lund University, Sölvegatan 12, Lund 223 62, Sweden; Thorbjörg Sigfúsdóttir and Ívar Örn Benediktsson, Institute of Earth Sciences, University of Iceland, Sturlugata 7, Reykjavík 101, Iceland; Emrys Phillips, British Geological Survey, The Lyell Centre, Research Avenue, Edinburgh EH14 4AP, UK and Emrys Phillips, Department of Geography, Queen Mary University of London, Mile End Road, London E1 4NS, UK; *received 8th October 2017, accepted 28th December 2017.*

During the Last Glacial Maximum (LGM; *c.* 26.5–20 thousand years ago (cal. ka BP), Clark *et al.* 2009), major ice sheets around the globe expanded to reach the continental shelf break (Dyke *et al.* 2002; Hughes *et al.* 2016). During the following deglaciation, they commonly experienced multiple phases of re-advance and retreat leaving behind a complex sequence of glacially deformed (glaciotectonized) sediments and landforms (e.g. Harris *et al.* 1997; Williams *et al.* 2001; Phillips *et al.* 2002; Thomas & Chiverrell 2007). The sediments and structures present within these glaciotectonic landforms can often be directly related to processes occurring at the margin (proglacial) and beneath (subglacial) glaciers, thus shedding light on past ice-sheet dynamics (i.e. Croot 1987; Bennett *et al.* 1999; Bennett 2001; Aber & Ber 2007; Benn & Evans 2010; Lee & Phillips 2013; Lee *et al.* 2013). Previous research on glaciotectonics has mostly focused on the structures associated with ice sheets and glaciers terminating in terrestrial settings (e.g. Bennett 2001; Bennett *et al.* 2004; Phillips *et al.* 2008; Lee *et al.* 2013), while relatively few studies have been performed on deformation related to marine-terminating glaciers.

Submarine landform systems formed at oscillating margins of marine-terminating glaciers have, however, been described from a number of locations within recently deglaciated fjords (Boulton *et al.* 1996, 1999; Ottesen & Dowdeswell 2006; Ottesen *et al.* 2008; Dowdeswell & Vásquez 2013; Flink *et al.* 2015), and associated with the terminal zones of retreating Weichselian ice sheets (e.g. Johnson & Ståhl 2010; Winkelmann *et al.* 2010; Ó Cofaigh *et al.* 2012; Johnson *et al.* 2013; Rydningen *et al.* 2013). Such landsystems commonly comprise large terminal moraines marking the maximum glacier extent, as well as streamlined landforms separated by series of transverse ridges formed during stillstands or small re-advances (Ottesen & Dowdeswell 2006; Ottesen *et al.* 2008; Winkelmann *et al.* 2010; Flink *et al.* 2015). Less is known about the internal architecture of subaquatically formed moraines and therefore the glacial processes that caused their formation. The primary reason for this is the general lack of subaerial sections through moraines known to have formed on the sea floor. However, available sections through individual subaqueous moraines as well as published interpretations of offshore seismic data have shown that they have commonly been formed as a result of glaciotectonism (Sættem 1994; Seramur *et al.* 1997; Bennett *et al.* 1999; Johnson *et al.* 2013), and/or ice-marginal sedimentary processes such as gravity flows and the outflow of subglacial meltwater (Lønne 1995; Lønne *et al.* 2001; Lønne & Nemec 2011).

This paper contributes to the study of glacier-induced deformation at the margins of marine-terminating glaciers

DOI 10.1111/bor.12306

by examining the glaciotectonism recorded by the Late Weichselian glaciomarine sediments exposed in Melasveit, lower Borgarfjörður, western Iceland (Fig. 1A, B). Exposed in the coastal cliffs is a sequence of marine deposits showing evidence of deformation (ductile shearing, thrusting) by ice. The stratigraphy of these sediments has previously been described by Ingólfsson (1987, 1988), with the aim of reconstructing the regional glacial history. The present study adopts Ingólfsson's stratigraphical framework and focuses on the internal structural architecture of this well-developed submarine glaciotectonic complex. The intensity and style of deformation are interpreted in terms of episodic ice-marginal folding and thrusting during the active retreat of a glacier flowing from Borgarfjörður immediately to the north (Fig. 1A; Ingólfsson 1987, 1988; Norðdahl *et al.* 2008; Ingólfsson *et al.* 2010).

The study area and its geological context

Melasveit is a lowland area situated between the fjords Hvalfjörður and Borgarfjörður (Fig. 1A, B). To the north-east is the mountain range of Hafnarfjall and Skarðsheiði, its highest peaks rising to over 1000 m above sea level (m a.s.l.) (Fig. 1A). The local bedrock is mainly composed of Neogene basaltic lava flows, which crop out in the mountains and along the coast (Franzson 1978; Ingólfsson 1988).

Evidence for glacial activity is widespread in the region (Ingólfsson 1988; Norðdahl *et al.* 2008). The mountain landscape of Hafnarfjall – Skarðsheiði is characterized by trough-shaped valleys, horns and cirques formed as a result of repeated glaciations during the Pleistocene (Ingólfsson 1988). Striations on exposed bedrock surfaces show that, at some point, ice flowing down Borgarfjörður, Hvalfjörður and the Svínadalur valley coalesced in the lower Borgarfjörður region (Fig. 1A; Ingólfsson 1988; Magnúsdóttir & Norðdahl 2000). The bedrock in Melasveit is blanketed by at least 30-m-thick, dominantly glaciomarine deposits of Late Weichselian age (Ingólfsson 1987, 1988). This sequence is overlain by stratified sand and gravel thought to be of Holocene age, and records a major marine transgression following the final deglaciation of the area (Ingólfsson 1987, 1988). The most notable depositional glacial landform in the lower Borgarfjörður region is the

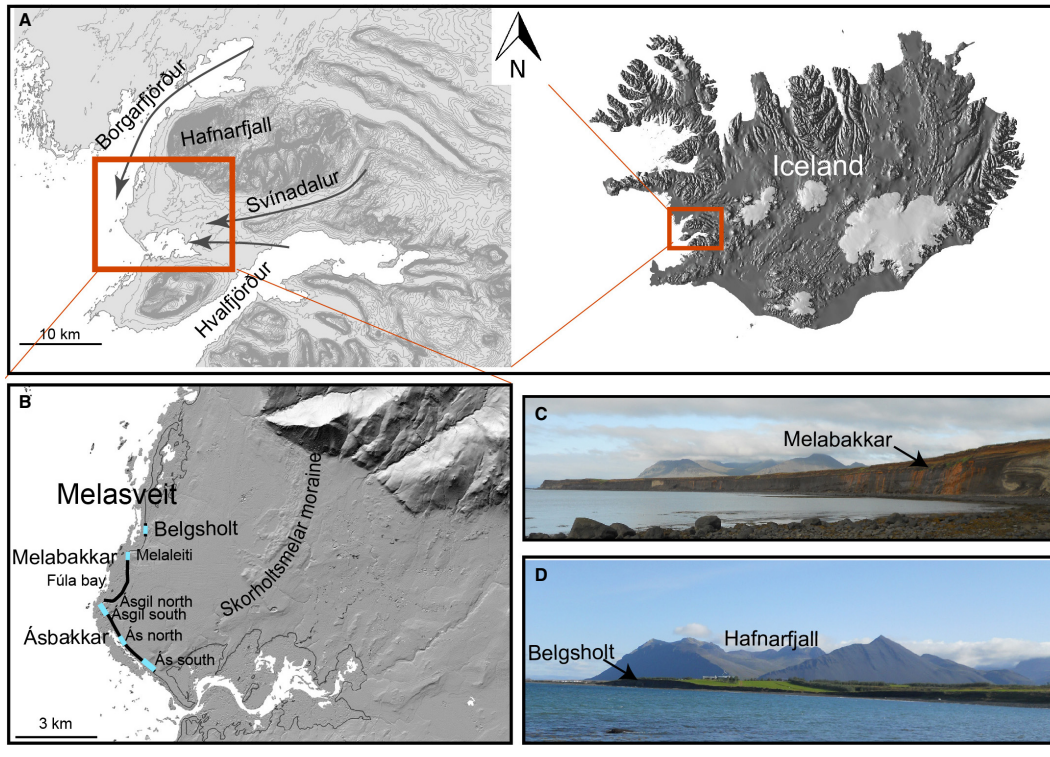

Fig. 1. A. The Melasveit study area (red box) and the surrounding regions. Arrows indicate the ice flow into the region during the Weichselian glaciation according to Ingólfsson (1988). B. A map of Melasveit. Thick black lines indicate the Belgsholt and Melabakkar-Ásbakkar coastal sections and blue lines the structural zones that were studied in detail in this paper. C. The northern part of the Melabakkar coastal cliff. D. The Belgsholt coastal section. Note the ridge-like shape of the landform that contains the section. [Colour figure can be viewed at www.boreas.dk]

Skorholtsmelar end moraine (Fig. 1B). This is a ~6-km-long arcuate landform that rises ~20–40 m over its flat surroundings and has been interpreted as marking the maximum position of a Late Weichselian ice advance from Borgarfjörður (Ingólfsson 1988; Hart & Roberts 1994; Norðdahl *et al.* 2008; Ingólfsson *et al.* 2010). The exact age of this moraine is not known, but it has been suggested that it formed during the Younger Dryas (Ingólfsson 1988), late Bølling (Norðdahl *et al.* 2008; Ingólfsson *et al.* 2010) or possibly both (Ingólfsson 1988). The southern side of the moraine is flanked by deltaic deposits reaching up to 52 m a.s.l., which indicates the minimum relative sea level during, or following the moraine formation. On its northern side, i.e. at the ice-contact slope, the surface is littered with erratic boulders (Ingólfsson 1988).

The lower Borgarfjörður region, including the Melasveit area, probably became ice free in the early Bølling, after a rapid collapse of an ice shelf off the west coast of Iceland (Ingólfsson 1987; Syvitski *et al.* 1999; Jennings *et al.* 2000; Norðdahl *et al.* 2008; Ingólfsson *et al.* 2010; Norðdahl & Ingólfsson 2015). The collapse of this marine-terminating ice mass was most probably driven by a global rise in sea level resulting from the decay of other major Northern Hemisphere ice sheets (Ingólfsson & Norðdahl 2001; Norðdahl & Ingólfsson 2015; Patton *et al.* 2017).

The Melasveit area was submerged during most of the Late Weichselian, with the highest relative sea level occurring in the early Bølling, immediately after the deglaciation of the West Iceland shelf (Norðdahl *et al.* 2008; Norðdahl & Ingólfsson 2015). Raised marine shorelines, radiocarbon dated to 14.7 cal. ka BP, show that the relative sea level in the region was up to ~150 m higher than present (Ingólfsson & Norðdahl 2001; Norðdahl & Ingólfsson 2015). The subsequent marked decrease in the volume of ice covering Iceland during the remainder of the Bølling and into the Allerød (13.9–12.8 cal. ka BP) led to a rapid isostatic rebound and thus marine shore regression. Glacier expansion in the Younger Dryas (12.8–11.7 cal. ka BP) caused renewed isostatic depression of the lower Borgarfjörður region and a rise in relative sea level of ~60–70 m. This led to the development of a younger series of raised marine terraces. During the Preboreal (11.7–10.0 cal. ka BP), glaciers re-advanced leading to yet another isostatic depression and relative sea-level rise in the region, up to ~65 m a.s.l. in the innermost part of Hvalfjörður (Fig. 1A; Norðdahl *et al.* 2008; Ingólfsson *et al.* 2010).

The locally deformed sequence of marine sediments, which is the focus of the present study, is now well exposed in coastal cliffs due to the postglacial isostatic uplift (Ingólfsson 1987, 1988; Norðdahl & Ingólfsson 2015). This provides a rare opportunity to study the interrelationships between glaciotectonics and sedimentation at the margin of a marine-terminating glacier. In most places such sequences remain concealed beneath the seabed.

Glaciotectonism observed in the coastal exposures in Melasveit has previously been attributed to an ice advance occurring shortly after 14.0 cal. ka BP, possibly as a result of the dynamic response of the western Iceland ice sheet following the earlier collapse of its marine-based component (Ingólfsson & Norðdahl 2001; Norðdahl *et al.* 2008; Ingólfsson *et al.* 2010). Furthermore Ingólfsson (1987, 1988) suggested another, more restricted, ice advance within the Younger Dryas based on stratigraphical evidence and radiocarbon dates.

Material and methods

The sedimentology and structural architecture of the Belgsholt and Melabakkar-Ásbakkar cliff sections (Fig. 1B–D) have been investigated using a range of macro-scale field techniques (Krüger & Kjær 1999; Evans & Benn 2004). The exposed sections were described in detail with particular emphasis being placed on recording the type of bedding, sediment type, bed geometry and structure (both sedimentary and glaciotectonic). The sediments were grouped into eight main sedimentary units (A–H) based upon lithofacies associations and other sediment properties, as well as their stratigraphical location. The terminology used for describing the glaciotectonic structures follows that normally used in bedrock structural geological studies (Phillips *et al.* 2011; Phillips 2017 and references therein). The geometry of folds, sense of displacement along thrusts and faults, as well as cross-cutting relationships between different sets of structures were systematically recorded. The orientation of fold axes, bedding, faults and joints measured in the field were plotted on a series of Schmidt equal-area lower hemisphere projections, and analysed using the Stereonet 9 software (Allmendinger *et al.* 2012; Cardozo & Allmendinger 2013). For ease of description, the Melabakkar-Ásbakkar cliffs were divided into several sub-sections, four of which were selected for more detailed analysis: Melaleiti, Ásgil, Ás-north and Ás-south (Fig. 1B). The sections are typically clean and free of surface debris due to the constant coastal erosion. As most of the cliffs are near-vertical only the lowermost parts could be accessed and examined in detail. The upper parts could only be approached at a few locations. The upper parts of the sections are thus mainly documented in the field using binoculars and by the detailed analysis of photomosaics and remotely sensed (LiDAR) images.

The Melabakkar-Ásbakkar cliffs and the Belgsholt section were scanned using a terrestrial, high-resolution RIEGL VZ1000 Light Detection and Ranging (LiDAR) Scanner in May 2014. The scanning was performed as a series of overlapping images spaced at 50–100 m intervals along the cliff sections. The position of the scanner was recorded using a differential Global Navigation System (dGNSS). After each scan, the relevant section of the cliff was photographed with a high-resolution digital camera mounted on top of the scanner in order to apply the right colour to each scan point. The data from the scanner were processed in the RiSCAN PRO software package supplied by RIEGL in order to align and merge the scans manually.

After the scans had been trimmed and aligned the data were exported into the Bentley Pointools program for visualization and measurements. Analysis of the LiDAR images and photomosaics enabled the construction of detailed cross-sections through this variably glaciotectonized sequence.

The radiocarbon dates used in this study were previously obtained by Ingólfsson (1987) and calibrated by Norðdahl & Ingólfsson (2015) with the Marine13 calibration curve (Reimer *et al.* 2013) using the Radiocarbon Calibration Program (CALIB). The dates were reservoir corrected by 365±20 years (ΔR = 24±23), which is the apparent age for living organisms in the sea around Iceland (Håkansson 1983).

Sedimentology of the Late Weichselian to Holocene sedimentary sequence

The sediments exposed in the cliffs at Melasveit can be divided into eight major sedimentary units (A–H), which are often quite heterogeneous. In the undeformed parts of the sequence, these units typically occur in their correct stratigraphical order. However, large-scale thrusting associated with glaciotectonism has resulted in the localized repetition and/or excision of parts of this sequence. The individual sedimentary units are described below and their spatial distribution shown in Fig. 2.

Sediment unit A

This is the structurally and stratigraphically lowermost, and most widely exposed unit in the Belgsholt and Melabakkar-Ásbakkar cliff sections (Figs 1B, 2). Its thickness ranges from 0 to ~25 m, measured from the base of the cliffs, but its lower contact is typically not exposed. An exception to this is at ~3000 m in the Melabakkar-Á sbakkar cliff (Fig. 2) where this unit rests directly on bedrock. The dominant facies within unit A is an extremely firm (hard), typically massive matrix-supported, greyish-

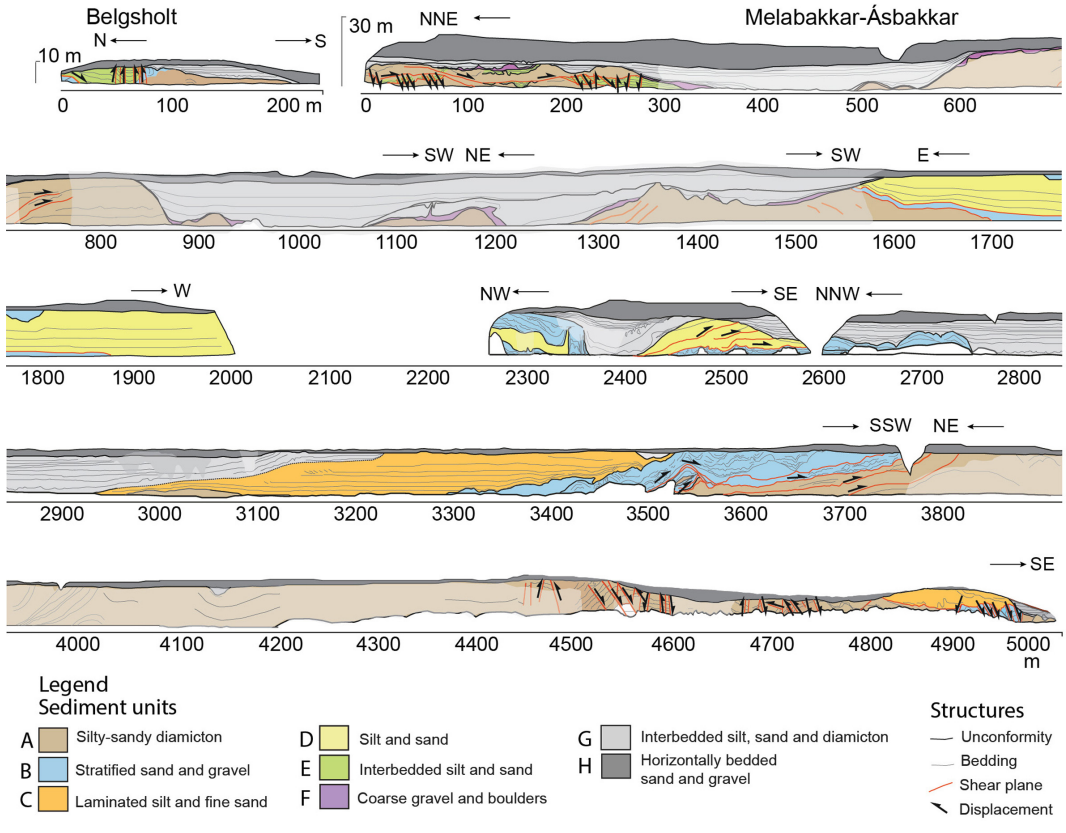

Fig. 2. Overview diagrams of the coastal cliffs from Belgsholt in the north throughout Melabakkar-Ásbakkar. The diagrams were drawn on the basis of terrestrial LiDAR images, except at ~400–2000 and 3900–4500 m, where photographs were used. The diagram is vertically exaggerated (2×). Shaded areas represent sections covered by water and debris that prevented detailed investigation of both structures and stratigraphy. [Colour figure can be viewed at www.boreas.dk]

brownish, silty-sandy diamicton that is locally rich in cobble-sized clasts (Fig. 3A). However, the characteristics of the diamicton vary along the cliffs. In the northern part of Melabakkar-Ásbakkar, most of the diamicton is heavily deformed, vaguely stratified and contains numerous irregular to lenticular-shaped sand intraclasts (up to several metres in length). Both the diamicton and sand intraclasts locally contain high concentrations of fragmented and occasionally intact mollusc shells (Fig. 3A). In the southern part of the Melabakkar-Ásbakkar cliff section, the unit A diamicton occurs interbedded with laterally extensive beds of poorly sorted sand, usually with irregular and gradational contacts. The sands locally contain small shell fragments.

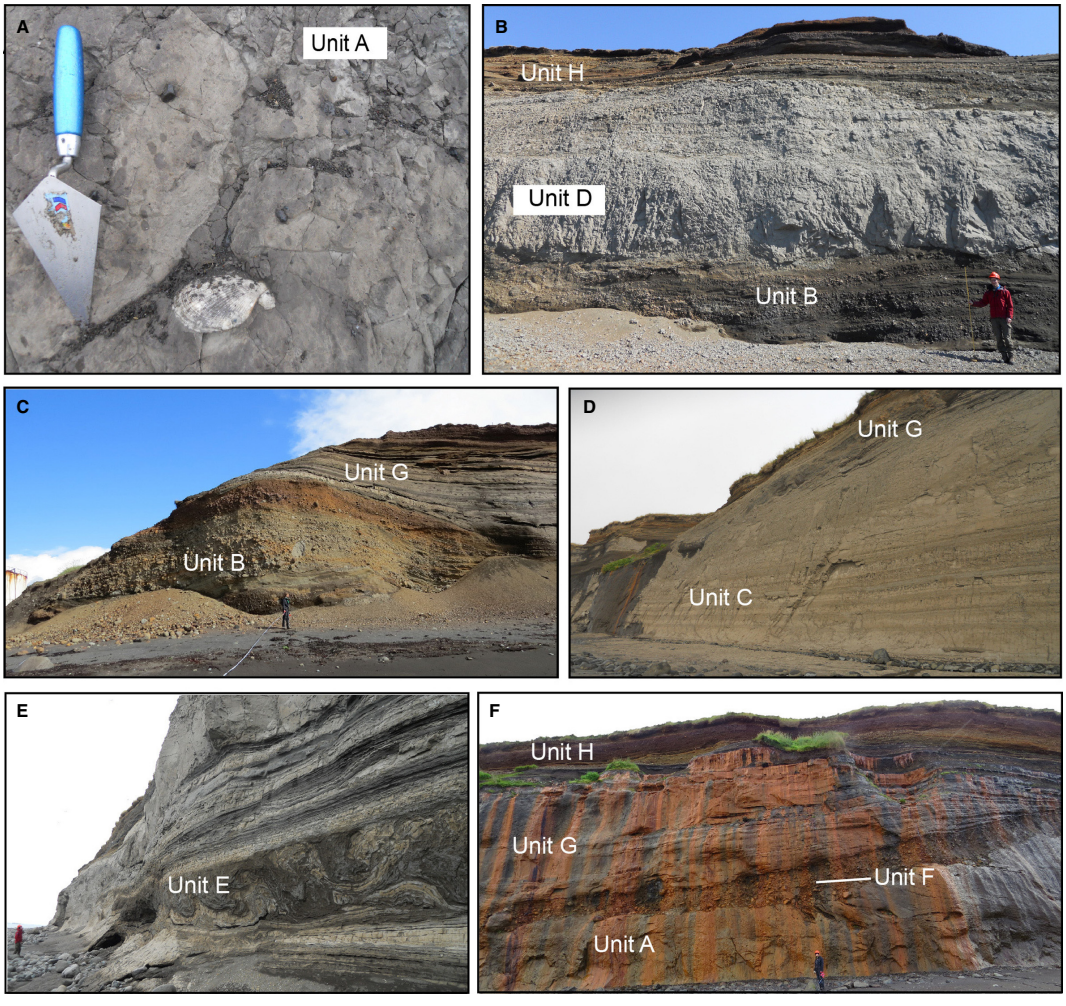

Fig. 3. Examples of sediment composition and contact configuration within some of the eight (A–H) identified sediment units within the Melabakkar-Ásbakkar coastal cliffs. A. Close-up view of the silty-sandy diamicton of unit A (Melaleiti at ~100 m, Fig. 2). Note the embedded unbroken *Chlamys islandica* shell. B. Unit D silts and sands overlaying unit B stratified sand and gravel. The contact between the sediment units is sheared and folded and is cross-cut by a number of small faults. On top is unit H beach-face sediment. Cliff section at around 2550 m (Fig. 2). C. Unit B locally upward coarsening beds of stratified sand and gravel; the gravel is mostly undeformed and forms a ~15-m-thick sediment pile, in turn overlain by undeformed unit G interbedded diamicton and sand. Cliff section at about 2650 m (Fig. 2). D. Unit C horizontally laminated silt and sand grading upwards into a heterogeneous diamicton. The basal sediment sequence is conformably overlain by unit G sandy beds, which at this location dip towards north. The unit A silty-sandy diamicton can be seen at beach level. Cliff section at ~3200 m (Fig. 2). E. Unit E interbedded silt and sand at the base of the cliff with unit A diamicton thrusted on top. Melaleiti cliff section at ~250 m (Fig. 2). F. Unit A silty-sandy diamicton, overlain by a 2-m-thick bed of massive gravel and boulders (unit F) with erosive contact in between. Stratified and undeformed unit G sediments drape the unit F gravel. Cliff section at ~1300–1350 m (Fig. 2). [Colour figure can be viewed at www.boreas.dk]

Ingólfsson (1987) concluded that the mollusc fauna within unit A belong to the *Macoma calcarea* community, indicative of deposition in a low-salinity, shallow water, boreal to mid-arctic fjord environment. Five radiocarbon-dated samples retrieved at different locations in the Melabakkar-Ásbakkar cliffs yielded ages ranging between *c*. 13.7–14.5 cal. ka BP.

Unit A sediments are interpreted as having been deposited in an ice-proximal to ice-distal marine setting, the sedimentary appearance most likely reflecting locally and temporally variable proximity to the ice margin at the time of deposition. The mollusc faunal assemblage within unit A is indicative of a shallow/near-shore environment with a high input of fresh water or glacial meltwater (Ingólfsson 1987, 1988). The massive, structureless nature of the diamicton suggests deposition of fines from suspension with the inclusion of coarser clasts as ice-rafted debris (IRD). Although such sediments may possess a planar lamination due to the variation in sediment input over time, it may have been erased due to bioturbation by molluscs (e.g. Ó Cofaigh & Dowdeswell 2001). Furthermore the lack of distinct stratification may also have been partly caused by homogenization due to post-sedimentary ductile deformation and liquefaction. The occurrence of interbedded sands suggests deposition in a more ice-proximal location, reflecting deposition from turbidity currents discharging from meltwater channels, deltas or outwash fans, causing winnowing of the sediments (Cowan *et al.* 1999; Boggs 2006). However, the locally high concentration of shells within the heterogeneous part of sediment unit A suggests deposition further away from the ice margin where temperatures were higher, bioactivity also high and sediment accumulation rate lower (Powell & Molnia 1989; Powell & Domack 1995; Jaeger & Nittrouer 1999; Ó Cofaigh & Dowdeswell 2001).

Sediment unit B

Unit B sediments are exposed at Belgsholt and at a few places within the Melabakkar-Ásbakkar cliffs, most notably between ~1600–2800 and 3300–3700 m (Fig. 2). This unit has an undulating geometry and its thickness is highly variable laterally with the thickest parts (>15 m) being exposed at Melabakkar-Ásbakkar between ~3400–3800 m. The dominant facies comprises alternating beds of well-sorted coarse to fine sand and cobble gravel beds, as well as frequent interbeds and lenses of massive fines (silt/fine sand) and silty-sandy diamicton (Fig. 3B, C). The diamicton layers/lenses within unit B are most prominent at Ás-north (Fig. 2, ~3600–3800 m) where they are up to ~3 m thick. The planar and trough-cross bedded sand and gravel beds are laterally discontinuous with erosive bases, the thickness of individual beds ranging from centimetres to over a metre. Unit B sediments are typically sheared, folded and faulted, except between 2600–2800 m (Fig. 2) where they form an up to 15-m-thick sequence of undeformed coarse, well-stratified gravel with subrounded to well-rounded pebble to boulder-sized clasts (Fig. 3C). Some beds contain a large amount of mollusc fragments with abraded edges; no whole, un-abraded shells were detected. The lower contacts of unit B are only exposed between 1600–1700 and 3500–3900 m (Fig. 2) where unit B overlies sediment unit A, and between ~2300–2400 where it rests upon sedimentary unit D (see below). The contacts of unit B with these other sediment packages frequently show evidence of shearing and tectonic mixing with the structurally underlying sediment units.

The sedimentary structures, large grain sizes, sorting and roundness of clasts, as well as a high content of shell fragments suggest that the sands and gravels of unit B were deposited from meltwater discharge in a relatively high-energy, marine environment. This type of environment frequently occurs at the margin of marine-terminating glaciers where coarse-grained sediments are brought into the ocean by subglacial meltwater streams (Powell & Molnia 1989; Powell & Domack 1995; Powell 2003). The massive, fine-grained sediment layers that interdigitate with the sorted sand and gravel may represent debrisflows and/or fall-out from suspension, both of which are common processes in ice-contact marine systems (Powell & Molnia 1989; Lønne 1995; Powell 2003). The shell fragments are likely to be reworked and therefore do not reflect the faunal assemblage living at the time of sediment deposition.

Sediment unit C

Unit C sediments are exposed between ~3000 and 3500 m at Melabakkar-Ásbakkar where they range from 1 to 20 m thick and unconformably overlie units A and B (Fig. 2). The dominant facies comprises planar and cross-laminated fine sand interbedded with massive silt. This sand and silt sequence is unconformably overlain by a massive silty-sandy and relatively clast-poor diamicton (Fig. 3D). The sediments of unit C have been subject to both ductile and brittle deformation immediately below the diamicton. No shells or shell fragments were found in the lower interbedded part of the sequence, while small fragments were observed in the diamicton.

The dominance of fine-grained laminated silts and sands with occasional outsized clasts suggests deposition in a glaciomarine setting in which the massive silt beds were deposited from suspension settling, while planar and cross-laminated sand formed from turbidity currents (Powell & Molnia 1989; Ó Cofaigh & Dowdeswell 2001). The absence of *in situ* mollusc shells suggests a hostile environment, either due to low temperatures and/or high sedimentation rate (Ó Cofaigh & Dowdeswell 2001). The diamicton in the upper part of unit C is interpreted as a massflow deposit (Ó Cofaigh & Dowdeswell 2001; Nichols 2009) containing reworked shell fragments. Emplacement of this massflow is thought to have resulted in the observed disruption of the underlying silts and sands. Alternatively, the diamicton could be interpreted as a subglacial traction

till deposited at the ice–bed interface. During its emplacement, the underlying unit C sediments may have been subjected to glaciotectonic deformation.

Sediment unit D

This sediment unit is up to ~25 m thick and was observed in the Melabakkar–Ásbakkar cliffs between ~600–700 m, 1600 and 2600 m, as well as within the southernmost part of this section between 4700–5000 m (Fig. 2). The dominant facies is a poorly sorted, massive fine sandy silt, often with bed thickness over 1 m, separated by much thinner (cm scale) beds of medium to coarse sand (Fig. 3B). Occasional pebble-sized clasts (up to a few cm) are found dispersed within the silt beds. The sediments of unit D are deformed and locally appear to have been homogenized to form a fine-grained, clast-poor diamicton. Unit D sediments have locally been thrust over unit B (e.g. Fig. 3B). The glaciotectonic contact between units B and D is irregular, and shows evidence of both brittle faulting and ductile shearing, as well as liquefaction and mixing between these sedimentary units (see below). A few small mollusc fragments (mm scale) were found, mostly in the lowermost parts of unit D, but no whole mollusc shells or larger fragments were detected. Ingólfsson (1987) has published three radiocarbon dates on shell fragments collected at ~2550 m (Fig. 2) that range in age between *c.* 13.4–13.5 cal. ka BP. This suggests a maximum age of sediment deposition during the Allerød.

Sediments of unit D are interpreted as having been deposited in an ice-proximal glaciomarine environment. The thick beds of massive sandy silt represent deposition by suspension settling from buoyant meltwater plumes and the pebble intraclasts deposited by means of debris rain-out from icebergs (Powell & Molnia 1989; Lønne 1995). The mollusc fragments are clearly redeposited, their age only giving a maximum age of sediment deposition. The absence of whole shells suggests a too hostile environment for mollusc fauna, possibly reflecting a high rate of sediment accumulation (Ó Cofaigh & Dowdeswell 2001).

Sediment unit E

Unit E sediments are exposed between ~10–100 m in Belgsholt (Fig. 2) where the unit is up to ~6 m thick, and in the Melabakkar-Ásbakkar section at ~0–300 m (Fig. 2) where at Melaleiti the unit is 8 m thick. The dominant facies comprises beds of well-sorted, both planar cross-bedded and planar laminated medium-grained sand, alternating with beds of massive silt. Bed thicknesses are generally in the cm- to dm-scale. In the lower part of unit E are occasional beds of gravel (bed thicknesses in the order of centimetres) and beds of sandy silty diamicton (up to ~1 m thick), the latter containing small mollusc fragments. The contacts between the beds of different facies are typically sharp and erosive, with the sand beds commonly containing silt intraclasts that are lithologically similar to the interbedded massive silts, indicative of localized penecontemporaneous erosion.

The appearance of the sediments within unit E varies along the cliff section. At Belgsholt, the sand and silt beds in the lowermost part are up to a few dm thick and commonly exhibit small-scale synsedimentary folds and overturned flame structures. The beds become thinner and less deformed upwards and in the uppermost ~3 m they contain abundant intact mollusc shells; identified species are *Balanus balanus*, *Buccinum undatum*, *Hiatella arctica* and *Macoma calcerea*. At the Melaleiti section there is no obvious vertical variation in bed thickness or grain size of unit E sediments. Synsedimentary folds and flame structures up to 50 cm in amplitude are common (Fig. 3E). At Belgsholt, the contact between unit E and units A and B is tectonic, while at Melaleiti the boundary between units E and A ranges from sharp to gradational.

The alternating planar- and cross-laminated sand with beds of massive silt suggest deposition from turbidity currents alternating with suspension settling of fine-grained sediments from meltwater plumes (Ó Cofaigh & Dowdeswell 2001). The flame structures are most likely a result of loading of water-saturated mud, with the resultant water-escape leading to the deflection upwards of the interbedded sand layers. The presence of these water-escape features within unit E is consistent with high rates of sedimentation. The loading was most likely accompanied by mass movement, leading to the overturning of the load structures in the direction of emplacement of the massflow (Boggs 2006). The diamicton beds in the lower part of unit E are thought to represent subaqueous sediment gravity flows with their emplacement having been accompanied by localized soft-sediment deformation (Lønne 1995; Boggs 2006). Together, this suggests a high-energy, unstable, depositional environment located close to the ice margin, while the upward fining trend, as well as the marine fauna, in the upper beds of unit E at Belgsholt suggests a progressively increasing distance from the ice front during deposition of unit E; potentially recording the retreat of the ice front. The marine fauna observed at Belgsholt indicates shallow coastal water and the presence *Buccinum undatum*, which is a sub-arctic species (Símonarson 1981), relatively warm water temperatures.

Sediment unit F

Unit F sediments were observed in the northern part of the Melabakkar-Ásbakkar cliffs between 0–2800 m (Fig. 2). The dominant facies is a massive clast-supported gravel with subrounded to rounded clasts and with a sandy matrix infill. Maximum particle size is generally around 0.5 m, although occasionally larger clasts, up to ~2 m in diameter, were also found. Unit F forms a thin (maximum thickness ~3 m) and undulating bed following the shape of the underlying topography. Its

lower contact is erosional, especially between 1000–1600 m, where the clast sizes also tend to be their largest (Fig. 3F). Sediment intraclasts that are clearly derived from underlying sedimentary units A and D are common within unit F. The southward tilted rip-up structures show that the palaeocurrent direction was towards the south. No mollusc shells were observed in the sediment.

The clast roundness and erosional lower contacts, as well as the large particle sizes, suggest sedimentation by running water in a high-energy environment. Massive boulder beds and lag deposits similar to those of unit F that contain frequent rip-up clasts due to erosion of underlying beds have been described in glacial outburst flood (jökulhlaup) deposits in Iceland (Maizels 1997; Marren 2005). The fact that unit F follows the undulating surface topography of underlying sedimentary units suggests that it was deposited under high pressure in a confined space where the fluid flow followed the topography of the substratum instead of accumulating in depressions, as would be expected in an unconfined setting. Based on this, unit F is interpreted as having been deposited at the ice/bed interface by pressurized subglacial meltwater flows. Similar coarse-grained sediments with erosive bases, argued to be diagnostic for subglacial excavation and deposition in subglacial cavities during high-energy flow conditions, have been described from Skeiðarárjökull in Iceland (Russell *et al.* 2006).

Sediment unit G

Unit G sediments are exposed at a few places within the Melabakkar-Ásbakkar cliff, most notably between 300–600, 900–1600 and 2500–3200 m (Fig. 2), and within the Belgsholt cliff section (between ~100–250 m; Fig. 2). They are undeformed, drape the topography of the underlying sediment units and are separated from these variably deformed sediments by a sharp contact (Fig. 3C, D, F). Unit G records an overall upward fining trend. The lower parts of the unit mainly consist of relatively thick beds of interbedded diamicton and sand (often >1-m-thick beds) as well as local occurrences of thin gravel beds (cm- or dm-scale), with erosional contacts. The silty-sandy diamicton beds are usually massive, while the sand beds show both planar and cross lamination. Evidence of soft-sediment deformation, such as convolute bedding and flame, ball and pillow structures, are commonly found within individual beds in the lower part of the unit. The upper parts of unit G commonly consist of planar-laminated silt and fine sand. No mollusc shells were found within unit G.

The diamicton beds that dominate the lower part of unit G are interpreted as deposited from high-density sediment gravity flows, common in ice-contact environments due to instable slopes, high sedimentation rates and calving (Powell & Molnia 1989; Lønne 1995; Boggs 2006). The interbedded planar to cross-bedded sands are thought to record traction deposition from more diluted sediment underflows. The soft-sediment deformation structures within these beds are indicative of fast sediment deposition resulting in localized liquefaction and water-escape. The absence of mollusc shells may also indicate high sedimentation rates, although it is also possible that this absence is due to unfavourable temperature conditions (Ó Cofaigh & Dowdeswell 2001; Boggs 2006). Measured depositional rates in front of contemporary retreating glacier margins in Alaska, Greenland and Svalbard are reported to be as high as several decimetres per year (Cowan *et al.* 1999; Jaeger & Nittrouer 1999; Gilbert *et al.* 2002; Trusel *et al.* 2010). The change in lithofacies upwards within unit G to a sequence dominated by laminated silt and fine sand suggests a progressive lowering of energy levels and increased distance from the sediment source, reflecting retreat of the ice margin. Sedimentation in the upper part of the sequence is thought to have been dominated by suspension settling of fine sediments out of a buoyant sediment plume (Ó Cofaigh & Dowdeswell 2001).

Sediment unit H

Unit H constitutes the stratigraphically youngest part of the sedimentary sequence and can be traced laterally along the entire Melabakkar-Ásbakkar section, and corresponds to the uppermost part of the succession identified by Ingólfsson (1987). Unit H ranges in thickness from ~10 m at 0–400 m to ~1 m in most places beyond 3000 m. This sedimentary unit is generally separated from the underlying units by a distinct unconformity (erosion surface). The dominant facies within unit H is horizontally bedded sands and gravels, which define an overall coarsening upwards sequence. However, in detail these sediments also exhibit smaller-scale changes in grain size both vertically and laterally. For example at ~300–400 m, the unit consists of cross-bedded gravel, whereas at ~500–700 m it comprises a 6-m-thick sequence of planar- and cross-laminated sand with occasional load structures. No detailed examination of unit H could be performed because of inaccessibility at the top of the cliffs.

Unit H sediments have previously been interpreted as comprising a complex, time-transgressive sequence of beach (littoral zone) sediments and aeolian sand that was formed during a marine regression and emergence of the landscape in the early Holocene (Ingólfsson 1987, 1988).

Structural architecture of Belgsholt and Melabakkar-Ásbakkar

The detailed internal structural architecture of the Belgsholt and Melabakkar-Ásbakkar sections are described below and illustrated in Fig. 2.

Belgsholt

The northernmost section, Belgsholt, occurs in an elongated, E–W trending ridge, situated approximately 500 m

northeast of the main Melabakkar-Ásbakkar cliff section (Fig. 1B). The ridge is cut by a transverse ~250-m-long, N–S orientated, 12-m-high subvertical coastal cliff (Fig. 4A). The northernmost ~100 m is clean and free from surface debris enabling a detailed examination of the internal architecture of the ridge. The remainder of the cliff section is partly obscured by surface wash and debris.

Structural architecture. – The Belgsholt section can be divided into two parts based on the style and relative intensity of deformation: (i) the northern part (0–110 m; Fig. 4A) characterized by the presence of a large syncline-anticline pair affecting units B and E and (ii) the southern part (110–250 m; Fig. 4A), which consists of undeformed laminated sediments (unit G) overlying deformed sand and diamicton (units A and B).

The sediments in the northern part of the section (0–110 m) are dominated by the interbedded silts and sands of unit E, resting upon the bedded sands and gravels of unit B. At this locality, the base of unit E is poorly defined and deformed with the small-scale folds along this boundary indicating that it has been modified by bedding-parallel shearing. The dominant deformation structure in the section is a large-scale syncline-anticline pair (~50–100 m; Fig. 4A). The syncline is upright with amplitude over 12 m and wavelength ~40 m with its axis plunging 4° to the ESE (Fig. 4B). Bedding-parallel shearing appears to have occurred prior to the folding as the tectonized contact between units E and B is folded by the syncline. The bedding within the core of the fold is offset by numerous, steeply inclined reverse faults (displacement in the order of cm or dm) that fan around the axis of the syncline (Fig. 4A, B). These faults have sharp planes and extend outwards to deform the structurally underlying stratified sand and gravels of unit B. Although deformed, primary sedimentary structures and relationships between the beds within unit E are well preserved. Between 70 and 100 m, the unit B sands and gravels occur within a south-verging anticline (Fig. 4A, C). Primary sedimentary features within the core of the anticline have been overprinted during deformation and the sand has been homogenized by liquefaction. The limbs of the anticline are cross-cut by minor faults (displacement of only mm to a few cm), mainly reverse faults, developed approximately orthogonal to the bedding surfaces.

The sequence exposed in the southern part of the Belgsholt section (110–250 m) is composed of the massive/heterogeneous silty-sandy diamicton (unit A) overlain by stratified sand and gravel (unit B). These lithofacies associations are interfingered and show evidence of soft-sediment deformation; probably as a result of synsedimentary compaction and loading of still wet sediments. Immediately adjacent to the south-verging anticline (between 90 and 110 m; Fig. 4A) both units A and B show evidence of locally intense, and highly disruptive, ductile

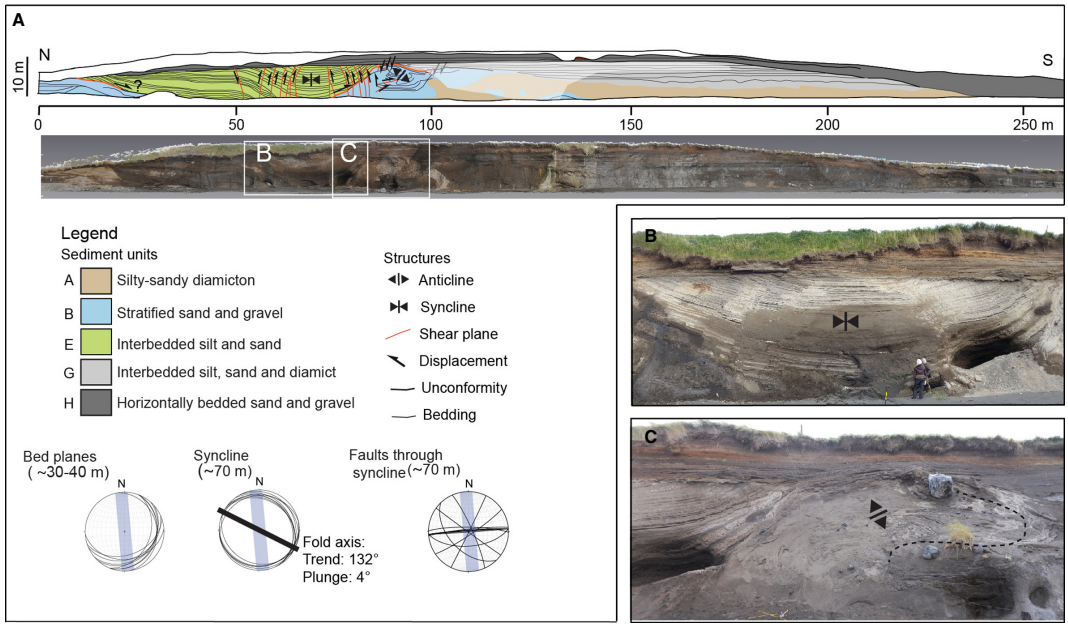

Fig. 4. The structural ridge at Belgsholt. A. A scale diagram of the Belgsholt section above a LiDAR image of the section. Directional data are plotted on lower hemisphere stereographic projections and the blue bars indicate the orientation of the section. The white boxes indicate the area covered by the photographs in B and C. B. A large syncline at ~70 m. C. An overturned, southward-verging anticline at ~90 m. Note the big boulder (1 m in diameter) approximately in the core of the anticline. [Colour figure can be viewed at www.boreas.dk]

deformation and associated liquefaction, and also contain a large number of intraclasts (individual clasts over 1 m in diameter) of sand. Relatively undeformed beds of silt and sand (unit G) unconformably overlie the deformed sequence from ~90 m southwards and the whole sequence is truncated by a horizontally bedded gravel unit (unit H).

Structural evolution. – The relatively simple internal architecture of the Belgsholt ridge is consistent with lateral (subhorizontal) compressive deformation, as a result of ice-push from the north/northeast. The south-verging syncline-anticline fold pair is interpreted as recording ductile folding as the ice advanced into the pre-existing marine sediments. Minor brittle faulting of the sediments within units B and E occurred as the sequence accommodated further compression imposed by the advancing ice.

The focusing of ductile deformation along the lithological boundary between unit E and the structurally underlying sands and gravels of unit B may simply reflect the marked lithological/rheological contrasts between these two units. This deformation probably occurred during the onset of glaciotectonic deformation at Belgsholt (i.e. prior to folding) and possibly records the earliest stages of shortening of the sediment wedge in response to initial ice-push. As the ice continued to advance, this tectonized boundary was folded into the upright syncline that dominates the northern part (Fig. 4A, B). Alternatively, this sheared boundary may represent an earlier formed bedding-parallel thrust resulting from the southerly transport of a detached slab of unit E sediments and its emplacement upon the sands and gravels of unit B.

The relative intensity and complexity of the deformation observed in the northern part of the Belgsholt section initially increase southward towards the central part of the section (~50–100 m), before fading out in the remaining part of the section (Fig. 4A). The sediments deformed by the south-verging anticline and immediately south of this fold show evidence of soft-sediment deformation and liquefaction (Fig. 4A, C). The fluidized sediments were remobilized and injected upwards in the form of diapirs and clastic dykes. There is no definitive evidence that the advancing ice overrode the sequence at Belgsholt (e.g. evidence for subglacial shearing): therefore, the diapirs and clastic dykes may simply be recording the escape of pressurized meltwater from the deforming sequence driven by a hydrostatic pressure gradient formed by the weight of the advancing ice. Compression of wet sediments immediately in front of the advancing ice mass would have resulted in an increase in pore-water pressure leading to liquefaction and injection of the remobilized sediments. Localized faulting of the sediments observed cutting through the diapirs and clastic dykes within units A and B indicates that deformation continued after liquefaction, consistent with dewatering of the sediments prior to the termination of glaciotectonic deformation.

Although the Belgsholt ridge has most likely undergone some erosion since its formation, the location of the most highly deformed part of the sequence below the crestline suggests that the ridge is a morphological expression of the glaciotectonics below. This is further supported by the structural reconstructions indicating ice movement from the north, approximately perpendicular to the trend of the ridge. Based on this association between the ridge morphology and the compressional nature of the glaciotectonics, as well as the localized nature of the deformation, the ridge is interpreted as an ice-shoved ridge (e.g. Aber & Ber 2007). The deformation is mostly confined to the proximal (northern) and central part of the ridge, which indicates that the former ice margin was located on the northern side of the ridge.

Melaleiti

The Melaleiti structural zone occurs at the northern end of the Melabakkar-Ásbakkar coastal cliffs, between 0 and 300 m (Fig. 2). At Melaleiti, the cliff is orientated NNE–SSW and rises vertically up to 30 m a.s.l. The cliff face is mostly dry allowing a detailed documentation of the sedimentary features and glaciotectonics. Bedrock outcrops are found at sea level just north of the section and ~100–200 m offshore.

The stratigraphy at Melaleiti can be divided into three main structural units (Fig. 5A): (i) the deformed sequence that dominates the lowermost ~13 m of the cliff section and forms the Melaleiti structural zone (units A and E); (ii) an undulating gravel bed (unit F) overlain by a sequence of alternating silt, sand and clast-poor diamicton (unit G); and (iii) the structurally higher Holocene sequence of littoral sediments (unit H; Ingólfsson 1987, 1988).

Structural architecture. – The Melaleiti structural zone consists of subhorizontal to gently northwards tilted, thrust-bound blocks comprising the silty-sandy diamicton of unit A and interbedded silts and sands of unit E.

In the northern part of the section (~0–80 m; Fig. 5A) the thrust blocks are separated by a poorly defined, undulating shear plane. Internally, the thrust-bound blocks are pervasively deformed showing evidence of homogenization due to ductile deformation and the contacts between the internal sediments (units A and E) are generally diffused. They are dissected by a series of southeast-dipping normal (extensional) faults, as well as some smaller-scale, steep, northwest-dipping, reverse and normal faults (Fig. 5A). These faults seem to be truncated by and therefore pre-date the shear plane. The displacement on both sets of faults is generally in the order of centimetres or decimetres. Most of the faults are undulating and commonly infilled/lined by massive, fine-grained sediments, which suggests that they acted as fluid pathways.

The middle part of the section (80–110 m; Fig. 5A) exhibits the most complicated deformation in the Melaleiti

zone. The most notable structures in this part are a number of southeast-dipping shear planes, which break up the thrust blocks of units A and E into a series of northward-dipping fault blocks. The fault blocks and the shear planes are cross-cut by undulating open, southward-dipping fractures that are infilled by massive sand-rich sediments. The shear planes are poorly defined and are frequently lined by deformed, fine-grained sediments. Although hard to estimate, the offset of internal bedding within unit E suggests that the displacement might be a few metres towards the southeast.

The southern part of the Melaleiti section (110–250 m; Fig. 5A) exhibits somewhat simpler and less penetrative deformation than the northern part. A gently northward-dipping discrete shear plane divides the sequence into two thrust blocks, each containing both units A and E. Although deformed, internal sediment features within unit E in both the upper and lower thrust blocks are easily recognizable and can be traced throughout a large part of this structural unit. However, the sediments immediately below the shear plane show evidence of intense ductile deformation (shearing and folding) that decreases in intensity and depth of penetration towards the south (Fig. 5A–D). The sediments in the footwall of this shear plane are cut by numerous reverse and normal faults (Fig. 5C, D). The dominant fault type varies laterally; in particular most of the faults between 100 and 150 m are north-dipping reverse (compressional) faults, whereas between ~180 and 300 m the faults are mainly extensional (normal) dipping both towards the southeast and northwest (Fig. 5A). Most of these faults only cut through the footwall although a few cross-cut and therefore post-date the thrust boundary and extend upwards into the hanging wall (Fig. 5A, D). Some of the faults are infilled by sand suggesting that these may have acted as fluid pathways (hydrofractures) (Rijsdijk *et al.* 1999; Phillips & Merritt 2008; van der Meer *et al.* 2009; Phillips & Hughes 2014). The upper block forms a large boudinage structure between 170 and 250 m (Fig. 5A, C).

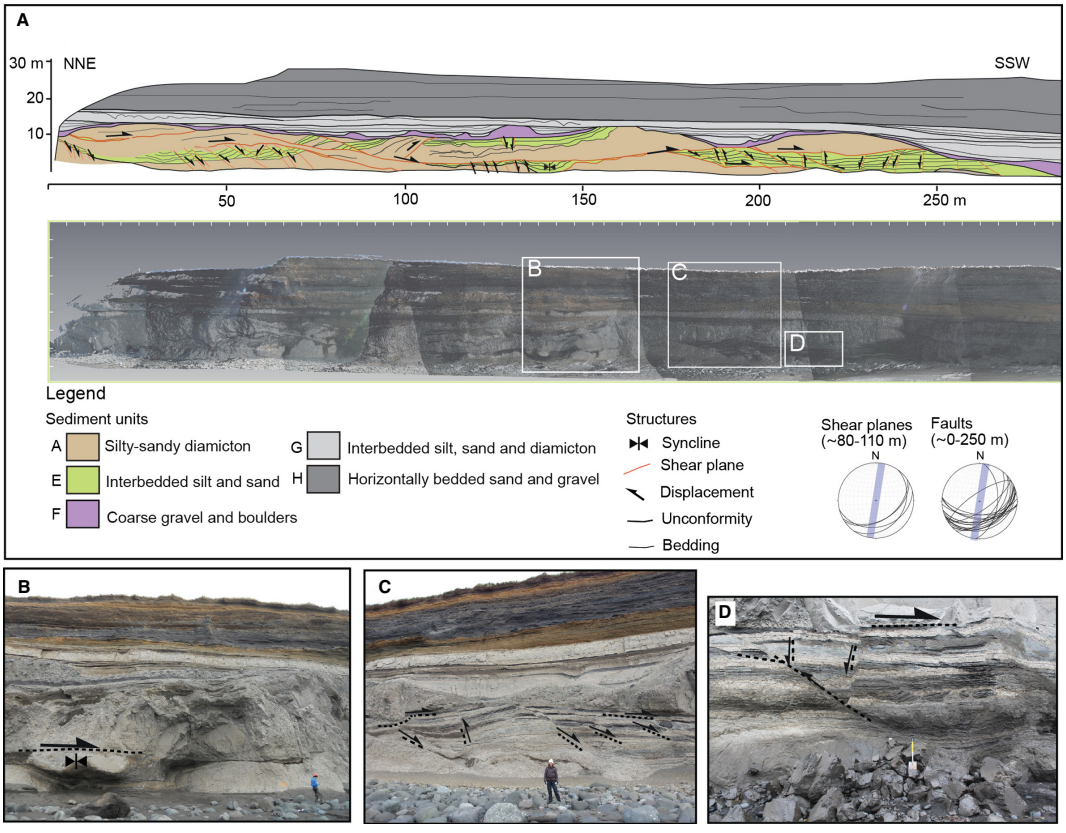

Fig. 5. A. A scale diagram and a LiDAR image of the Melaleiti structural zone. Directional data are plotted on lower hemisphere stereographic projections and the blue bars indicate the orientation of the section. The white boxes indicate the area covered by the photographs in B–D. B. Stacked rafts of unit A silty-sandy diamicton overlying deformed unit E interbedded silt and sand. Note the person for scale. C. Boudinaged raft of silty-sandy diamicton of unit A with faulted unit E bedded sediments below. D. A close-up view of faults cutting through unit E sediments. Spade for scale. [Colour figure can be viewed at www.boreas.dk]

Structural evolution. – The overall structural architecture of the Melaleiti section indicates a thrust zone where blocks composed of the marine diamicton of unit A and interbedded sands and silts of unit E have been thrusted and stacked as a result of subhorizontal compressional deformation (Fig. 6). Such thrust-stack sequences generally form in an ice-marginal or proglacial position due to gravity spreading and compression from the rear by the forward movement of the ice (e.g. Aber *et al.* 1989; Bennett *et al.* 1999; Boulton *et al.* 1999; Bennett 2001; Pedersen 2005; Phillips *et al.* 2008, 2017; Benediktsson *et al.* 2010, 2015; Benn & Evans 2010). Based on the configuration of these thrust blocks and orientation of faults, this deformation was caused by an ice-push from the northwest (Fig. 5A). The overall decrease in strain from north to south can therefore be explained by a decreasing amount of stress transferred from the source of tectonic pressure, i.e. an advancing ice margin, towards the foreland.

Shear zones like the one separating the thrust-blocks at the southern part of Melaleiti are commonly found below glacially transported sediment rafts where the displacement is facilitated by a thin water-lubricated detachment (e.g. Benediktsson *et al.* 2008; Phillips & Merritt 2008). Vaughan-Hirsch *et al.* (2013) argue that elevated pore-water pressures during glaciotectonism can lead to liquefaction of the sediments within the shear zone, lowering their cohesive strength and thereby aiding forward movement of the overriding thrust block. Therefore, based on the nature of contacts, the detachment and transportation of the thrust sheets at Melaleiti are thought to have been facilitated by elevated pore-water pressures during glaciotectonism. The tectonic thickening may have caused a build-up of pore-water pressures within the developing thrust stacks leading to hydrofracturing when the pressure exceeded the cohesive strength of the sediments and the depressurization of the lubricated detachments (Rijsdijk *et al.* 1999, 2010; Phillips & Merritt 2008). Subsequently the forward movement of the thrust sheets was accommodated by extensional deformation in the lower thrust sheet causing the formation of normal faults. The sediments became increasingly well drained towards the distal (south) part of the moraine reflected by the better defined fault/fracture planes towards the south. Similar patterns of continuing brittle deformation after a fall in pore-water pressures are known from both modern and past glacial environments (e.g. Benediktsson *et al.* 2008, 2010; Phillips & Merritt 2008). The thrust blocks are draped by the subglacial gravel of unit F showing that the zone was overridden by a glacier after the ridge was formed. This may have resulted in further extensional deformation of the thrust stacks, such as the boudinage structure of the upper thrust block (between 150 and 250 m; Fig. 2) and a set of extensional faults dissecting the thrust blocks and the boundary between (Fig. 6).

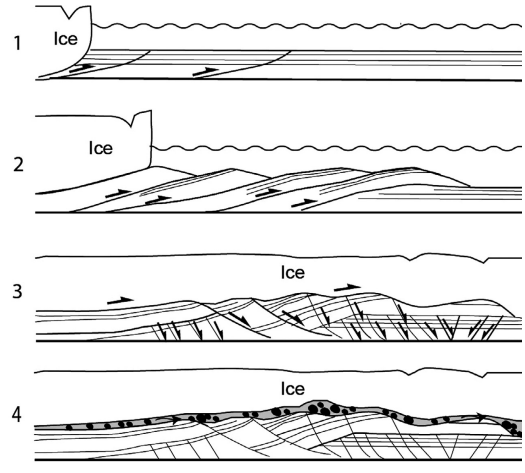

Fig. 6. A sequential model showing the formation of the Melaleiti structural zone.

Fúla Bay

The Fúla Bay comprises several subzones occurring between 400 and 2000 m (Fig. 2). The overall architecture of these zones is only briefly described because a detailed investigation was hampered by overhangs and frequent rock falls as well as water and thin debris cover on the cliff face.

Structural architecture. – The structural zones in Fúla are mostly composed of the deformed sediments of units A, B and D. The deformed units A and D as well as local occurrences of unit B in between form a small number of ridges, the two largest of which are up to 30 m high (at 600–900 and 1300–2000 m; Fig. 2). The architecture of the ridge at 600–900 m indicates that it comprises stacked thrust blocks dipping towards the northwest (ranging 276–316°; Fig. 7). Numerous normal faults with a down-throw to the south (ranging 156–216°; Fig. 7) were identified in the lowermost parts of the ridge (Fig. 2). However, it was typically not possible to determine the amount of fault displacement or how far up the sequence the faults extended. The ridge between 1300–2000 m mainly consists of apparently subhorizontally bedded unit D resting upon heavily deformed units A and B. The most part of unit D, however, is only weakly deformed although the lower contacts are sheared, folded and dissected by numerous compressional and extensional faults (Fig. 2).

The coarse gravel and boulder bed of unit F, interpreted as a subglacial deposit that caps the deformational zone at Melaleiti, can also be traced along the entire Fúla zone (Figs 2, 3F). The gravel follows the ridge-like topography of the deformed unit A below and is equally thick on the ridge crests as in the swales between the ridges.

Structural evolution. – The zone located between 600 and 900 m comprises a thrust-stack sequence indicating

Fig. 7. A photograph of the Fúla Bay thrust zone at ~730 m (Fig. 2). Directional data are plotted on lower hemisphere stereographic projections and the blue bars indicate the orientation of the section. [Colour figure can be viewed at www.boreas.dk]

that it was formed by a subhorizontal, compressional deformation in an ice-marginal or proglacial position (Bennett *et al.* 1999; Boulton *et al.* 1999; Bennett 2001; Phillips *et al.* 2008, 2017; Benn & Evans 2010). The orientations of the thrust sheets and faults suggest an ice flow from the northwest (Fig. 7). The lower contacts of unit D within the structural zone between 1300–2000 m are interpreted as a thrust boundary based on the shearing and folding concentrated along the contacts. Although no structural measurements could be carried out in this part of the cliffs, it is likely that the glaciotectonic stress direction was also from the north/northwest. Between 1600–2000 m the cliff is orientated E–W, approximately perpendicular to the main glaciotectonic stress direction, making the beds appear horizontal in the cliff wall. The presence of the subglacial gravel of unit F on top of all the ridges in Fúla Bay indicates that they were overridden and perhaps also eroded and reshaped by a glacier after the thrust stacks were formed. The southward-dipping faults detected within the Fúla structural zone (Fig. 7) might have developed in response to this subglacial modification.

Ásgil

The Ásgil structural zone is located in the central part of the Melabakkar-Ásbakkar cliffs, north of the Ásgil gully, between ~2250 and 2600 m (Figs 2, 8A). The cliff face at this site is subvertical and orientated northwest–southeast. The southern part of the section is mostly clean and well exposed allowing detailed documentation of deformation structures, whereas the northern part (2250–2400 m; Fig. 8A) is partially concealed by surface wash and debris.

Ásgil can be divided into three main structural units: (i) the deformed zone comprising stratified gravel of unit B and interbedded silts and sands of unit D. These deformed sediments rest on unit A, which is not exposed in the cliffs but can be seen on the foreshore at low tide; (ii) the interbedded unit G, which overlaps the underlying deformed units; and (iii) the uppermost Holocene sequence of littoral gravels (unit H).

The Ásgil deformed zone is divided into two parts based on the style of deformation; (i) the northern part (2250–2400 m, Fig. 8A), which is dominated by large-scale folds and (ii) the southern part (~2400–2700 m, Fig. 8A), which is characterized by stacked, northward-dipping thrust blocks.

Ásgil north – structural architecture. – The northern part of the Ásgil section (2250–2400 m; Fig. 8A) is characterized by a few upright to gently northward-verging folds, which become progressively tighter towards the southeast with amplitudes of up to about 20 m and deform the ice-marginal sand and gravel of unit B and the silts and sands of unit D.

The northernmost fold is an open syncline (2300–2330 m; Fig. 8A), followed by a closed anticline at 2330–2350 m (Fig. 8A). They both appear to have fold axes trending approximately southwest–northeast based on measurements from the southeastwards-dipping fold limb. Two or three tight/isoclinal folds are also found at ~2350 m (Fig. 8A). Despite being deformed, primary sedimentary structures (e.g. bedding) are usually well preserved within the sands and gravels of unit B. The folds are dissected by a number of fractures and minor faults (displacement in the order of mm to cm), many of which seem to radiate from the centre of the folds (Fig 8A; ~2300–2350 m). Based on the stratigraphy and the proximity to the southernmost thrust zone at Fúla Bay (1300–2000 m; Fig. 2) these are interpreted to be part of the same structural zone.

Ásgil north – structural evolution. – The large folds present in the northern part of the section (at ~2250–2400 m; Fig. 8A) most likely post-date the southern part as they do not show any indications of being overprinted by stress from the northwest (high relief and a lack of overturning) and the sediments affected by the folding appear to structurally overlie the deformation zone at

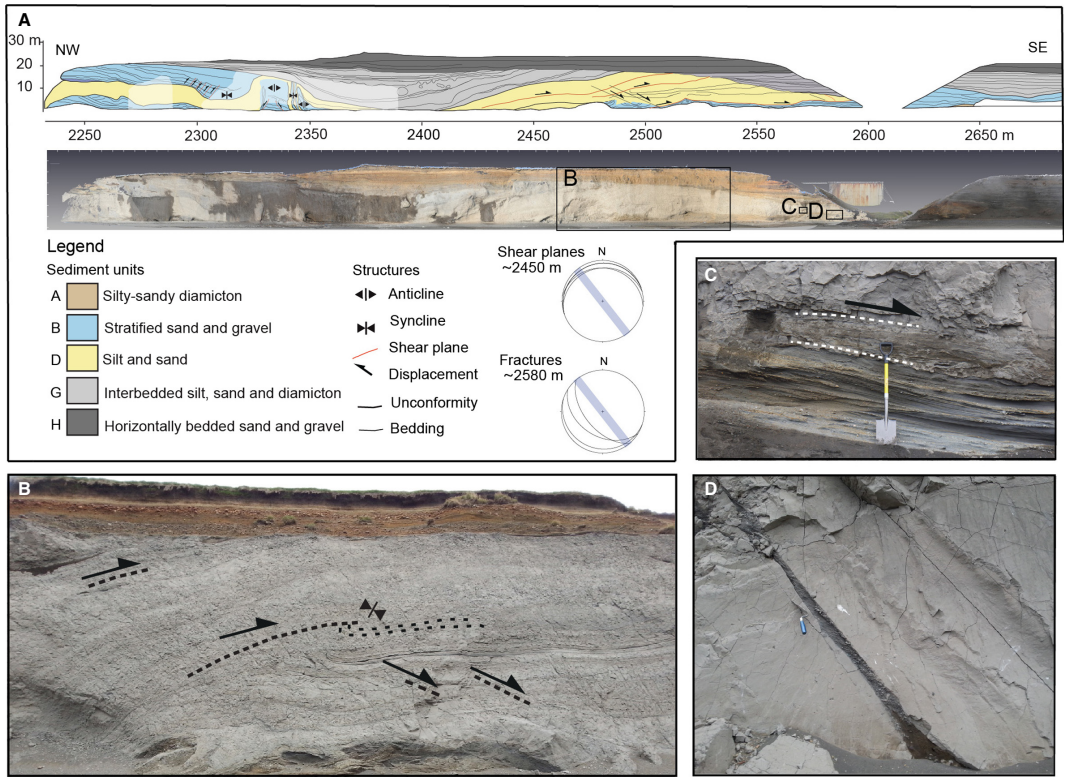

Fig. 8. A. A scale diagram and a LiDAR image of the Ásgil section. Directional data are plotted on lower hemisphere stereographic projections and the blue bars indicate the orientation of the section. The black boxes on the LiDAR image indicate locations of the photographs in B–D. B. Imbricated thrust blocks of unit D at ~2475 m. The lower thrust block is folded and dissected by normal faults with a southwest dip. C. Deformed zone separating the silts and sands of unit D above and the stratified sand and gravel of unit B below. D. A hydrofracture dissecting a bed of massive sandy-silt belonging to unit D, infilled with sorted coarse sand from unit B below. [Colour figure can be viewed at www.boreas.dk]

Ásgil-south. The folds might be glaciotectonic, possibly representing proglacial deformation formed as the ice was forming the thrust stacks observed south of the zone at Fúla Bay (1300–2000 m; Fig. 2). Alternatively, they could have formed during slumping in response to large-scale gravity flows as the glacier retreated from the area (Boggs 2006). The radiating geometry of most of the faults dissecting the folds suggests that these were developed in response to horizontal shortening of the sediment as it was folded.

Ásgil south – structural architecture. – The most notable large-scale structures at the southern part of Ásgil (2400–2650 m; Fig. 2) are a number of stacked, convex upward thrust-bound blocks of the silts and sands of unit D (Fig. 8A). Measurement of the lowermost block shows that it dips towards the north (Fig. 8A). Internally unit D exhibits deformation structures indicative of shearing, apparently from a northerly direction (e.g. folds and augen structures; Fig. 8B).

The lowermost thrust block rests on the subhorizontally bedded sands and gravels of unit B. The level of internal deformation within unit B changes laterally. Between 2450 and 2550 m (Fig. 8A), unit B is heavily folded and the boundary between units B and D is diffused. A number of fractures and minor faults, with a displacement usually in the order of millimetres or centimetres, cross-cut the silts and sands (unit D), and the sands and gravels of unit B (Fig. 8A, B). The deformation gradually becomes less penetrative southward and at the southernmost part of the section most of the sands and gravels of unit B show little or no evidence of deformation. However, in this area the boundaries between units B and D are defined by a thin and highly distorted zone (~50 cm) of layered clay, silt and gravels (Fig. 8C). This zone is locally offset by both small- and large-scale faults and fractures (Fig. 8A, D), including a set of steeply inclined, southwest-dipping open fractures consistent with water-escape structures/hydrofractures formed by the escape of pressurized water under or in

front of ice margins (Rijsdijk *et al.* 1999; Kjær *et al.* 2006; Benediktsson *et al.* 2008; van der Meer *et al.* 2009). These hydrofractures extend upward into unit D. They are up to a few metres long and their widths are in the order of centimetres and are infilled by massive and sorted sediments, mainly sand and fine gravel (Fig. 8D). The sediment infillings of some of these fractures exhibit various sedimentary structures typical of fluid transport, such as planar parallel-bedding and cross-bedding.

The stratified sand and gravel (unit B) continues at the other side of the Ásgil gully. It is unconformably overlain by a coarse gravel and together they form an up to 15-m-high and 200-m-long multi-crested pile of well-bedded, sorted sand, gravel and boulder gravel of unit B (Figs 2, 3C). The inclined bedding (foresets) within the unit is consistent with an apparent palaeoflow direction towards the southeast. Primary sedimentary structures such as planar- and trough-cross beddings are intact and there are no clear signs of glaciotectonic deformation.

Ásgil south – structural evolution. – The structural architecture of the southern part of the Ásgil section, which comprises northward-dipping thrust stacks, is consistent with its formation in response to thrusting and compressional deformation (Fig. 9; i.e. Bennett 2001; Benediktsson *et al.* 2008, 2015; Pedersen 2014; Phillips *et al.* 2017). Based on this, the Ásgil zone is interpreted as an ice-marginal/proglacial moraine deposited by a glacier advancing from the north (Boulton *et al.* 1999; Bennett 2001). This was accompanied by release of glacial meltwater and the deposition of the ice-marginal sands and gravels of unit B both before and after the termination of the glacial advance.

The highly deformed boundary between units B and D (Fig. 8A; ~2450–2600 m) provides evidence for displacement of the lowermost block along this interface indicating that the thrust blocks of unit D partially overrode the ice-marginal sediments of unit B. This would have caused elevated pore-water pressures in the ice-marginal sands and gravels in response to the thickening of the thrust stack causing liquefaction, hydrofracturing and injection of sand and gravel into the base of the lowermost thrust block (Rijsdijk *et al.* 1999; Kjær *et al.* 2006; Benediktsson *et al.* 2008; van der Meer *et al.* 2009). The localized faulting of the sediments further indicates that some minor deformation continued after the sediments had been drained.

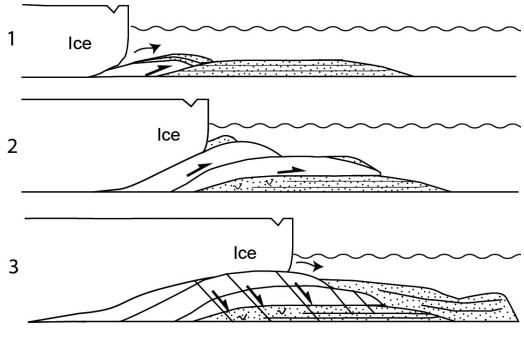

Fig. 9. A sequential model explaining the formation of the southern part of the Ásgil structural zone.

The large accumulation of coarse sand and gravels of unit B at the southern (distal) end of the zone show very little signs of deformation. These sands and gravels are interpreted as a subaquatic fan and were most likely formed as the ice margin stood still after the cessation of the advance (Fig. 9). As the fan is undeformed it shows that the area did not experience further glacial pushing or overriding after the moraine was formed.

Ás

The Ás structural zone is located in the Melabakkar-Á sbakkar cliffs between ~3400 and 5000 m (Fig. 2), which makes it the largest of the structural zones in the entire cliff section and the only one that has a clear morphological expression. A detailed analysis was carried out in two separate parts of the Ás structural zone; the northern part at 3500–3700 m (Fig. 2) and the southern part at 4500–5000 m (Fig. 2). These parts are called Ás-north and Ás-south, respectively. The cliff face between these two parts (at 3800–4500 m; Fig. 2) was largely obscured due to surface wash and debris cover. However, large-scale folds and northward-dipping thrusts could be identified through the surface wash, clearly showing that this part of the cliff is also deformed.

Ás-north – structural architecture. – The cliff face at Ás-north is subvertical and is orientated NW–SE (326–146°). The northern part of the section is ~23 m high, mostly clean and well exposed, allowing a detailed examination, whereas the lowermost ~10 m of the southern part (3575–3680 m; Fig. 10A) is covered in surface wash and debris.

The stratigraphy at Ásgil can be divided into three main structural units: (i) the deformed zone comprising the silty-sandy diamicton of unit A and the stratified sands and gravels of unit B; (ii) laminated sand and silt of unit C overlain by the bedded sand and diamicton of unit G; and (iii) the uppermost Holocene sequence of littoral gravel with erosional lower contacts (unit H).

The most prominent structure is an asymmetrical ridge-like feature at around 3550 m (Fig. 10A, B). This feature comprises a series of folded and thrusted sediments including a large-scale (amplitude at least 30 m and wavelength ~15 m), southwest-verging, overturned, tight anticlinal fold affecting the silty-sandy diamicton of unit A and stratified sand and gravel of unit B. This fold overlies a smaller, overturned anticline consisting entirely of unit A. The ridge is deformed by a large number of faults that cut through the sediments on both sides of this

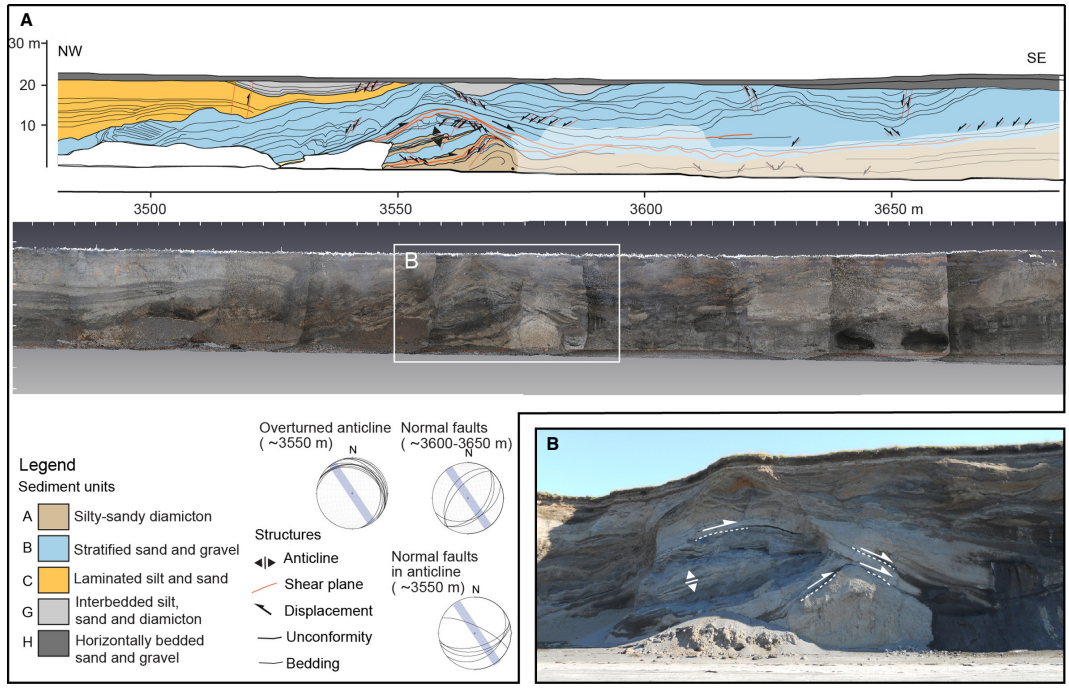

Fig. 10. A. A scale diagram and a LiDAR image of the Ás-north section. Directional data are plotted on a lower hemisphere stereographic projection and the blue bars indicate the orientation of the section. The white box indicates the location of the photograph in B. B. A large overturned, southwestward-verging and deformed anticlinal fold affecting units A and B. It is truncated by a number of shear planes with an apparent sense of displacement towards the south and dissected by a number of both extensional and compressional faults. [Colour figure can be viewed at www.boreas.dk]

feature. These faults are generally curved with a displacement ranging from a few cm to several dm. Most of the faults cutting through the lower limb of the large anticline are normal faults dipping either to the southeast or the northeast whereas both reverse and normal faults are prominent in the upper parts.

The convex upper surface of the ridge is capped by an up to 20-m-thick unit of diamictons and stratified sand and gravel of unit B. Internally these gravel and sand beds are undulating and often folded and boudinaged (e.g. at around 3600 m). These beds and the diamicton of unit A can be followed to about 3800 m in the cliff where they have an apparent northward dip with slightly convex upward configuration (Fig. 2). These beds are internally deformed by a number of small faults, mainly normal faults. A number of measurements on fault planes in the lowermost unit (unit A) showed that the faults dip both to the northwest or the southeast (Fig. 10A). An approximately 0.5-m-thick layer of deformed (ductile) sediment mélange of folded and layered silt, sand and gravel, which appears to originate mostly from unit B, separates the stratified sand and gravel from the undeformed laminated silt and sand of unit G above.

Ás-north – structural evolution. – The Ás-north zone is, similar to the Belgsholt, Melaleiti and Ásgil zones, mainly characterized by compressive deformation as a result of pressure from a glacier advancing from the north (northeast–northwest) based on the southwest-verging anticlinal folds and the overall northward dip of the thrusted sediment blocks (Fig. 11; e.g. Bennett 2001; Benediktsson *et al.* 2008; Pedersen 2014). The large anticline can be interpreted as recording ductile folding as the ice pushed into the sequence (Fig. 11). Continued ice-push stacked up the sediments above it and in front (south) of this fold, and led to the overturning of this anticline. Thrust faults developed in the upper limb and extensional faults in the lower limb of the anticline formed in response to the overturning and subsequent extension of the fold (Fig. 11).

Comparably to Ásgil, the advance was accompanied an ice-marginal deposition of sands and gravels of unit B, which were subsequently deformed (faulted and boudinaged) possibly in response to continued ice-sheet advance. Together with the overturning of the fold this indicates that the moraine underwent subglacial modification (Fig. 11; Aber *et al.* 1989; Pedersen 2000; van der Wateren *et al.*

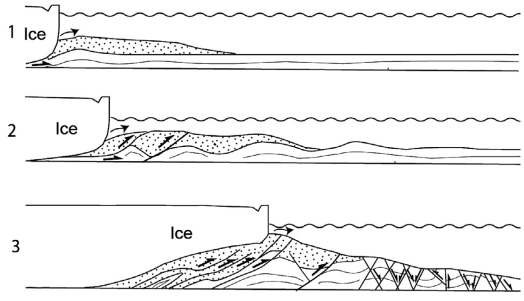

Fig. 11. A sequential model showing the formation of the Ás structural zone (north and south).

2000; McCarroll & Rijsdijk 2003). However, some of the small normal faults within the gravel (unit B) might have formed by gravity collapse. The sediment mélange capping unit B can be interpreted as a glaciotectonite formed by subglacial shearing of the pre-existing sediments (Evans *et al.* 2006; Benn & Evans 2010; Ó Cofaigh *et al.* 2011). Alternatively, the mélange can be interpreted as a gravity flow deposited as the ice retreated from the moraine.

Ás-south – structural architecture. – Ás-south is the southernmost part of the Ás structural zone (4500–5000 m; Figs 2, 12). The section wall is 12–20 m high, steeply inclined and orientated NW–SE. Most of the section was visible and easily accessible, which enabled detailed mapping and measurements of sediments and structures.

Ás-south can be divided into three main structural units: (i) the folded and faulted zone comprising the stratified sand and gravel of unit B and stratified silty-sandy diamicton of unit A overlain by deformed silts and sands of unit D; (ii) the silts and sands of unit G with erosive lower contacts that overlies the northern end of unit 1; and (iii) the uppermost Holocene sequence of littoral gravels (unit H).

This section comprises a folded and thrusted sequence composed of units A and B that is cross-cut by open fractures and numerous faults with sharp fault planes. The folds usually become smaller in amplitude towards the south. Between ~4800 and 4950 m (Fig. 12A) units A and B are overlain by indistinctively bedded, silts and sands of unit D, which exhibit ductile deformation structures such as boudins and augen structures. The faults found in the lower units (A and B) usually do not extend upwards into unit D indicating that the faulting pre-dates the deposition of unit D.

Most of the faults form a conjugate set of southeast-northwest dipping normal faults. The displacement along the planes is commonly in the range of a few cm to a few dm although some have an offset of over a metre. This fault pattern is most conspicuous between 4500–4650 m (Fig. 12A) where the faults cross-cut a large, anticlinal open fold with an approximately northeast-southwest trending fold axis (Fig. 12A, B), and also in the southernmost part of the cliff between 4800–5000 m (Fig. 12A, C).

In the middle part of the section (4650–4850 m; Fig. 12A), the sequence exhibits a more complex deformation history. Units A and B are folded, thrust repeated and dissected by a number of normal (extensional) and reverse (compressional) faults. These faults cut the sequence at various angles: the normal faults mostly dip to the northwest or the southeast but thrust faults mainly have a southward dip (Fig. 12A). The fault offsets range from several cm to a few m. A few open fractures infilled by diamicton cut through units A and B in this part of the section. The complicated nature of the deformation in this area made it very hard to trace laterally the individual structural units especially

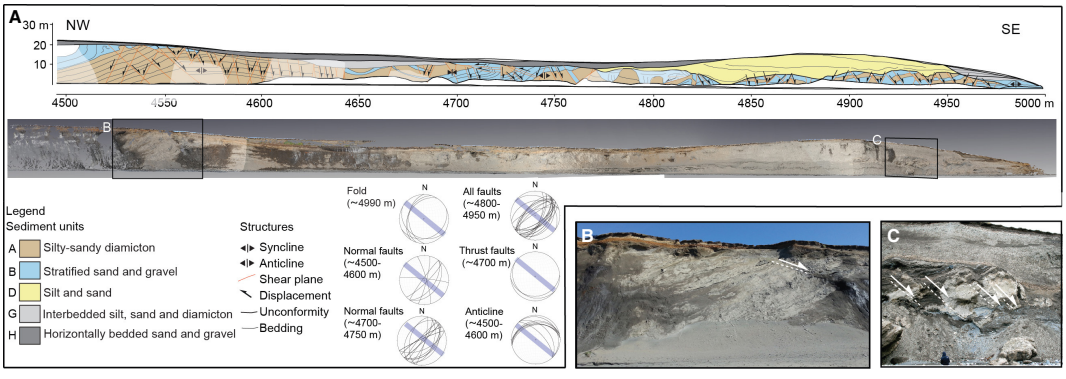

Fig. 12. A. A scale diagram and a LiDAR image of the Ás-south section. Directional data are plotted on lower hemisphere stereographic projections and the blue bars indicate the orientation of the section. The black boxes indicate the locations of the photographs in B and C. B. The northern limb of an open anticlinal fold affecting the stratified diamicton of unit A. The fold is dissected by numerous normal faults. C. Faulted sediments of units A and B overlain by sheared and deformed diamicton of unit D. [Colour figure can be viewed at www.boreas.dk]

between 4750 and 4800 m (Fig. 12A) where the deformation was most intense.

Ás-south – structural evolution. – The large folds indicate that the sequence experienced shortening due to subhorizontal compression consistent with deformation in an ice-marginal or proglacial setting (e.g. Boulton *et al.* 1999; Benediktsson *et al.* 2010). The orientations of the large anticline between 4500–4650 m and the small syncline at around 4980 m (Fig. 12A) could indicate glaciotectonic stress from either the northwest or southeast. The same applies to the system of the conjugate normal faults. The sense of offset along the thrust faults in the central part of the section (~4700–4750 m; Fig. 12A) that cross-cut units A and B indicates that these units were affected by a northwestwards-directed stress. This is in contrast with all other evidence from the cliffs indicating ice flow from the north. However, these thrust faults are small, they are only seen in a restricted part of the section and the cliff section probably only reveals part of the glaciotectonic zone due to the erosive base of units G and H; hence, they could simply be backthrusts formed in response to localized stress (Boulton *et al.* 1999; Benediktsson *et al.* 2010). Many of the faults and fractures that cross-cut the folds are open and infilled by typically massive, coarse sediment indicating extension and subsequent infilling of these fractures. The geometry of the conjugate fault system implies that it was formed by ice-push in association with the folding (Fig. 12A).

There is no unequivocal structural or sedimentological evidence that can tell if the deformation of the sequence was induced by stress from the northwest or southeast. However, as this zone appears to be linked to the tectonic zone at Ás-north (see Fig. 2), pressure from the northwest seems most plausible. In addition, the decreasing amplitude of the folds towards the southeast suggests a decreasing stress in that direction and corresponds to multi-crested end-moraine complexes described from modern (e.g. Boulton *et al.* 1999; Benediktsson *et al.* 2010) and Late Weichselian (Phillips *et al.* 2017) glacier environments. This zone is therefore interpreted to represent proglacial folding and faulting of the sediment package in front (south) of the Ás-north thrust zone (Fig. 11).

Discussion

The overall configuration and the internal architecture of the structural zones in the coastal cliffs in Melasveit indicate a series of subaquatic moraines formed during the interplay between glaciotectonic deformation and ice-marginal sedimentation. After the glacier retreated from the area these moraines were covered by glaciomarine, marine and littoral sediments; consequently, the ridges have no or very little topographical expression on the modern land surface. Below we propose a model for the formation of the structural zones/moraines seen in the coastal cliffs in Melasveit and discuss their implications for the regional ice dynamics and glaciotectonic processes below marine-terminating glaciers (Figs 13, 14).

Direction of ice flow

Directional elements measured in this study, such as large-scale faults, thrusts, fold axes and fold vergence indicate that the glaciotectonic stress was applied from the northwest and north/northeast. Thus, the glacier responsible for the glaciotectonics most likely advanced from Borgarfjörður, which agrees with previous research on the glacial geology and glacial history of this area (Fig. 1A; e.g. Ingólfsson 1987, 1988; Hart 1994; Ingólfsson & Norðdahl 2001; Norðdahl & Pétursson 2005; Norðdahl *et al.* 2008; Ingólfsson *et al.* 2010; Norðdahl & Ingólfsson 2015). Based on the predominant southeastward sense of shearing the lobate-shaped glacier might have flowed locally from the fjord (Fig. 14).

Hart (1994) and Hart & Roberts (1994) proposed that the deformation in the southernmost part of Melabakkar-Ásbakkar (~4400–5000 m; Fig. 2) was caused by a glacier moving from the south. Although our study revealed a few southward-dipping thrust faults at Ás-south (Fig. 12A; ~4700–4750 m), which could support that hypothesis, these were only found at one location and are small scale compared to the overall deformation observed in the Melabakkar-Ásbakkar cliffs. Also, Ás-south is structurally connected to Ás-north where the glaciotectonic stress direction is most definitely from the north/northwest. Therefore, we suggest that the entire deformation was induced by a glacier flowing southwards from Borgarfjörður.

The formation of the Belgsholt and Melabakkar-Ásbakkar structural zones – a sequential model

The internal architecture of the structural zones/moraines is dominated by thrusting and stacking of detached thrust blocks with varying degrees of folding, ductile shearing and brittle faulting (extensional and compressional). Thus, each zone/moraine was formed in the compressional regime of the glacier in an ice-marginal and/or proglacial position and are thus interpreted as moraines formed during advances or stillstands during an overall stepwise northward retreat (e.g. Bennett *et al.* 1999; Boulton *et al.* 1999; Bennett 2001; Phillips *et al.* 2002, 2008, 2017; Benediktsson *et al.* 2010; Benn & Evans 2010; Johnson *et al.* 2013). The moraines are thought to reflect periods where the glacier was grounded transmitting shear stress into the sediments. Between the moraines are zones with no or negligible evidence of glaciotectonic deformation possibly reflecting periods of retreat and lifting of the glacier from the seabed.

The southernmost and largest moraine at Melabakkar-Ásbakkar, the Ás moraine (Ás-north and Ás-south

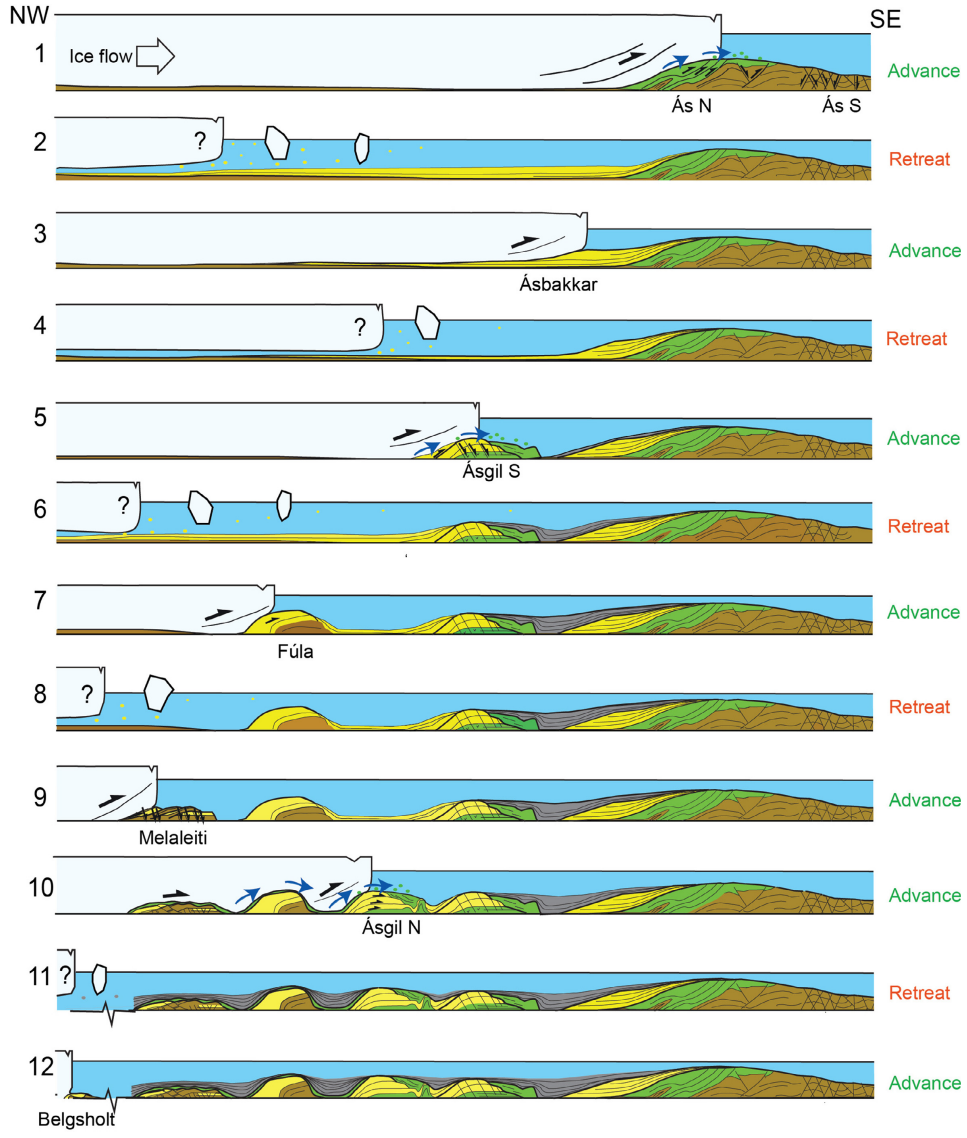

Fig. 13. A conceptual sequential model demonstrating the formation of the glaciotectonic moraines exposed in the coastal cliffs of Belgsholt and Melabakkar-Ásbakkar. The sequence of events is described in the Discussion section. Black arrows indicate displacement and blue arrows indicate water flow. Brown: pre-existing fossiliferous silty-sandy glaciomarine diamicton (unit A), green: ice-marginal/subglacial fluvial sediments (units B and F), yellow: deformed laminated/bedded glaciomarine sediments (units C, D and E) and grey: undeformed, bedded glaciomarine sediments (unit G). [Colour figure can be viewed at www.boreas.dk]

combined) is thought to represent the maximum extent of the glacier. The location of the Ás thrust moraine, the southeast-directed sense of ice-push derived from the glaciotectonic structures, and its subtle morphological expression suggest that this moraine system represents a lateral extension of the Skorholtsmelar end-moraine complex further inland (see Fig. 1B), as suggested by Ingólfsson (1988). However, the lack of exposures and obvious morphological expressions of the moraine in the area between the coast and the Skorholtsmelar moraine means that this correlation remains tentative. A sequential glaciotectonic model is proposed for the formation of the moraines/structural zones at Melabakkar-Ásbakkar and Belgsholt associated with the active retreat of a

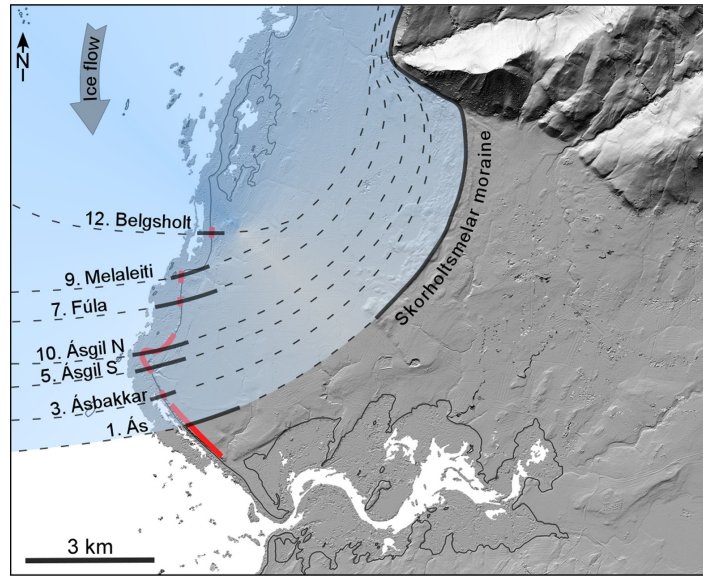

Fig. 14. A hillshade map of the study area showing the location of the moraines exposed in the coastal cliffs (red lines) and the configuration of the moraines based on structural data from this study (black solid lines). Note that the configuration of the youngest moraine at Belgsholt was formed by glaciotectonic stress from the north while the stress forming all the older moraines was, at least locally, applied from the northwest. Black dashed lines are an approximation of the configuration of the ice margin during each advance, partly based on the correlation between the Skorholtsmelar moraine and the Ás structural zone. The numbers refer to the relative timing of advances (see Fig. 13). [Colour figure can be viewed at www.boreas.dk]

glacier back to Borgarfjörður (Figs 13, 14). The model is described in 12 stages below.

1. The first stage commenced with the advance of the glacier out of Borgarfjörður into the bay (Fig. 1A). Once out of the fjord, the ice spread laterally, extending southward to its proposed maximum limit in the Ás area where it deformed marine sediments of Bølling age (unit A; Ingólfsson 1988; Ingólfsson *et al.* 2010) to form a prominent, multi-crested thrust moraine (~3500–5000 m; Fig 2). The penecontemporaneous deposition of the ice-marginal sediments of unit B occurred during this advance with the earlier deposited parts of this sequence also being deformed as the glacier continued to advance. The structural architecture of the ice-proximal part of the moraine (Ás-north) is dominated by thrust stacks and overturned folds whereas the ice-distal part of the moraine (Ás-south) comprises open folding of the marine and ice-marginal sediments (units A and B), which are also cross-cut by both extensional and compressional faults. These folds observed at Ás-south are thought to have formed at, or some distance in front (proglacial) of, the advancing ice margin as a result of the propagation of stress into the forefield.
2. The glacier retreated northwards to an unknown position north of Ás and the laminated silts and sands of unit C were deposited.
3. The glacier re-advanced resulting in erosion and deformation of the uppermost part of unit C (seen in Ásbakkar between ~3100–3300 m; Fig. 2). There is no constructional landform visible in the cliff section at this place but only an erosive contact with mainly ductile deformation below. Therefore this remains uncertain.
4. The glacier retreated and the silts and sands of unit D were deposited.
5. The stage 4 retreat was followed by another re-advance causing a thrust stacking at the ice margin and the formation of a moraine at Ásgil-south (~2600 m; Figs 2, 8A). This advance was accompanied by a deposition of the ice-marginal outwash sediments of unit B at Ásgil (Fig. 8A, B) that were subsequently deformed by the ice-push. The subaqueous fan was deposited at the ice margin when the glacier had reached a stillstand position (between 2600–2800 m; Figs 2, 3C). This fan is undeformed indicating that it was not overridden after it had been deposited. The depression between the ice margin (at Ásgil-south) and the deformation zone at Ásbakkar was gradually infilled by the bedded sediments of unit G.

6. The glacier retreated further north and the silts and sands of unit D found north of Ásgil were deposited.
7. Re-advances or oscillations of the ice margin resulted in ice-marginal thrusting and folding of units A, B and D, and the development of the recessional thrust moraines at Fúla around 600–900 m and possibly other smaller ridges in Fúla Bay.
8. The glacier retreated to the north of the Melabakkar-Ásbakkar coastal cliffs and deposited the interbedded silts and sands of unit E exposed at Melaleiti.
9. The glacier re-advanced causing the thrust stacking and brittle faulting of sediment units A and E observed at Melaleiti at around 0–300 m (Fig. 2).
10. The glacier advanced to a position somewhere around 2000 m, overriding the thrust-block moraine at Melaleiti and the recessional thrust moraines at Fúla Bay (0–2000 m; Fig. 2). This resulted in a subglacial deformation, erosion and deposition of subglacial gravels and boulders of unit F on-lapping the thrust-block moraine at Melaleiti and the moraines at Fúla Bay. A moraine composed of imbricated thrust-stacked blocks and a subaquatic fan of unit B (between 1500–2000 m; Fig. 2) was formed at the ice margin at Ásgil-north. The folds seen at Ásgil-north (~2250–2400 m; Fig. 2) most likely represent proglacial folding of the distal (southern) side of the moraine fan. Alternatively, these folds could have been formed due to slumping on the unstable slopes of the moraines at Ásgil or Fúla.
11. The glacier retreated and the depressions between the moraines were rapidly infilled by the upward fining sequence of the bedded marine sediments of unit G (Fig. 2). The lithofacies of unit G are undeformed and overlap the recessional moraines in Fúla Bay and the thrust-block moraine at Melaleiti with little or no discernible lateral variation in grain size. This indicates concurrent sediment deposition and rapid glacier retreat from Ásgil-north without the formation of ice-marginal fans or deformation of the bedded glaciomarine sedimentary infill between the ridges. The glacier retreated to some place north of the study area and the upward fining sequence of unit E exposed at Belgsholt was deposited.
12. This stage occurred following a further phase of retreat and is characterized by the ice-marginal to proglacial folding and thrusting observed at Belgsholt, which is the northernmost and youngest structural zone/-moraine exposed in the coastal cliffs of Melasveit.

Timing of the glacier advances

The exact age of the glacial advances in Melasveit is unknown. Ten radiocarbon dates have been published from the deformed sediments (units A and D) within the Melaleiti, Ásgil and Ás structural zones ranging between *c*. 13.4 and 14.6 cal. ka BP (Ingólfsson 1987, 1988; Ingólfsson *et al.* 2010; Norðdahl & Ingólfsson 2015). These dates only record the maximum ages of deformation events. Due to the lack of *in situ* fossils within the undeformed sediments separating the ridges it has not been possible to determine the minimum age for these events. Ingólfsson (1988) suggested two separate advances based on radiocarbon dates and the stratigraphy of the cliff sections; the first occurring in the late Bølling or Allerød (just after *c*. 14.0 cal. ka BP) and the second during the Younger Dryas. However, our model involves a highly dynamic glacier that advanced and retreated multiple times, possibly during a single overall phase of retreat. Our data also indicate that the glaciomarine sediments rapidly accumulated in front of the oscillating glacier continuously providing material for the construction of new moraines. Although it is hard to estimate how rapid this deposition was, studies have shown that deposition rates of ice-proximal sediments similar to the bedded glaciomarine sediments within and between the Melasveit ridges can be in the order of decimetres or even metres per year (Eyles *et al.* 1985; Cowan *et al.* 1999; Jaeger & Nittrouer 1999; Gilbert *et al.* 2002; Trusel *et al.* 2010).

Based on our model and the age of the sediments in the Melabakkar-Ásbakkar cliffs (Ingólfsson 1988; Ingólfsson *et al.* 2010), the formation of all of the moraines may have occurred after *c*. 13.4 cal. ka BP, or most likely during the Younger Dryas chronozone (*c*. 12.8–11.7 cal. ka BP). During that time, glaciers in Iceland are known to have expanded considerably and the regional relative sea level was high enough to allow the deposition of the up to 30-m-thick marine sediments between and stratigraphically on top of the deformed moraine ridges (Norðdahl *et al.* 2008; Ingólfsson *et al.* 2010).

Conclusions

We have constructed a model of an active retreat of a Late Weichselian, marine-terminating glacier based on detailed mapping of the stratigraphy and glaciotectonics exposed in the coastal cliffs of Belgsholt and Melabakkar-Ásbakkar in Melasveit, lower Borgarfjörður.

- The glaciotectonics reveal a series of well-preserved moraines formed by a marine-terminating glacier advancing from the Borgarfjörður fjord, north of the study area.
- Each moraine marks a former ice-marginal position. Their internal structures are dominated by large-scale thrusting and stacking of detached blocks of marine sediments with varying degrees of folding, ductile shearing and brittle faulting. This deformation was accompanied by the deposition of ice-marginal subaquatic fans that were largely deformed by continued ice-push and integrated into the glaciotectonics.

- The southernmost and largest structural zone exposed in the Melabakkar-Ásbakkar coastal cliffs is a multi-crested terminal moraine indicating the maximum extent of the Borgarfjörður glacier. The other moraines in the series generally become younger towards the north representing oscillatory advances during an overall northward retreat.
- During this active retreat, glaciomarine sediments were continuously deposited in front of the glacier as source material for new moraines. As the glacier receded, the depressions between the ridges were rapidly infilled by glaciomarine sediments and later, after the isostatic rebound of the area, covered by littoral and aeolian sediments.
- Although the exact age of the glacial advances in Melasveit is unknown, previously obtained radiocarbon ages of marine shells within the deformed marine sediments suggest that these advances most likely occurred during the Younger Dryas chronozone.
- This case study exemplifies glaciotectonic and depositional processes occurring in ice-marginal/proglacial marine environments. It highlights the dynamic nature of marine-terminating glaciers and may aid in the understanding and interpretation of their sedimentological and geomorphological records.

Acknowledgements. – This project was funded by the Icelandic Research Fund (grant no. 141002-051 to Í.Ö. Benediktsson) and the Royal Physiographic Society in Lund (grants to Th. Sigfúsdóttir and Í.Ö. Benediktsson), with support from the British Geological Survey (to E. Phillips, M. Kirkham, E. Haslam). The LiDAR scanning and photographing of the Melabakkar-Ásbakkar coastal cliffs by Matthew Kirkham and Ed Haslam is gratefully acknowledged. We would like to thank Sandrine Roy, Heimir Ingimarsson and Kim Teilmann for their invaluable assistance and discussions in the field, and Ólafur Ingólfsson and Hreggviður Norðdahl for fruitful discussions on the glacial history of the area. Furthermore, we also thank Per Möller for his useful comments on the manuscript and James Aber and Matthew Bennett for constructive reviews that helped us improve this paper. E. Phillips publishes with the permission of the Executive Director of the British Geological Survey, NERC.

References

Aber, J. S. & Ber, A. 2007: *Glaciotectonism*. 256 pp. *Developments in Quaternary Science 6*. Elsevier, Amsterdam.

Aber, J. S., Croot, D. G. & Fenton, M. M. 1989: *Glaciotectonic Landforms and Structures*. 200 pp. *Glaciology and Quaternary Geology Series*. Kluwer Academic Publishers, Dordrecht.

Allmendinger, R. W., Cardozo, N. C. & Fisher, D. M. 2012: *Structural Geology Algorithms: Vectors and Tensors*. 302 pp. Cambridge University Press, Cambridge.

Benediktsson, Í. Ö., Möller, P., Ingólfsson, Ó., van der Meer, J. J. M., Kjær, K. H. & Krüger, K. 2008: Instantaneous end moraine and sediment wedge formation during the 1890 surge of Brúarjökull, Iceland. *Quaternary Science Reviews 27*, 209–234.

Benediktsson, Í. Ö., Schomacker, A., Johnson, M. D., Geiger, A. J., Ingólfsson, Ó. & Guðmundsdóttir, E. R. 2015: Architecture and structural evolution of an early Little Ice Age terminal moraine at the surge-type glacier Múlajökull, Iceland. *Journal of Geophysical Research 120*, 1895–1910.

Benediktsson, Í. Ö., Schomacker, A., Lokrantz, H. & Ingólfsson, Ó. 2010: The 1890 surge end moraine at Eyjabakkajökull, Iceland: a re-assessment of a classic glaciotectonic locality. *Quaternary Science Reviews 29*, 484–506.

Benn, D. I. & Evans, D. J. A. 2010: *Glaciers and Glaciation*. 802 pp. Hodder Education, London.

Bennett, M. R. 2001: The morphology, structural evolution and significance of push moraines. *Earth-Science Reviews 53*, 197–236.

Bennett, M. R., Hambrey, M. J., Huddart, D., Glasser, N. F. & Crawford, K. 1999: The landform and sediment assemblage produced by a tidewater glacier surge in Kongsfjorden, Svalbard. *Quaternary Science Reviews 18*, 1213–1246.

Bennett, M. R., Huddart, D., Waller, R. I., Cassidy, N., Tomio, A., Zukowskyj, P., Midgley, N. G., Cook, S. J., Gonzalez, S. & Glasser, N. F. 2004: Sedimentary and tectonic architecture of a large push moraine: a case study from Hagafellsjökull - Eystri, Iceland. *Sedimentary Geology 172*, 269–292.

Boggs, S. 2006: *Principles of Sedimentology and Stratigraphy*. 662 pp. Pearson Prentice Hall, Upper Saddle River.

Boulton, G. S., van der Meer, J. J. M., Beets, D. J., Hart, J. K. & Ruegg, G. H. J. 1999: The sedimentary and structural evolution of a recent push moraine complex: Holmstrømbreen, Spitsbergen. *Quaternary Science Reviews 18*, 339–371.

Boulton, G. S., van der Meer, J. J. M., Hart, J., Beets, D., Ruegg, G. H. J., van der Wateren, F. M. & Jarvis, J. 1996: Till and moraine emplacement in a deforming bed surge - an example from a marine environment. *Quaternary Science Reviews 15*, 961–987.

Cardozo, N. & Allmendinger, R. W. 2013: Spherical projections with OSXStereonet. *Computers and Geosciences 51*, 193–205.

Clark, P. U., Dyke, A. S., Shakun, J. D., Carlson, A. E., Wohlfarth, B., Mitrovica, J. X., Hostetler, S. W. & McCabe, A. M. 2009: The last glacial maximum. *Science 325*, 710–714.

Cowan, E. A., Seramur, K. C., Cai, J. & Powell, R. D. 1999: Cyclic sedimentation produced by fluctuations in meltwater discharge, tides and marine productivity in an Alaskan fjord. *Sedimentology 46*, 1109–1126.

Croot, D. G. 1987: Glacio-tectonic structures: a mesoscale model of thin-skinned thrust sheets? *Journal of Structural Geology 9*, 797–808.

Dowdeswell, J. A. & Vásquez, M. 2013: Submarine landforms in the fjords of southern Chile: implications for glacimarine processes and sedimentation in a mild glacier-influenced environment. *Quaternary Science Reviews 64*, 1–19.

Dyke, A. S., Andrews, J. T., Clark, P. U., England, J. H., Miller, G. H., Shaw, J. & Veillette, J. J. 2002: The Laurentide and Innuitian ice sheets during the Last Glacial Maximum. *Quaternary Science Reviews 21*, 9–31.

Evans, D. J. A. & Benn, D. I. 2004: *A Practical Guide to the Study of Glacial Sediments*. 266 pp. Arnold, London.

Evans, D. J. A., Phillips, E. R., Hiemstra, J. F. & Auton, C. A. 2006: Subglacial till: formation, sedimentary characteristics and classification. *Earth-Science Reviews 78*, 115–176.

Eyles, C. H., Eyles, N. & Miall, A. D. 1985: Models of glaciomarine sedimentation and their application to the interpretation of ancient glacial sequences. *Palaeogeography, Palaeoclimatology, Palaeoecology*, *51*, 15–84.

Flink, A. E., Noormets, R., Kirchner, N., Benn, D. I., Luckman, A. & Lovell, H. 2015: The evolution of a submarine landform record following recent and multiple surges of Tunabreen glacier, Svalbard. *Quaternary Science Reviews 108*, 37–50.

Franzson, H. 1978: *Structures and petrochemistry of the Hafnarfjall-Skarðsheiði central volcano and the surrounding basalt succession, W-Iceland*. Ph.D. thesis, University of Edinburgh, 264 pp.

Gilbert, R., Nielsen, N., Möller, H., Desloges, J. R. & Rasch, M. 2002: Glacimarine sedimentation in Kangerdluk (Disko Fjord), West Greenland, in response to a surging glacier. *Marine Geology 191*, 1–18.

Håkansson, S. 1983: A reservoir age for the coastal waters of Iceland. *Geologiska Föreningens i Stockholm Förhandlingar 105*, 65–68.

Harris, C., Williams, G., Brabham, P., Eaton, G. & McCarroll, D. 1997: Glaciotectonized Quaternary sediments at Dinas Dinlle, Gwynedd, North Wales, and their bearing on the style of deglaciation in the Eastern Irish Sea. *Quaternary Science Reviews 16*, 109–127.

Hart, J. K. 1994: Proglacial glaciotectonic deformation at Melabakkar-Asbakkar, west Iceland. *Boreas 23*, 112–121.
Hart, J. K. & Roberts, D. H. 1994: Criteria to distinguish between subglacial glaciotectonic and glaciomarine sedimentation, I. Deformation styles and sedimentology. *Sedimentary Geology 91*, 191–213.
Hughes, A. L. C., Gyllencreutz, R., Lohne, Ø. S., Mangerud, J. & Svendsen, J. I. 2016: The last Eurasian ice sheets – a chronological database and time-slice reconstruction, DATED-1. *Boreas 45*, 1–45.
Ingólfsson, Ó. 1987: The Late Weichselian glacial geology of the Melabakkar- Ásbakkar coastal cliffs, Borgarfjörður, W-Iceland. *Jökull 37*, 57–81.
Ingólfsson, Ó. 1988: Glacial history of the lower Borgarfjörður area, western Iceland. *Geologiska Föreningens i Stockholm Förhandlingar 110*, 293–309.
Ingólfsson, Ó. & Norðdahl, H. 2001: High relative sea level during the Bølling interstadial in Western Iceland: a reflection of ice-sheet collapse and extremely rapid glacial unloading. *Arctic, Antarctic, and Alpine Research 33*, 231–243.
Ingólfsson, Ó., Norðdahl, H. & Schomacker, A. 2010: Deglaciation and Holocene glacial history of Iceland. *Developments in Quaternary Sciences 13*, 51–68.
Jaeger, J. M. & Nittrouer, C. A. 1999: Marine record of surge-induced outburst floods from the Bering Glacier, Alaska. *Geology 27*, 847–850.
Jennings, A., Syvitski, J., Gerson, L., Grönvold, K., Geirsdóttir, Á., Harðardóttir, J., Andrews, J. & Hagen, S. 2000: Chronology and paleoenvironments during the late Weichselian deglaciation of the southwest Iceland shelf. *Boreas 29*, 163–183.
Johnson, M. D. & Ståhl, Y. 2010: Stratigraphy, sedimentology, age and palaeoenvironment of marine varved clay in the Middle Swedish end-moraine zone. *Boreas 39*, 199–214.
Johnson, M. D., Benediktsson, Í. Ö. & Björklund, L. 2013: The Ledsjö end moraine – a subaquatic push moraine composed of glaciomarine clay in central Sweden. *Proceedings of the Geologists Association 124*, 738–752.
Kjær, K. H., Larsen, E., van der Meer, J. J. M., Ingólfsson, Ó., Krüger, J., Benediktsson, Í. Ö., Knudsen, C. G. & Schomacker, A. 2006: Subglacial decoupling at the sediment/bedrock interface: a new mechanism for rapid flowing ice. *Quaternary Science Reviews 25*, 2704–2712.
Krüger, J. & Kjær, K. H. 1999: A data chart for field description and genetic interpretation of glacial diamicts and associated sediments - with examples from Greenland, Iceland, and Denmark. *Boreas 28*, 386–402.
Lee, J. R. & Phillips, E. 2013: Glacitectonics : a key approach to examining ice dynamics, substrate rheology and ice-bed coupling. *Proceedings of the Geologists' Association 124*, 731–737.
Lee, J. R., Phillips, E., Booth, S. J., Rose, J., Jordan, H. M., Pawley, S. M., Warren, M. & Lawley, R. S. 2013: A polyphase glacitectonic model for ice-marginal retreat and terminal moraine development: the Middle Pleistocene British Ice Sheet, northern Norfolk, UK. *Proceedings of the Geologists' Association 124*, 753–777.
Lønne, I. 1995: Sedimentary facies and depositional architecture of ice-contact glaciomarine systems. *Sedimentary Geology 98*, 13–43.
Lønne, I. & Nemec, W. 2011: The kinematics of ancient tidewater ice margins: criteria for recognition from grounding-line moraines. *Geological Society of London, Special Publications 354*, 57–75.
Lønne, I., Nemec, W., Blikra, L. H. & Lauritsen, T. 2001: Sedimentary architecture and dynamic stratigraphy of a marine ice-contact system. *Journal of Sedimentary Research 71*, 922–943.
Magnúsdóttir, M. & Norðdahl, H. 2000: Aldur hvalbeins og fornra fjörumarka í Akrafjalli (English summary: re-examination of the deglaciation history of the area around Akrafjall in South-western Iceland). *Náttúrufræðingurinn 69*, 177–188.
Maizels, J. 1997: Jökulhlaup deposits in proglacial areas. *Quaternary Science Reviews 16*, 793–819.
Marren, P. M. 2005: Magnitude and frequency in proglacial rivers: a geomorphological and sedimentological perspective. *Earth-Science Reviews 70*, 203–251.
McCarroll, D. & Rijsdijk, K. F. 2003: Deformation styles as a key for interpreting glacial depositional environments. *Journal of Quaternary Science 18*, 473–489.
van der Meer, J. J. M., Kjær, K. H., Krüger, J., Rabassa, J. & Kilfeather, A. A. 2009: Under pressure: clastic dykes in glacial settings. *Quaternary Science Reviews 28*, 708–720.
Nichols, G. 2009: *Sedimentology and Stratigraphy*. 432 pp. Wiley-Blackwell, Oxford.
Norðdahl, H. & Ingólfsson, Ó. 2015: Collapse of the Icelandic ice sheet controlled by sea-level rise? *Arktos 1*, p. 13.
Norðdahl, H. & Pétursson, H. G. 2005: Relative sea-level changes in Iceland: new aspects of the Weichselian deglaciation of Iceland. *In* Caseldine, C., Russel, A., Harðardóttir, J. & Knudsen, Ó. (eds.): *Iceland-Modern Processes and Past Environments*, 25–78. *Developments in Quaternary Science 5*.
Norðdahl, H., Ingólfsson, Ó., Pétursson, H. G. & Hallsdóttir, M. 2008: Late Weichselian and Holocene environmental history of Iceland. *Jökull 58*, 343–364.
Ó Cofaigh, C. & Dowdeswell, J. A. 2001: Laminated sediments in glacimarine environments: diagnostic criteria for their interpretation. *Quaternary Science Reviews 20*, 1411–1436.
Ó Cofaigh, C., Dunlop, P. & Benetti, S. 2012: Marine geophysical evidence for Late Pleistocene ice sheet extent and recession off northwest Ireland. *Quaternary Science Reviews 44*, 147–159.
Ó Cofaigh, C., Evans, D. J. A. & Hiemstra, J. F. 2011: Formation of a stratified subglacial 'till' assemblage by ice-marginal thrusting and glacier overriding. *Boreas 40*, 1–14.
Ottesen, D. & Dowdeswell, J. A. 2006: Assemblages of submarine landforms produced by tidewater glaciers in Svalbard. *Journal of Geophysical Research 111*, F01016, https://doi.org/10.1029/2005jf000330.
Ottesen, D., Dowdeswell, J. A., Benn, D. I., Kristensen, L., Christiansen, H. H., Christensen, O., Hansen, L., Lebesbye, E., Forwick, M. & Vorren, T. O. 2008: Submarine landforms characteristic of glacier surges in two Spitsbergen fjords. *Quaternary Science Reviews 27*, 1583–1599.
Patton, H., Hubbard, A., Bradwell, T. & Schomacker, A. 2017: The configuration, sensitivity and rapid retreat of the Late-Weichselian Icelandic ice sheet. *Earth Science Reviews 166*, 223–245.
Pedersen, S. A. S. 2000: Superimposed deformation in glaciotectonics. *Bulletin of the Geological Society of Denmark 46*, 125–144.
Pedersen, S. A. S. 2005: Structural analysis of the Rubjerg Knude glaciotectonic complex, Vendsyssel, northern Denmark. *Geological Survey of Denmark and Greenland Bulletin 8*, 192 pp.
Pedersen, S. A. S. 2014: Architecture of glaciotectonic complexes. *Geosciences 4*, 269–296.
Phillips, E. 2017: Glacitectonics. *In* Menzies, J. & van der Meer, J. J. M. (eds.): *Past Glacial Environments*, 467–502. Elsevier, Amsterdam.
Phillips, E. & Hughes, L. 2014: Hydrofracturing in response to the development of an overpressurised subglacial meltwater system during drumlin formation: an example from Anglesey, NW Wales. *Proceedings of the Geologists' Association 125*, 296–311.
Phillips, E. & Merritt, J. 2008: Evidence for multiphase water-escape during rafting of shelly marine sediments at Clava, Inverness-shire, NE Scotland. *Quaternary Science Reviews 27*, 988–1011.
Phillips, E., Cotterill, C., Johnson, K., Crombie, K., James, L., Carr, S. & Ruiter, A. 2017: Large-scale glacitectonic deformation in response to active ice sheet retreat across Dogger Bank (southern central North Sea) during the Last Glacial Maximum. *Quaternary Science Reviews 179*, 24–47.
Phillips, E. R., Evans, D. J. A. & Auton, C. A. 2002: Polyphase deformation at an oscillating ice margin following the Loch Lomond Readvance, central Scotland, UK. *Sedimentary Geology 149*, 157–182.
Phillips, E., Lee, J. R. & Burke, H. 2008: Progressive proglacial to subglacial deformation and syntectonic sedimentation at the margins of the Mid-Pleistocene British Ice Sheet: evidence from north Norfolk, UK. *Quaternary Science Reviews 27*, 1848–1871.
Phillips, E., Lee, J. R. & Evans, H. M. 2011: *Glacitectonics - Field Guide*, 362 pp. Quaternary Research Association, Pontypool.
Powell, R. D. 2003: Subaquatic land systems: fjords. *In* Evans, D. J. A. (ed.): *Glacial Landsystems*, 313–347. Arnold, London.

Powell, R. D. & Domack, E. W. 1995: Modern glaciomarine environment. *In* Menzies, J. (ed.): *Modern Glacial Environments: Processes, Dynamics, and Sediments; Glacial Environments 1*, 445–486. Butterworth-Heinemann, Oxford.

Powell, R. D. & Molnia, B. F. 1989: Glacimarine sedimentary processes, facies and morphology of the south-southeast Alaska shelf and fjords. *Marine Geology 85*, 359–390.

Reimer, P. J., Bard, E., Bayliss, A., Beck, J. W., Blackwell, P. G., Bronk Ramsey, C., Buck, C. E., Cheng, H., Edwards, R. L., Friedrich, M., Grootes, P. M., Guilderson, T. P., Haflidason, H., Hajdas, I., Hatté, C., Heaton, T. J., Hoffmann, D. L., Hogg, A. G., Hughen, K. A., Kaiser, K. F., Kromer, B., Manning, S. W., Niu, M., Reimer, R. W., Richards, D. A., Scott, E. M., Southon, J. R., Staff, R. A., Turney, C. S. M. & van der Plicht, J. 2013: IntCal13 and Marine13 radiocarbon age calibration curves 0-50,000 years cal BP. *Radiocarbon 55*, 1869–1887.

Rijsdijk, K. F., Owen, G., Warren, W. P., McCarroll, D. & van der Meer, J. J. M. 1999: Clastic dykes in over-consolidated tills: evidence for subglacial hydrofracturing at Killiney Bay, eastern Ireland. *Sedimentary Geology 129*, 111–126.

Rijsdijk, K. F., Warren, W. P. & van der Meer, J. J. M. 2010: The glacial sequence at Killiney, SE Ireland: terrestrial deglaciation and polyphase glacitectonic deformation. *Quaternary Science Reviews 29*, 696–719.

Russell, A. J., Roberts, M. J., Fay, H., Marren, P. M., Cassidy, N. J., Tweed, F. S. & Harris, T. 2006: Icelandic jökulhlaup impacts: implications for ice-sheet hydrology, sediment transfer and geomorphology. *Geomorphology 75*, 33–64.

Rydningen, T. A., Vorren, T. O., Laberg, J. S. & Kolstad, V. 2013: The marine-based NW Fennoscandian ice sheet: glacial and deglacial dynamics as reconstructed from submarine landforms. *Quaternary Science Reviews 68*, 126–141.

Sættem, J. 1994: Glaciotectonic structures along the southern Barents shelf margin. *In* Warren, W. P. & Croot, D. G. (eds.): *Formation and Deformation of Glacial Deposits*, 95–113. A.A. Balkema, Rotterdam.

Seramur, K. C., Powell, R. D. & Carlson, P. R. 1997: Evaluation of conditions along the grounding line of temperate marine glaciers: an example from Muir Inlet, Glacier Bay, Alaska. *Marine Geology 140*, 307–327.

Símonarson, L. 1981: Upper Pleistocene and Holocene marine deposits and faunas on the north coast of Nugssuaq, West Greenland. *Grønlands Geologiske Undersøgelse 140*, 1–107.

Syvitski, J. P., Jennings, A. E. & Andrews, J. T. 1999: High-resolution seismic evidence for multiple glaciation across the southwest Iceland Shelf. *Arctic, Antarctic, and Alpine Research 31*, 50–57.

Thomas, G. S. P. & Chiverrell, R. C. 2007: Structural and depositional evidence for repeated ice-marginal oscillation along the eastern margin of the Late Devensian Irish Sea Ice Stream. *Quaternary Science Reviews 26*, 2375–2405.

Trusel, L. D., Powell, R. D., Cumpston, R. M. & Brigham-Grette, J. 2010: Modern glacimarine processes and potential future behaviour of Kronebreen and Kongsvegen polythermal tidewater glaciers, Kongsfjorden, Svalbard. *Geological Society, London, Special Publications 344*, 89–102.

Vaughan-Hirsch, D. P., Phillips, E., Lee, J. R. & Hart, J. 2013: Micromorphological analysis of poly-phase deformation associated with the transport and emplacement of glaciotectonic rafts at West Runton, north Norfolk, UK. *Boreas 42*, 376–394.

van der Wateren, F. M., Kluiving, S. J. & Bartek, L. R. 2000: Kinematic indicators of subglacial shearing. *In* Maltman, A. J., Hubbard, B. & Hambrey, M. J. (eds.): *Deformation of Glacial Materials*, 259–278. *Geological Society, London, Special Publications 176*.

Williams, G. D., Brabham, P. J., Eaton, G. P. & Harris, C. 2001: Late Devensian glaciotectonic deformation at St Bees, Cumbria: a critical wedge model. *Journal of the Geological Society 158*, 125–135.

Winkelmann, D., Jokat, W., Jensen, L. & Schenke, H.-W. 2010: Submarine end moraines on the continental shelf off NE Greenland-Implications for Lateglacial dynamics. *Quaternary Science Reviews 29*, 1069–1077.

Paper II

Quaternary Research

doi:10.1017/qua.2019.48

Micromorphological evidence for the role of pressurised water in the formation of large-scale thrust-block moraines in Melasveit, western Iceland

Thorbjörg Sigfúsdóttir[a,b]*, Emrys Phillips[c], Ívar Örn Benediktsson[b]

[a]Department of Geology, Lund University, 22362 Lund, Sweden
[b]Institute of Earth Sciences, University of Iceland, 101 Reykjavík, Iceland
[c]British Geological Survey, The Lyell Centre, Edinburgh EH14 4AP, United Kingdom
*Corresponding author. e-mail address: thorbjorg.sigfusdottir@geol.lu.se.

(Received January 31, 2019; Accepted July 10, 2019)

Abstract

Pressurised meltwater has a major impact on ice dynamics, as well as on sedimentary and deformational processes occurring below/in front of glaciers and ice sheets, but its role in glaciotectonic processes is yet to be fully understood. This study explores micro- and macroscale structures developed within décollements in two thrust-block moraines of Late Weichselian age in Melasveit, western Iceland. The aim is to investigate how pressurised subglacial meltwater can aid the dislocation and transport of large, unfrozen and unlithified sediment blocks by glaciers. A detailed model is constructed for the development of the thrust-block moraines and the microscale processes occurring along their detachments during thrusting. The detachments are characterized by relatively thin zones of crosscutting hydrofractures, which reflect fluctuating water pressures during glaciotectonism. Little evidence of shearing is observed along the leading edges of the thrusts in both moraines. This is supported by high water pressures along the detachments and indicates that the thrust blocks were initially decoupled from the underlying deposits. As the thrust moraines evolved, an increased amount of shear occurred in between events of sediment liquefaction, hydrofracturing, and fluid escape. This was followed by progressive locking up of the detachments and eventual cessation in the accretion of the thrust blocks.

Keywords: Glaciotectonic thrusting; micromorphology; subaquatic moraines; hydrofractures; glacier dynamics; Late Weichselian; Iceland

INTRODUCTION

Pressurised meltwater beneath glaciers and ice sheets is believed to have a major effect on ice sheet dynamics, as well as deformation and sedimentary processes (e.g., Boulton et al., 1974; Boulton and Caban, 1995; Hiemstra and van der Meer, 1997; Rijsdijk et al., 1999; Phillips and Auton, 2000; Boulton et al., 2001; Khatwa and Tulaczyk, 2001; Baroni and Fasano, 2006; Kjær et al., 2006; Phillips et al., 2007; van der Meer et al., 2009; Sole et al., 2011; Moon et al., 2014). Increased porewater pressures can cause accelerated flow (basal sliding) attributable to decoupling between the ice and its bed, as well as enhanced sediment remobilisation and deformation because of reduced sediment shear strength (e.g., Piotrowski and Tulaczyk, 1999; Boulton et al., 2001; Fischer and Clarke, 2001; Phillips et al., 2012, 2018; Evans, 2018). Deformation influenced by elevated water pressures can either result in the pervasive weakening of the sediment pile or be focused along discreet, water-lubricated detachments (Alley, 1989; Fischer and Clarke, 2001; Kjær et al., 2006; Phillips and Merritt, 2008). The development of such low-friction detachments/décollements is thought to have a considerable effect on the style and magnitude of glaciotectonics facilitating the transport of large thrust blocks of sediment and/or bedrock (Aber and Ber, 2007; Phillips and Merritt, 2008; Burke et al., 2009; Rüther et al., 2013; Vaughan-Hirsch et al., 2013) leading to the construction of large thrust-block or composite moraines (Croot, 1987; Bennett, 2001; Pedersen, 2005; Aber and Ber, 2007; Benediktsson et al., 2008; Phillips et al., 2017; Vaughan-Hirsch and Phillips, 2017; Sigfúsdóttir et al., 2018).

It has been argued that the presence of a well-developed permafrost layer in front of the advancing glacier above the

Cite this article: Sigfúsdóttir, T., Phillips, E., Benediktsson, Í. Ö. 2019. Micromorphological evidence for the role of pressurised water in the formation of large-scale thrust-block moraines in Melasveit, western Iceland. *Quaternary Research* 1–22. https://doi.org/10.1017/qua.2019.48

detachments can aid in the construction of large thrust-block moraines as it allows stress to be transmitted far into the forefield of the glacier (Aber et al., 1989; Evans and England, 1991; Boulton and Caban, 1995; Boulton et al., 1999; Bennett, 2001, or the base of the frozen layer acts as a focus for detachment above which deformation occurs (Burke et al., 2009; Benediktsson et al., 2015).

Furthermore, it has been argued that the freezing of sediments and/or bedrock to the base of the glacier is important for transportation of detached, largely intact thrust blocks (or rafts/megablocks) (Clayton and Moran, 1974; Banham, 1975; Bluemle and Clayton, 1984; Ruszczynska-Szenajch, 1987; Aber, 1988). However, it has increasingly been shown that overpressurised water within the substratum can cause the detachment and emplacement of large, unconsolidated thrust blocks without the ground being frozen (Moran et al., 1980; van der Wateren, 1985; Broster and Seaman, 1991; Aber and Ber, 2007; Benediktsson et al., 2008; Phillips and Merritt, 2008; Benn and Evans, 2010; Phillips et al., 2017; Vaughan-Hirsch and Phillips, 2017). Such sediment blocks can be transported over long distances; for example, thrust-bound rafts of glaciomarine sediments in Clava, Scotland, were shown to have been transported subglacially at least 50 km from their origin aided by fluid flow along the décollement surfaces (Phillips and Merritt, 2008).

However, a detailed understanding of the processes occurring along the major detachments formed during glaciotectonism has yet to be established, including how input of pressurised water controls variations in deformation styles and how that relates to the evolution of a large thrust-block complexes. This article presents the results of a micro- and macroscale investigation of the detachments developed within two thrust-block moraines in Melasveit, western Iceland. As these moraines were formed in a submarine environment, it can be assumed that the sediments were unfrozen at the time of deformation. This study uses micromorphology to investigate the changing style of deformation during the transport and emplacement of the thrust blocks. The factors controlling the style and magnitude of deformation are discussed—in particular, the effect of the introduction of pressurised water along the bounding thrusts during this process. The results of this study are presented in a conceptual sequential model and discussed in the wider context of the interrelationships between glacier dynamics, submarginal hydrology, and glaciotectonics.

Location of the study area and its geologic context

The Melasveit district of western Iceland is a coastal lowland area situated between the fjords of Borgarfjörður and Hvalfjörður (Fig. 1a). The geology of the area is dominated by a >30-m-thick sequence of Late Weichselian to Holocene glaciomarine to deltaic sediments overlying a striated bedrock surface (Ingólfsson, 1987, 1988; Sigfúsdóttir et al., 2018). The bedrock in the Melasveit area is mainly composed of Neogene basaltic lava flows, which are thought to have largely originated from the extinct Hafnarfjall-Skarðsheiði central volcano located to the northeast (Franzson, 1978).

The Melasveit district was covered by ice during the Last Glacial Maximum (LGM) and was subsequently deglaciated rapidly between ca. 15 and 14.7 cal ka BP, following the collapse of the marine-based western sector of the Icelandic Ice Sheet (Ingólfsson, 1987, 1988; Syvitski et al., 1999; Jennings et al., 2000; Norðdahl et al., 2008; Ingólfsson et al., 2010; Norðdahl and Ingólfsson, 2015; Patton et al., 2017). As a result, the relative sea level in the region was up to at least 125–150 m higher than present (Ingólfsson and Norðdahl, 2001; Norðdahl and Ingólfsson, 2015). Consequently, this low-lying area remained below sea level throughout most of the Late Weichselian leading to the deposition of a thick sequence of glaciomarine sediments.

The relative sea level fluctuated considerably during this time, reaching a maximum during a phase of renewed glacier expansion in both the Younger Dryas (ca. 12.9–11.7 cal ka BP) when the relative sea level was about 60–80 m higher than present and again in the Early Preboreal (ca. 11.7–10.1 cal ka BP) (Ingólfsson, 1988; Norðdahl et al., 2008; Ingólfsson et al., 2010).

After the initial deglaciation of Melasveit during the Bølling chronozone, a large outlet glacier in Borgarfjörður advanced from the north while the area was still isostatically depressed and culminated in the construction of the Skorholtsmelar end moraine (Fig. 1b) (Ingólfsson, 1987, 1988; Ingólfsson et al., 2010; Sigfúsdóttir et al., 2018). This also resulted in large-scale glaciotectonic deformation of the glaciomarine sediments exposed in the greater than 5-km-long and up to 30-m-high coastal cliffs of Melabakkar-Ásbakkar and a smaller coastal section at Belgsholt (see Fig. 1b and c) (Ingólfsson, 1987, 1988; Hart, 1994; Hart and Roberts, 1994; Sigfúsdóttir et al., 2018). Building on the pioneering stratigraphic framework of Ingólfsson (1987, 1988), a detailed investigation of the stratigraphy and glaciotectonic architecture of these coastal sections by Sigfúsdóttir et al. (2018) showed that a series of at least six buried ice-marginal/proglacial moraines is recorded in the cliffs (Fig. 1c). The internal structure of the moraines records large-scale glaciotectonic thrusting and folding of glaciomarine sediments, usually interleaved with penecontemporaneous, ice-marginal sands and gravels (Fig. 1c). The southernmost and largest moraine, called Ás in the cliffs, is more than 1.5 km wide and is correlated with the Skorholtsmelar moraine ridge a few kilometres farther inland and marks the maximum position of the post-LGM advance in the area (Fig. 1b). Sigfúsdóttir et al. (2018) suggested that the moraines north of Skorholtsmelar-Ás were formed as the glacier readvanced several times during an overall active retreat. Glaciomarine sediments were continuously being deposited and largely deformed during subsequent advances of the glacier. In general, the moraines become younger toward the north, the Belgsholt moraine being the youngest in the series (Sigfúsdóttir et al. 2018; Fig. 1b and c).

Based on this investigation and previously published radiocarbon ages from the glaciotectonised sediments

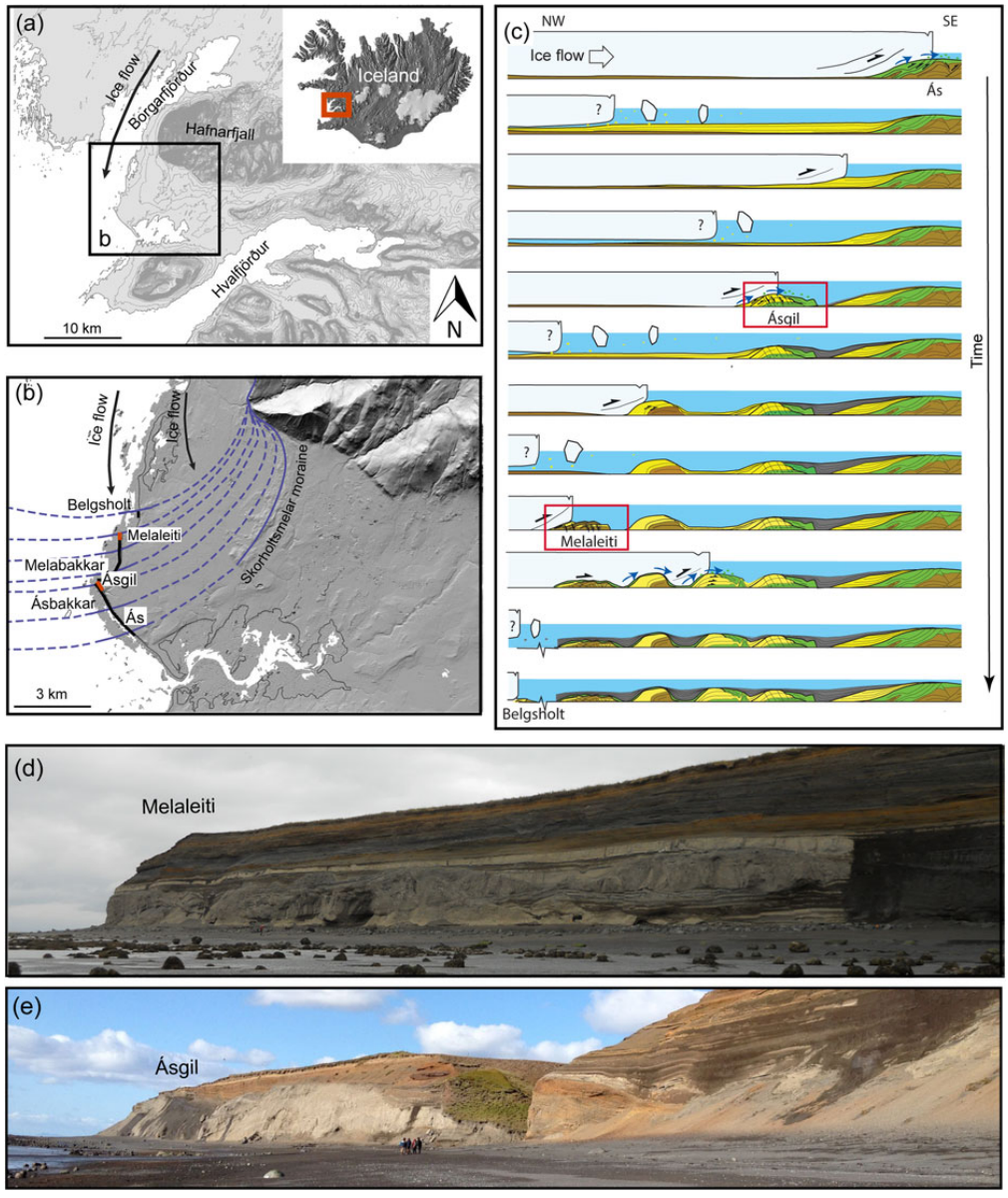

Figure 1. (a) The location of the Melasveit study area (black box) in western Iceland. The arrow indicates the direction of ice flow into the area during the Late Weichselian. (b) A digital elevation model (Arctic DEM) of Melasveit. Thin black line represents the present coastline, and the thick black lines denote the Melabakkar-Ásbakkar coastal cliffs. The red lines indicate the location of the Melaleiti and Ásgil thrust-block moraines in the cliffs. The curved, solid blue lines indicate the extent of the Late Weichselian glacier from the north based on the configuration of the Skorholtsmelar end moraine and the location of the buried moraines in the coastal sections. The dashed lines are the interpreted lateral extent of the ice margins (Sigfúsdóttir et al., 2018). (c) A conceptual sequential model showing the formation of the glaciotectonic moraines that are exposed in the Melabakkar-Ásbakkar and Belgsholt coastal cliffs. Each moraine inside (to the left of) the outermost moraine (Ás-Skorholtsmelar) marks a readvance of the glacier during an active retreat. The red boxes highlight the formations of the Ásgil and Melaleiti moraines. Black arrows indicate displacement; blue arrows, water flow; brown, preexisting glaciomarine sediments (unit A); green, meltwater deposits (units B and F); yellow, syntectonic glaciomarine sediments (units C–E); and grey, posttectonic, undeformed glaciomarine sediment (unit G) (Sigfúsdóttir et al. 2018). (d) An overview of the coastal section at Melaleiti. (e) An overview of the coastal section at Ásgil. The moraine is exposed to the north (left side) of the ravine, whereas associated submarine fan and overlying glaciomarine sediments are exposed on the southern side (right side). (For interpretation of the references to colour in this figure legend, the reader is referred to the web version of this article.)

(Ingólfsson, 1987, 1988; Norðdahl and Ingólfsson, 2015), Sigfúsdóttir et al. 2018 concluded that the readvances and subsequent active retreat of the Borgarfjörður glacier occurred after ca. 13.4 cal ka BP. This suggests that the moraines were formed during the Younger Dryas (Sigfúsdóttir et al., 2018). As the glacier retreated, the sedimentary basins between the moraines were progressively infilled by well-bedded, undeformed glaciomarine sediments (Fig. 1c). The entire glaciogenic sequence is unconformably overlain by littoral sands and gravels of early Holocene age (Ingólfsson, 1987, 1988).

The present study focuses on two of the moraines exposed in Melabakkar-Ásbakkar: Melaleiti and Ásgil (Fig. 1b–e). Both of these moraines show a relatively simple structural architecture with easily identified and accessible basal thrusts, thus allowing the deformation history to be confidently reconstructed. These moraines can be classified as thrust-block moraines (see Benn and Evans 2010 and references therein) and are characterised by a number of stacked, low-angle/subhorizontal thrust blocks (nappes), which show little evidence of large-scale folding. The geometry of the moraines is typical for glaciotectonic landforms formed by low-frictional sliding, supported by the relatively rigid nature of the thrust-block deposits (van der Wateren, 1995; Huddart and Hambrey, 1996; Boulton et al., 1999; Bennett, 2001). Based on this macro- to microscale study, a model is proposed that aims to link the microscale processes recorded along the bases of these two thrust blocks to each phase in the structural evolution of the thrust-block moraines.

METHODS

The large-scale glaciotectonics and stratigraphy of the Melabakkar-Ásbakkar cliff section have previously been described by Sigfúsdóttir et al. (2018), who divided this variably deformed glaciomarine sequence into eight informal sedimentary units (A–H); the same tectonostratigraphic framework has been adopted here. The detailed analysis of the macro- and microscale deformation structures associated with the emplacement of the thrust-bound blocks of glaciomarine sediments into the moraines is focused on the Melaleiti and Ásgil sections (Fig. 1b–e). Particular emphasis is placed on understanding the nature of the deformation associated with the prominent thrust planes, which form the basal detachments to the allochthonous blocks.

A total of 16 orientated samples (Ásgil 1 to 10 from Ásgil and Mel 11 to 16 from Melaleiti) were collected from within these basal detachments for detailed micromorphological and microstructural analysis. Each sample was collected using a $10 \times 10 \times 5$ cm aluminium Kubiena tin. The position of the sample within the thrust zone, its orientation relative to magnetic north, depth, and way up were recorded. The samples were taken from different parts of the basal detachment in order to provide detailed information on the style and intensity of deformation within these glaciotectonic contacts, as well as to examine the role played by pressurised water during the transport and emplacement of the thrust blocks. Each sample was sealed in two plastic bags and kept in cold storage prior to sample preparation at the British Geological Survey's thin section laboratory (Keyworth, Nottingham, UK). Sample preparation involves the replacement of porewater by acetone, which is then progressively replaced by a resin and allowed to cure. Large format orientated thin sections were taken from the centre of each of the prepared samples, thus avoiding artefacts associated with sample collection. Each large format thin section was cut orthogonal to the stratification/bedding within the sediment and parallel to the main ice movement direction in the study area. The thin sections were examined using a standard petrologic microscope and stereomicroscope allowing the detailed study of the microstructures at a range of magnifications. The terminology used to describe the various microtextures developed within these sediments in general follows that proposed by van der Meer (1987, 1993) and Menzies (2000) with modifications. Detailed maps of the range of sediments and microstructures present within the thin sections were obtained using the methodology of Phillips et al. (2010) (also see Phillips et al., 2012; Neudorf et al., 2013; Vaughan-Hirsch et al., 2013). Because of the large number of thin sections analysed, microstructural analysis of the 12 most representative thin sections, which illustrate the complete range of structural relationships, are included in this article. However, interpretive diagrams and high-resolution scans of the remaining four thin sections are included as Supplementary Material.

RESULTS

The Ásgil thrust-block moraine

The ice-marginal thrust-block moraine at Ásgil is located approximately halfway across the Melabakkar-Ásbakkar coastal cliffs (2400–2600 m measured from the northern end of the cliffs; Fig. 1b). It comprises at least two stacked, gently northward-dipping thrust-bound blocks of compact, weakly stratified to massive glaciomarine silt and sand (unit D; Fig. 2a; Sigfúsdóttir et al., 2018). The silt is poorly sorted, locally clay rich, massive to weakly laminated, and relatively thickly bedded (the thickest beds are more than 1 m thick). The interbedded sand is sorted and considerably thinner bedded (up to ~10 cm). The silt and sand largely retain their primary bedding, but locally, mainly within the lower thrust block, the sediments have undergone ductile shearing (augen structures and folds) and homogenisation. Each thrust block is more than 150 m long and about 10 m thick and is dissected by a number of steeply inclined joints and southerly dipping normal (extensional) faults.

Although not common, a small number of normal faults were observed crosscutting the detachment separating the thrust blocks, indicating that this phase of faulting postdated the development of the thrust stack. The base of the thrust stack rests on a few-metres-thick unit of stratified sand and gravel (unit B; Fig. 2a). These sands and gravels are folded and faulted and record a southward sense of shearing (based on vergence of folds and displacement along faults). The relative intensity of this deformation decreases toward

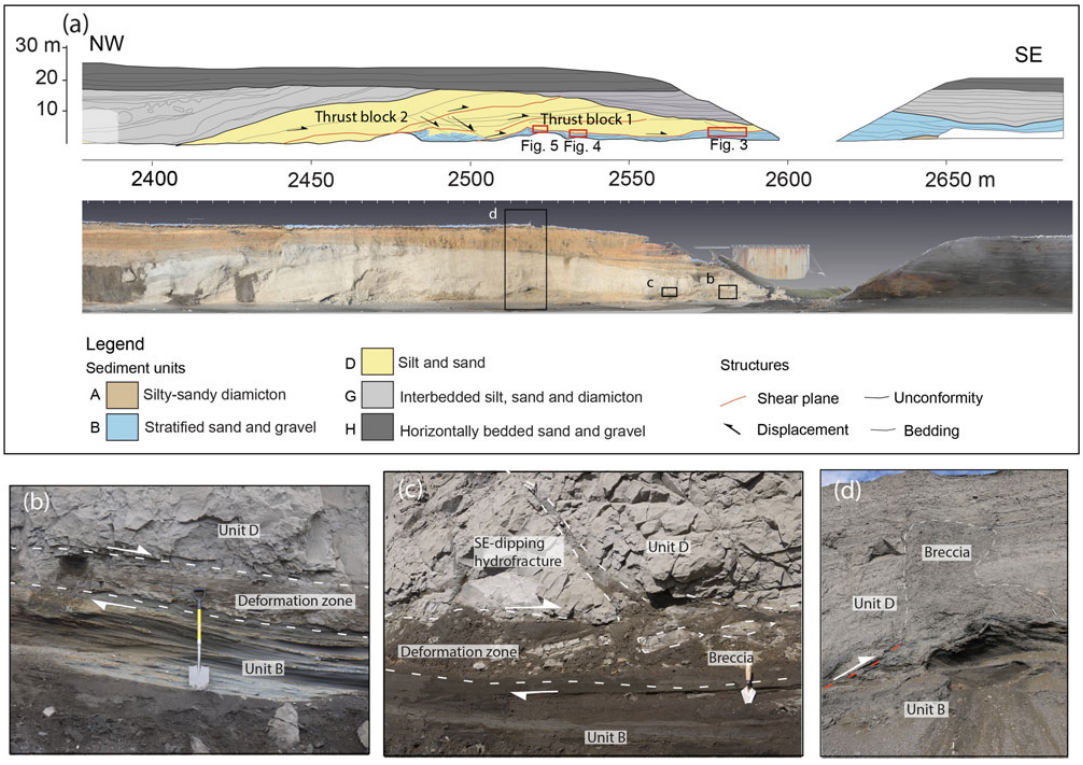

Figure 2. (a) A scale diagram and a LIDAR (light detection and ranging) scan of the Ásgil thrust-block moraine and overlying deposits (modified from Sigfúsdóttir et al., 2018). The scale bar indicates the distance from the northernmost point of the Melabakkar-Ásbakkar coastal cliffs. The red boxes indicate the sample locations and the area covered by Figures 3–5. The black boxes mark the locations of photographs in panels (b)–(d). The photographs show the detachment separating the thrust block from the footwall sand and gravel below. (b) A photo of the basal detachment at southern part of the Ásgil moraine. The deformation is focused within a ~50-cm-thick zone at the base of the thrust block, whereas the underlying deposits are largely undeformed (unit B). (c) A photo taken at ~2570 m showing elongated intraclasts (dashed outlines) within fluidised sand at the base of the thrust block. Hydrofractures infilled by coarse sands extend upward and dissect the overlying thrust block. (d) A photo taken at ~2520 m. The lower boundaries of the thrust block are diffused and deformed by folds and faults. A ~10-m-high and 2-m-thick clastic breccia extends upward into the thrust blocks, evidence of high water pressures. (For interpretation of the references to colour in this figure legend, the reader is referred to the web version of this article.)

the south. The sand and gravel can be traced laterally to the south of the thrust stack where they are unconformably overlain by a sequence of coarse gravel and boulders. This coarse-grained clastic sequence forms a greater than 15-m-thick and 200-m-wide multicrested sediment pile located on the ice-distal side of the thrust stack. Based on its sedimentology and stratigraphic location, Sigfúsdóttir et al. (2018) interpreted this sequence as an ice-contact fan deposited during the same readvance that resulted in the construction of the adjacent thrust stack. Despite some localised folding and faulting, this fan does not exhibit any macroscale glaciotectonic structures indicative of subglacial shearing, which suggests that the fan was not overridden after its formation.

The thrust-block moraine and the ice-contact fan rest on a glaciomarine diamicton (unit A of Sigfúsdóttir et al., 2018), which is exposed in the foreshore at low tide. This silty-sandy diamicton probably directly overlies the underlying basalt bedrock as the latter crops out ~150 m farther toward the northwest. The thrust-block moraine is overlain by an undeformed, glaciomarine sequence of interbedded silts, sands, and diamictons (unit G; Fig. 2a), which were deposited after the glacier had retreated from this recessional limit. The glaciomarine sequence is in turn unconformably overlain by early Holocene littoral sand and gravel (unit H; Fig. 2a) deposited during the isostatic adjustment of the area (Ingólfsson, 1987, 1988).

At Ásgil, the present study has focused on the deformation associated with the transport and emplacement along the basal detachment of the thrust-block moraine

Macroscale description of the basal detachment

Southeast of ~2550 m (Fig. 2a), the lowermost part (~0.5–1 m) of the thrust block is characterised by a distinct

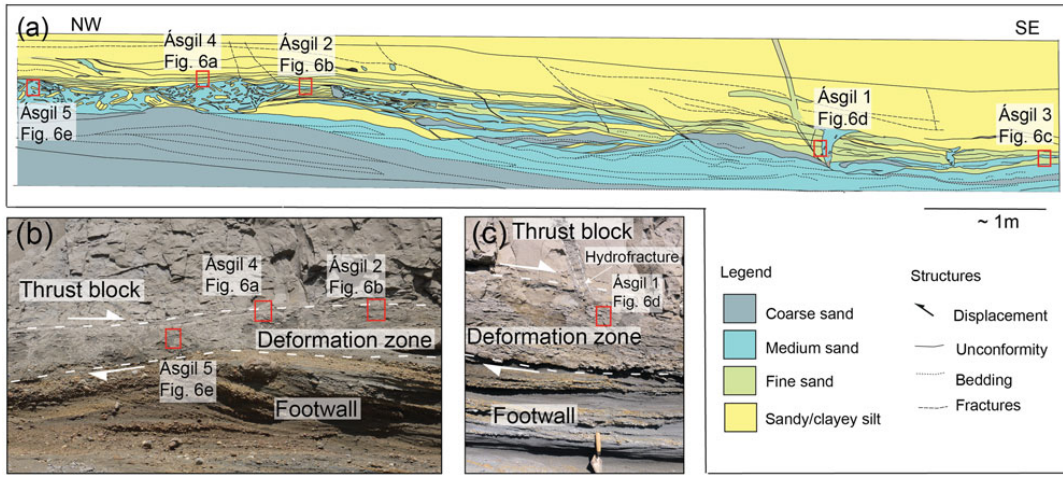

Figure 3. (colour online) (a) A section drawing showing the part of the detachment where samples Ásgil 1–5 were collected. The location is marked in Figure 2a. (b) A part of the detachment where samples Ásgil 2, 4, and 5 were collected. (c) A photograph of location of samples Ásgil 1. Note a trowel for scale.

deformation zone. This zone exhibits a number of erosive, crosscutting layers of sorted sand and gravel that are either massive or stratified. The crosscutting geometry of these layers is inconsistent with representing a primary (sedimentary) bedded sequence and can most simply be explained as hydrofractures formed by fracturing and subsequent infill by sediments (Rijsdijk et al., 1999; van der Meer et al., 2009; Phillips et al., 2012; Ravier et al., 2015). These hydrofractures are commonly subhorizontal, formed semiparallel to the base of the thrust blocks and the primary bedding within these sediments (Figs. 2b, 2c and 3). Because of their location along the detachments, it is most likely that these crosscutting sediment-filled hydrofractures were formed as pressurised water exploited the basal detachment of the developing thrust-block moraine (see *Microscale deformation structures*) (Phillips and Merritt, 2008). The largest sills (hydrofractures) are up to ~30 cm thick, have highly erosive margins, and are infilled with coarse sand and granule-sized gravel. The sediments filling these hydrofractures also locally contain angular, elongate to tabular-shaped blocks (up to ~50 cm long and 10 cm thick) of fine-grained silt and sand that are lithologically similar to the marine sediments contained within the overlying thrust block (Fig. 2c).

Although most of the hydrofractures form subhorizontal sill-like features, a number of high-angle to steeply inclined dykes, mostly dipping toward the southwest, were also observed (Fig. 2c). These steeply inclined sediment-filled fractures are up to ~20 cm wide and ~8 m in length and are filled by either a sandy breccia or well-sorted, stratified sand and gravel—the latter often exhibiting layering at an angle to the hydrofracture margins. These dyke-like features are rooted in the deformed basal zone and locally transect the entire thrust block. They are often (but not always) wedge shaped in form with the broadest part at the base of the thrust block, tapering toward the top located higher in the cliff, possibly suggesting that these sediment-filled features propagated upward from the base of the developing thrust stack.

The relative intensity of deformation within the basal detachment of this imbricate thrust stack gradually increases toward the north. Below this relatively thin deformed zone, in the southern part of the section, there is little evidence of glaciotectonic disturbance within the unit B sand and gravel indicating that negligible shear propagated downward into these underlying deposits (Figs. 2b, 2c and 3). In the northern part of the Ásgil section (between ~2450 and 2550 m; Fig. 2a), the contact between the thrust block and the underlying unit B stratified sand and gravel is poorly defined. In this area, these two tectono-sedimentary units appear to have been partially intermixed, possibly because of liquefaction and injection of sand and gravel upward into the base of the thrust block resulting in large-scale brecciation and disruption within the overlying thrust block (cf. Rijsdijk et al., 1999) (Figs. 2d, 4 and 5). In the northern part of the section, the hydrofractures and their host deposits of unit D, as well as the underlying unit B sand and gravel, are folded and thrust repeated, with the vergence of the folds recording a sense of shearing toward the south. Both sediment units and the boundary between them are crosscut by minor faults, which cut the sediments at different angles.

Microscale deformation structures

Ten thin sections were collected within the lowermost part of the thrust block at Ásgil at three locations (Figs. 3, 4 and 5; see relative location in Fig. 2) in order to examine the deformation structures developed close to the southern leading edge of the thrust block (at ~2580–2590 m; Fig. 2a, samples

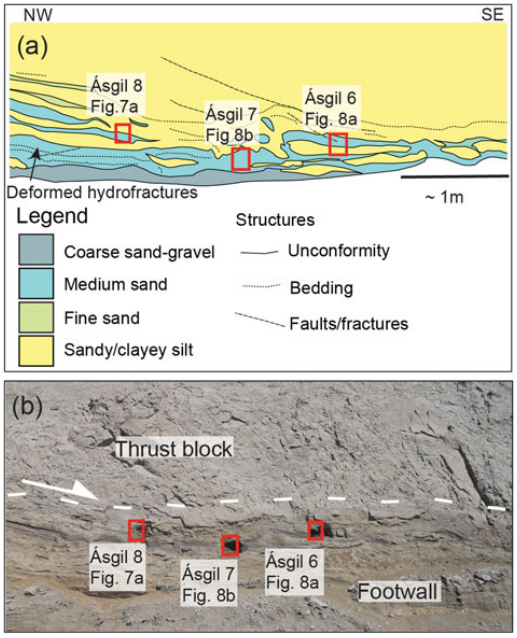

Figure 4. (colour online) (a) A diagram showing the details of the basal detachment where samples Ásgil 6–8 were collected. The sample location is marked in Figure 2a. Note that this is a less detailed diagram than Figure 3. (b) A photograph of the sampling location.

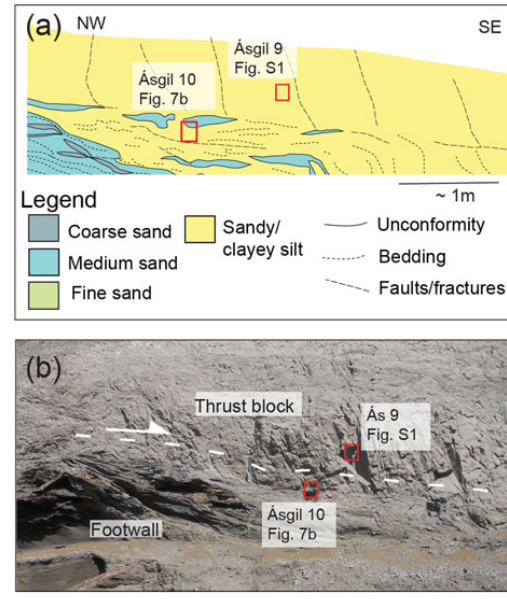

Figure 5. (colour online) (a) A diagram showing the basal detachment where samples Ásgil 9 and 10 were collected. The sample location is marked in Figure 2a. Note that this is a less detailed diagram than Figure 3. (b) A photograph of the sampling location.

Ásgil 1–5; Fig. 3) and farther north at a deeper structural level along the basal detachment (at 2520–2535 m; Fig. 2a, samples Ásgil 6–10; Figs. 4 and 5). In thin section, the fine sand, silt, and sandy diamicton, which not only form the thrust block but also the host sediments within the deformed, basal zone of the thrust stack, are lithologically similar indicating that they were derived from a similar source (provenance).

Microstructures developed close to the leading edge of the basal detachment (samples Ásgil 1–5). The position of samples Ásgil 1–5 within the deformed zone marking the basal detachment close to the leading edge of the thrust-block moraine is shown in Figure 3. These thin sections reveal that, although on a macroscale this zone appears highly deformed, this deformation is less apparent on a microscale with the samples being largely composed of finely stratified silt and silty clay, with subordinate amounts of fine sand (Fig. 6a–c). The contacts between these layers are undulating to irregular in form and range from sharp to diffuse/gradational. The clay layers commonly possess a moderate to well-developed, layer-parallel plasmic fabric defined by optically aligned clay minerals. In sample Ásgil 4 (Fig. 6a), this birefringent clay (crossed polarised light) is locally fragmented with the fractures filled by homogenised silt and fine sand. In sample Ásgil 2 (Fig. 6b), and, to a lesser extent, samples Ásgil 3 (Fig. 6c) and 4 (Fig. 6a), the stratification is offset by at least one set of gently to moderately northwest-dipping (apparent dip in plane of section provided by the thin sections) normal microfaults and a set of moderately southeast-dipping structures. These small-scale faults (displacements on the order of a few millimetres) appear to show a close spatial relationship to the lenses and layers of coarser-grained sand.

The stratification within the fine silts and silty/sandy clays is locally crosscut and disrupted by irregular (erosive) lenses/layers of fine- to coarse-grained sand. These crosscutting relationships indicate that the introduction of these coarser-grained sediments postdated the formation of the stratification within the finer-grained sediments. The coarse sand is matrix poor (low clay content) and varies from massive (homogeneous) to weakly normally graded (fining upward). The coarse-sand grains are typically subrounded to rounded in shape, with the finer sand grains being more angular in appearance. Sand- and gravel-sized particles within these sediments are mainly composed of basaltic rock (lithic) fragments consistent with the predominantly basaltic bedrock in the region. Fresh, angular fragments of basaltic and silicic volcanic glass are also common detrital components. In sample Ásgil 3, the introduction of the coarse sand (see lower part of the thin section; Fig. 6c) resulted in the disruption/fragmentation of the adjacent stratified silt and fine sand. This coarse sand contains angular to irregular fragments of laminated silt and clay that are lithologically similar to, and therefore thought to have been derived from, the adjacent stratified sediments. Some of these clasts are

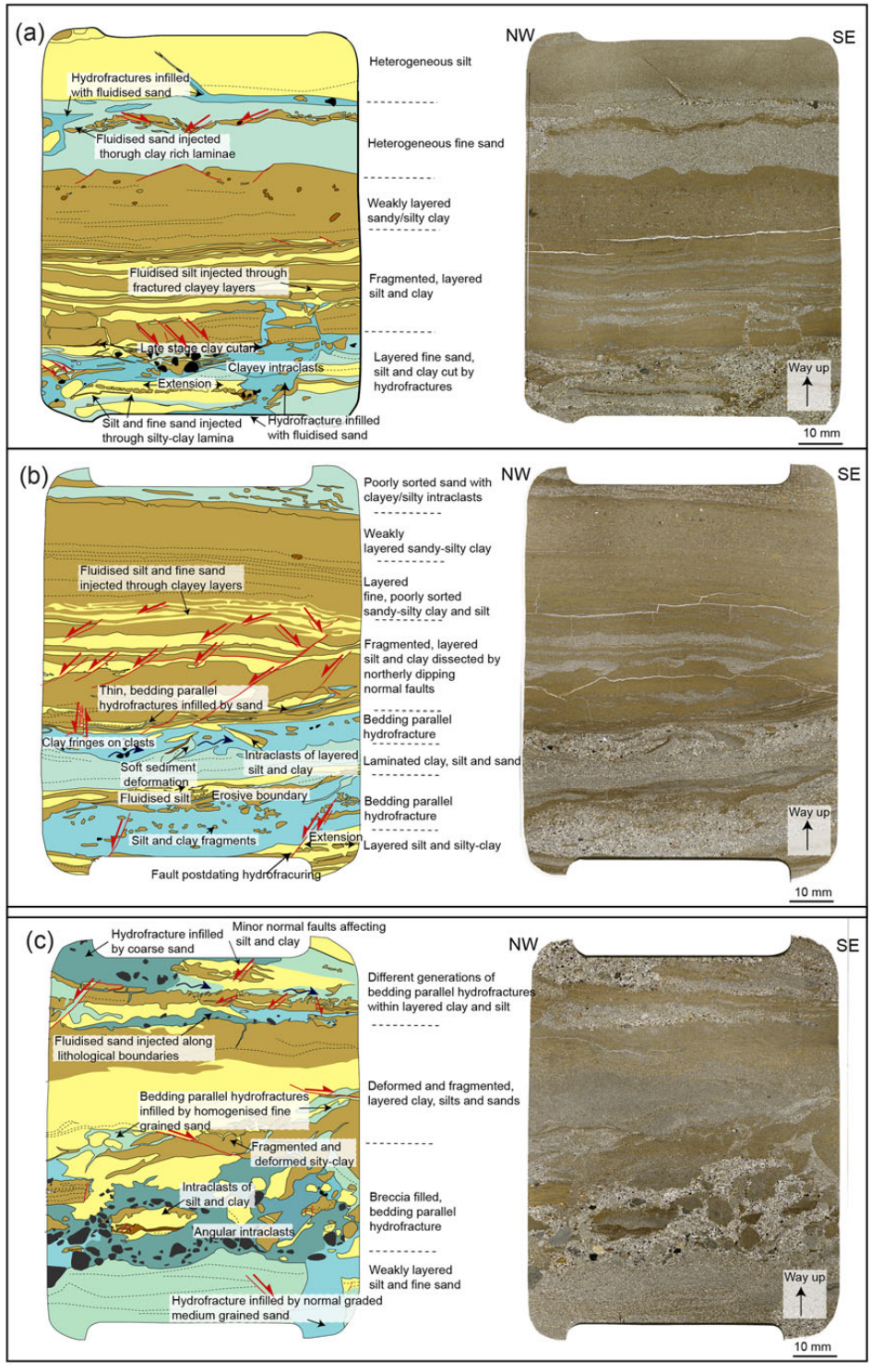

Figure 6. (Continued)

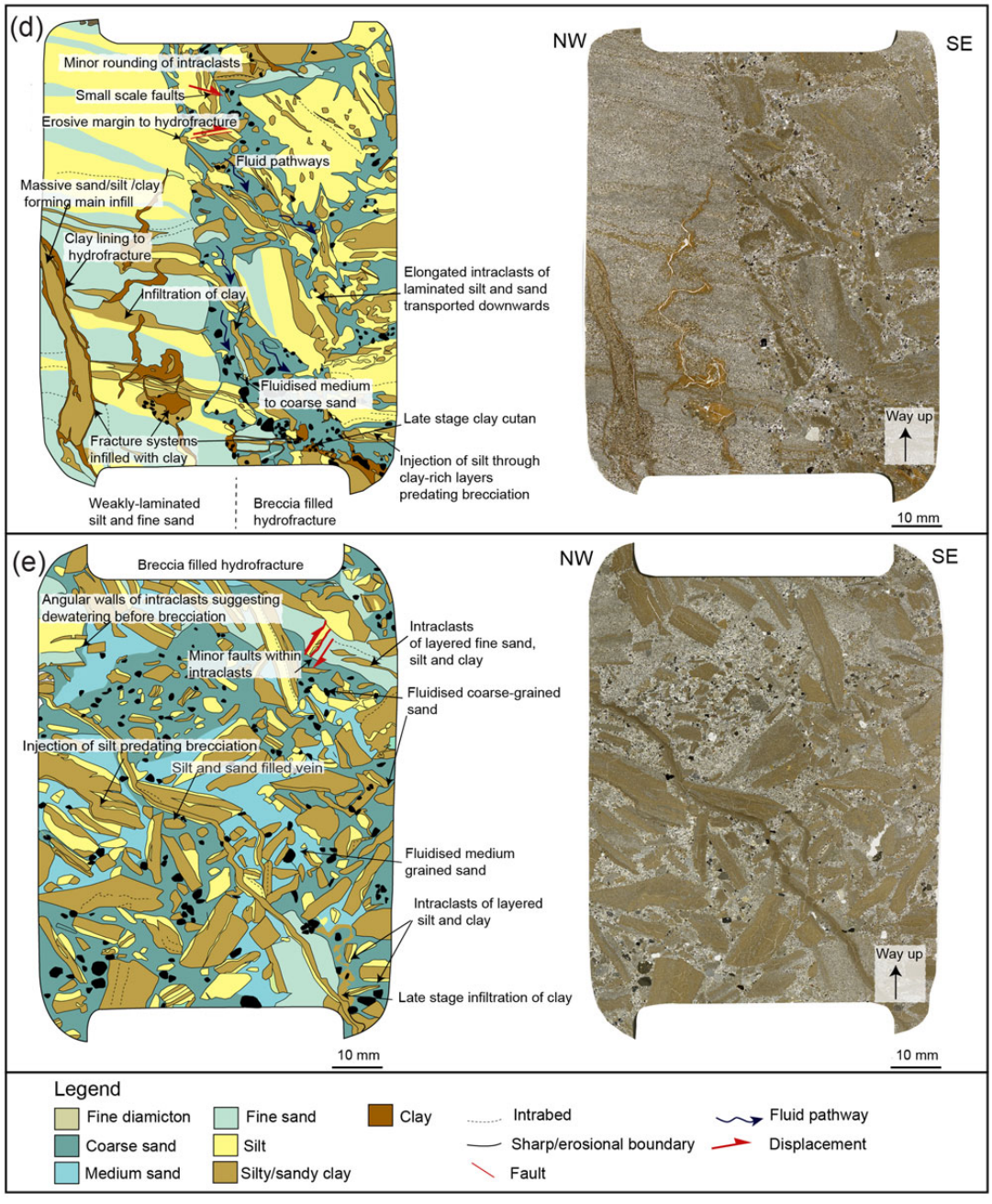

Figure 6. (colour online) Interpretation diagrams and scans of thin sections Ásgil 1–5. These thin sections were collected from a deformed zone at the base of the lowermost thrust block, close to the leading edge of the Ásgil moraine. Their relative location can be seen in Figure 3. These thin sections are dominated by layered, fine-grained sediments that have undergone repeated phases of sediment liquefaction, injection, and hydrofracturing. Samples Ásgil 4 (a), Ásgil 2 (b), and Ásgil 3 (c) are characterised by hydrofractures formed subparallel to the stratification of the fine-grained host deposits. Sample Ásgil 1 (d) shows the margins of a steep, breccia-filled hydrofracture. Sample Ásgil 5 (e) shows the infilling of a subhorizontal, breccia-filled hydrofracture.

composed of highly birefringent (under crossed polarised light) clay in which the optically aligned clay minerals define a moderate- to well-developed plasmic fabric. In samples Ásgil 2 (Fig. 6b) and 4 (Fig. 6a), the clay clasts within the medium-sand layers are much smaller in size and are more rounded in shape, indicative of a greater degree of rounding (abrasion) during transport. In sample Ásgil 4 (Fig. 6a), the medium-sand layer near the bottom of the thin section is linked to a fine-scale network of fractures (veins) filled by the same sediment. This network is injected into the adjacent clay and comprises two subvertical sand-filled veins connected to a number of subhorizontal veins, which occur parallel to the fine-scale lamination/stratification within the clay. The fine- to medium-sand layer in the upper part of this sample (Fig. 6a) contains a thin clay layer that is broken into a series of tabular segments with the intervening fractures filled by sand. Both the sand and clay layers are crosscut by an irregular vein of pale-coloured, medium-grained, matrix-poor sand. In the lower part of sample Ásgil 2 (Fig. 6b), the boundary between the medium- and fine-grained sand layers is complex and folded by a number of flame-like, asymmetrical disharmonic folds. The shape of these folds is consistent with an apparent sense of shear toward the southeast.

The microtextural relationships described previously suggest that the sand layers were injected into the preexisting stratified silts and clays. This process would have accompanied the brecciation and disruption of these fine-grained host sediments with the fragments dislodged from the walls of the developing sediment-filled hydrofracture being incorporated into the coarse sand during the injection process. The crosscutting relationships observed between the sand layers suggest that there were several phases of injection. Injection of the later coarser-grained sands, prior to the dewatering of the earlier formed sand, may have resulted in the observed soft-sediment deformation (disharmonic folding) in response to shear along the boundary between the two layers. In contrast, the more coherent silts and clays underwent brittle deformation with the normal (extensional) faulting as these stratified host sediments accommodated the expansion (increase in volume) of the sequence occurring in response to the injection of the liquefied coarse sand. In samples Ásgil 2 (Fig. 6b), Ásgil 3 (Fig. 6c), and Ásgil 4 (Fig. 6a), the coarser sand layers occur parallel/subparallel to the stratification within the host silt and silty clay indicating that injection of these sediments exploited this preexisting layering.

Samples Ásgil 1 (Fig. 6d) and Ásgil 5 (Fig. 6e) were taken from larger hydrofractures filled by a mud, clast-rich breccia, which is composed of elongated to irregular clasts of weakly stratified fine sand, silt, and clay set within a matrix of medium- to coarse-grained sand. The sandy matrix to the breccia varies from massive (sample Ásgil 1; Fig. 6d) to "patchy"/"mottled" in appearance because of the variation in its grain size from fine to coarse sand (sample Ásgil 5; Fig. 6e). Sample Ásgil 1 was taken from the margin of a prominent (up to 20 cm wide and 8 m long), steeply southeast-dipping, sediment-filled fracture system that crosscuts fine-grained weakly layered clayey silt, silt, and fine sand at the base of the thrust block (Fig. 3a and c). Sample Ásgil 5 (Fig. 6e) was collected from an approximately 50-cm-wide, subhorizontal breccia-filled hydrofracture that cuts through the finely layered sediments at the base of the thrust block (Fig. 3a and b). The laminated silt and clay intraclasts within the breccia range from being angular to rounded in shape, possibly reflecting a variation in the degree of rounding (abrasion) of the clasts during transport and injection of this coarse-grained sediment into the developing hydrofracture. However, the degree of rounding of these clasts appears to be dependent on lithology, with the sandy intraclasts tending to become more rounded with more diffused clast margins. The orientation of bedding preserved within the large clasts indicates that during transport (injection) they have been rotated (tilted) and possibly overturned. The clay layers within the clasts are locally broken, and the fractures infilled by silt and fine sand, indicating that these sediments have potentially recorded several phases of liquefaction, remobilisation, and injection prior to brecciation associated with the formation of the large-scale hydrofracture system. In sample Ásgil 1 (Fig. 6d), the margins of the hydrofracture are irregular, and it appears that some of the clasts contained within the breccia have been ripped (eroded) from the host sediments of this fracture system. Elongate clasts immediately adjacent to the wall of the hydrofracture show a preferred shape alignment parallel to or at a low angle to the margin of the fracture (Fig. 6d). In contrast, toward the interior of the vein the clasts are apparently more randomly orientated or may possibly define a subhorizontal preferred shape alignment (see Fig. 6d). In the lower, southeastern corner of the thin section, the breccia is cut by a complex network of clay veins. These veins are filled by finely laminated, highly birefringent clay (cutan). The sediments forming the host to this breccia-filled hydrofracture occur on the left-hand (northern) side of the thin section (Fig. 6d). The weakly developed to diffuse stratification developed within these silts and fine sands has an apparent dip toward the southeast. In the lower left-hand corner of the thin section, this stratification is crosscut by two thin (<10 mm) sediment-filled veins composed of clay and sandy clay (Fig. 6d). The larger of these two veins is layered with an outer layer of clay lining the fracture walls and a central infilling of massive clayey sand. A similar clay-filled, southeast-dipping vein was also observed cutting through the breccia within sample Ásgil 5 (Fig. 6e) where it is filled by weakly layered clayey silt and silt with this layering occurring parallel to the fracture walls.

Microstructures developed at a deeper structural level of the basal detachment (samples 6–10). Thin sections Ásgil 6–10 (Figs. 7 and 8; Supplementary Fig. 1) were collected within the deformed zone associated with the basal detachment at a deeper structural level at the thrust-block moraine (Figs. 4 and 5). Sample Ásgil 9 (Supplementary Fig. 1) was collected from the thrust block and comprises homogenised silts and sands (a diamicton). Samples Ásgil 8 and 10 (Fig. 7) were taken from fine-grained sediments comprising the base of the thrust block and samples. Ásgil 6 and 7

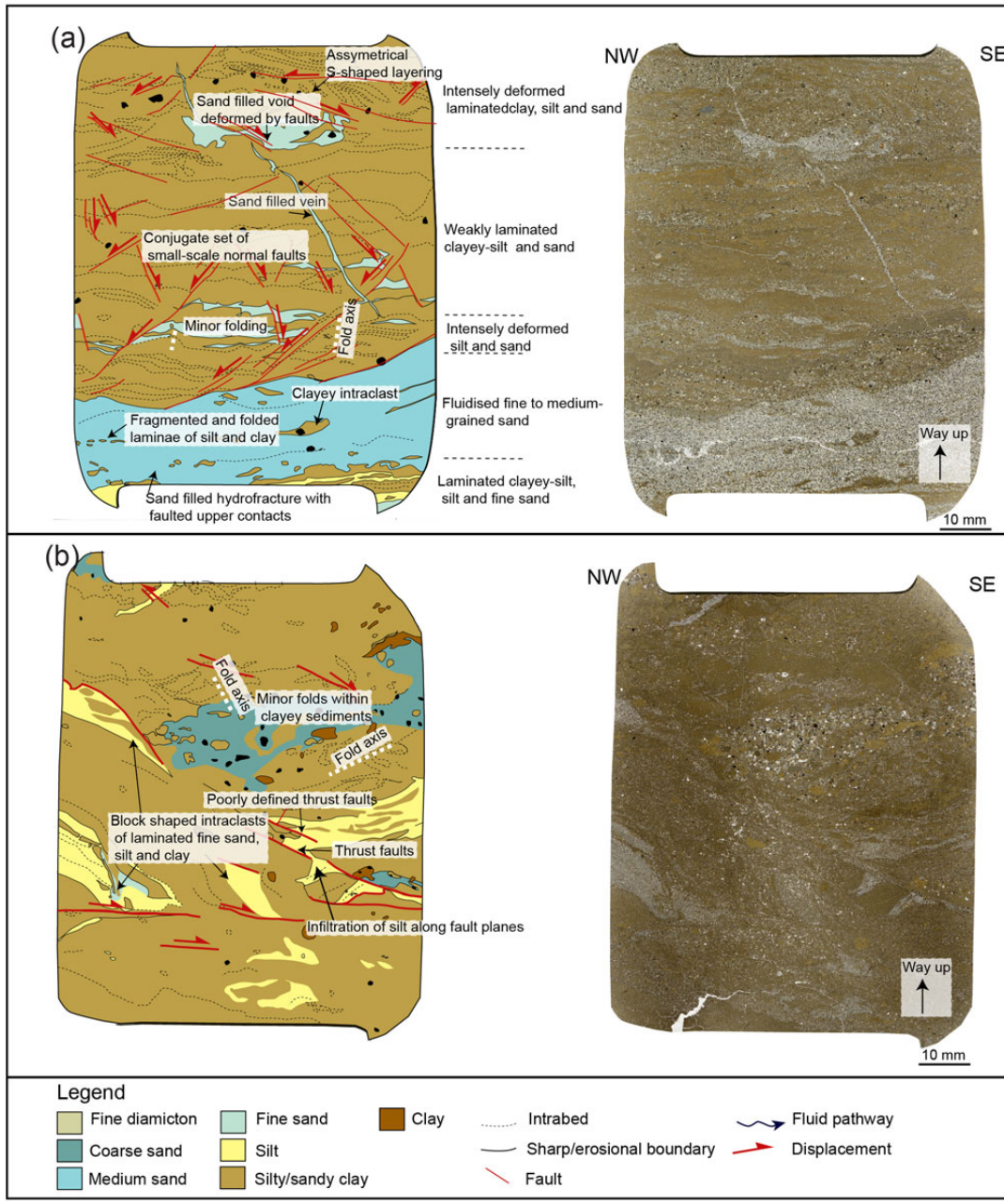

Figure 7. (colour online) Interpretation diagrams and scans of thin sections Ásgil 8 (a) and Ásgil 10 (b). These thin sections were sampled from the base of the lowermost thrust block at a structurally deeper part of the moraine. The location of the thin sections can be seen in Figures 4 and 5. They reveal fine-grain, stratified sediments that have undergone alternating phases of shearing (folding, faulting) and hydrofracturing.

(Fig. 8) were taken from subhorizontal hydrofractures that crosscut these fine-grained deposits (Figs. 4 and 5).

Thin sections Ásgil 8 and Ásgil 10 (Fig. 7) are dominated by finely stratified silty clay, silt, and very fine sand, which are lithologically similar (grain size, sorting, and stratification) to the finely stratified clay, silt, and sand forming the host to the hydrofracture system in samples Ásgil 1–5 (Fig. 6). However, much more disruption is observed in samples Ásgil 8 and 10

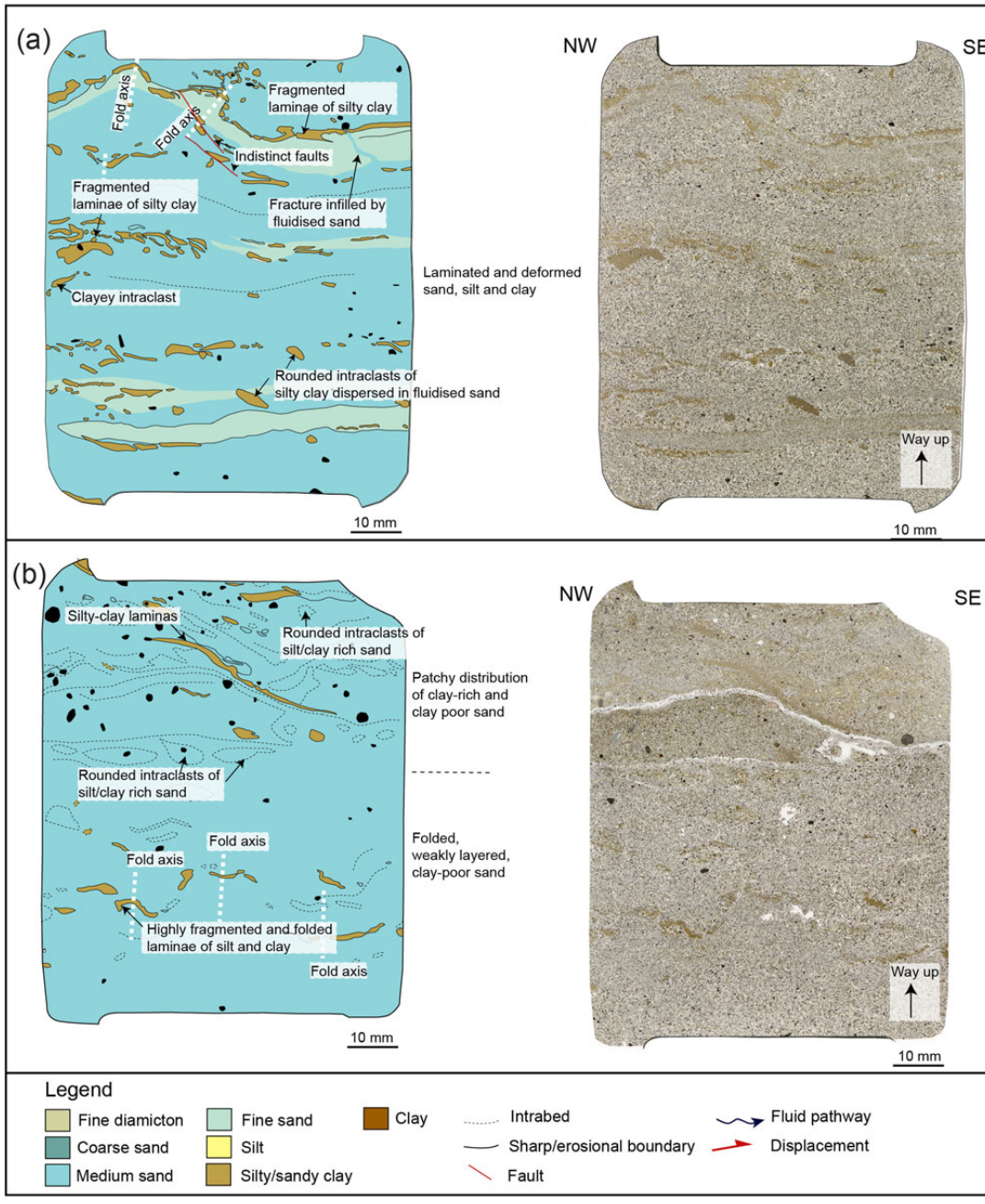

Figure 8. (colour online) Interpretation diagram and scans of samples Ásgil 6 (a) and Ásgil 7 (b). These thin sections were sampled from large hydrofractures dissecting the fine-grained sediment in the base of the lowermost thrust block at a structurally deeper part of the moraine. The locations of the thin sections can be seen in Figure 4.

(Fig. 7). The sediments have a mottled appearance as the stratification is diffused/gradational and the beds/laminae are undulating and discontinuous. This may possibly be attributable to an increase in the amount of layer-parallel shear accommodated by the laminated sediments within this structurally deeper and more complex part of the basal detachment. In sample Ásgil 8 (Fig. 7a), the stratification is mostly subhorizontal/weakly folded with the disruption of

the layers increasing upward. The stratification is offset by a poorly defined, conjugate set of normal microfaults with apparent dips both toward the northwest and southeast. In the lower part of this finely stratified subunit, the faults have a moderate to steep dip, but in the upper part, the faults tend to have lower dips. In the upper part of sample Ásgil 8 (Fig. 7a), the layers are tilted between two of these low-angle faults resulting in an asymmetrical S-shaped layering between these two faults. The faulted and folded stratified sediments are truncated by an apparently southeast-dipping sand vein (see Fig. 7a). The vein is about 0.5 mm thick with a sharp boundary and a steplike form and is infilled with massive fine-grained sand with high intergranular porosity. The crosscutting, erosive geometry, and sorted infilling is consistent with this sand vein being formed by injection and subsequent deposition of the sand. A larger sand vein/hydrofracture dominates the lowermost part of thin section Ásgil 8 (Fig. 7a). This hydrofracture is seen in the lower ~4 cm of the thin section where it has an apparent dip toward the northwest. The sediments within it comprise medium-grained sand that is lithologically similar to the sands seen in samples Ásgil 6 and Ásgil 7 (see below). The sand typically possesses a high intergranular porosity and low matrix content. The individual sand grains are subrounded to angular in shape. Within the sand are fragmented silt and clay laminae, as well as variably aligned fragments (intraclasts) of silty clay, which define a weakly developed/preserved layering that dips toward the northwest. The intraclasts have smooth edges indicative of rounding during transport. The upper boundary of the hydrofracture is defined by an approximately 1-cm-thick deformed layer of unsorted silt, sand, and clay that is offset by a set of northwest-dipping faults associated with small-scale folds. The faults are crosscut by the sand vein, so the injection of the sand postdated the small-scale faulting of the host sediments. In sample Ásgil 10 (Fig. 7b), the stratification within the clayey silt/silty clay is highly disrupted, and the laminae are tilted, folded, and possibly overturned. In between the clay-rich layers that dominate the thin section are layers of sorted silt and very fine sand with sharp boundaries. In the middle-upper part of the thin section is a lens of coarse-grained sand with diffused edges. All these sediments are dissected by a number of faults. The faults are poorly defined, and some have sand lining possibly deposited by water flowing along the fault walls. The faults have a very gentle to moderate dip toward the southeast (apparent dip), but because of complex deformation of the sample, it was difficult to estimate the direction of offset along the fault planes, although most of them appear to record apparent displacement toward the southeast.

Samples Ásgil 6 and 7 (Fig. 8) were taken from subhorizontal layers of sand with erosional margins, consistent with being hydrofractures (Fig. 4). The thin sections show that the sand within the hydrofractures is weakly stratified to heterogeneous and is interbedded with layers of silt and clayey silt possibly reflecting fluctuations of the velocity of the water flowing through the fractures. The sand is fine to medium grained and possesses an intergranular porosity and variable amounts of a fine-grained matrix. Most of the sand grains are subrounded to angular in shape and composed of a similar range of components as the sand layers in samples Ásgil 1–5 (Fig. 6). The contacts between the layers are irregular, and the silty-clay layers tend to be very fragmented, possibly because of brecciation of the rigid clay layers in response to the liquefaction and ductile deformation of the open-packed silt and sand. Although the alignment of elongate clasts appears to preserve the original stratification within the hydrofractures, some of the clay fragments are randomly dispersed within the sand indicating the longer transport path of these clasts. These "dispersed" fragments tend to have rounded and rather diffuse edges. The weakly preserved stratification is deformed by a number of upright to steeply inclined, asymmetrical, southeast-verging folds (Fig. 8). This indicates that after the hydrofractures formed, the sediments underwent a minor folding, possibly as a result of transmission of shear into the deposits during the thrust-block transport.

Overall, samples Ásgil 6 to 8 and 10 (Figs. 7 and 8) show higher intensity of faulting and folding compared with thin sections Ásgil 1–5 (Fig. 6). This is consistent with the observed, larger-scale increase in complexity and magnitude of deformation toward the northern, structurally deeper part of the detachment. The lithologic similarities and the tectonostratigraphic location of the finely layered silty clay, silt, and sand (see Ásgil 8 and 10; Fig. 7) to those seen at the front of the thrust (Ásgil 1 to 5; Fig. 6) may suggest that these are part of the same deformation/hydrofracture zone. However, the fine-grained host sediments and the crosscutting hydrofracture system seen in thin sections Ásgil 1–5 (Fig. 6) have lost some of their identity because of folding and faulting resulting from increased shearing transmitted into the deposits, probably because of increased overburden pressures during thrust stacking. Shearing was interrupted by events of sediment liquefaction and injection resulting in brecciation and hydrofracturing. The hydrofractures may have developed along weaknesses in the sediments, both parallel to bedding and along preexisting fault planes. The new hydrofractures also underwent faulting and folding to different degrees (Ásgil 6 to 8 and 10; Figs. 7 and 8). This indicates that the level of friction and transmission of shear varied along the detachment, possibly because of fluctuating porewater pressures related to hydrofracturing and water escape.

Melaleiti thrust-block moraine

The thrust-block moraine at Melaleiti is located in the northernmost part of the Melabakkar-Ásbakkar coastal cliffs. It is more than 300 m across and 10 m high and comprises several subhorizontal or gently north-dipping, stacked thrust-bound allochthonous blocks (Fig. 9). Each block is composed of two main sedimentary units—a massive, silty-sandy, very compact, and deformed glaciomarine diamicton of unit A, and unit E consisting of interbedded silt and sand with occasional, thin layers of gravel and diamicton (Sigfúsdóttir et al., 2018). The thrust blocks are dissected by a large

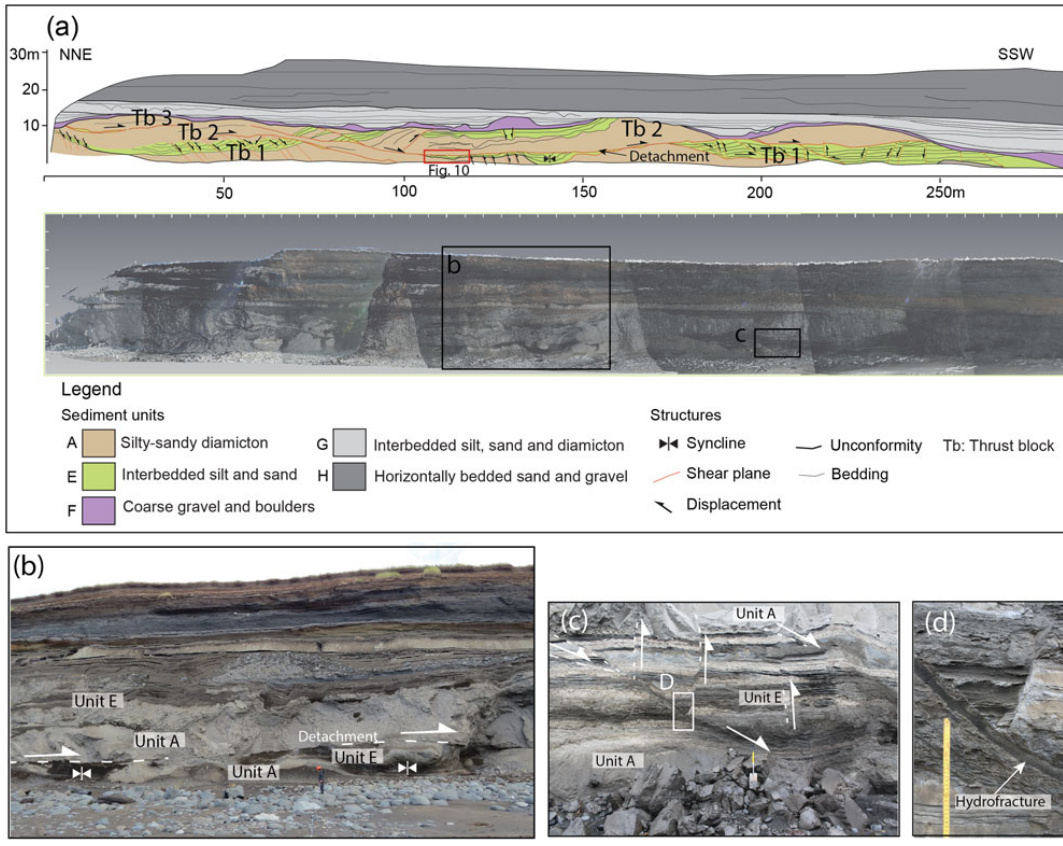

Figure 9. (a) A scale diagram and a LIDAR (light detection and ranging) scan of the Melaleiti thrust-block moraine (modified from Sigfúsdóttir et al., 2018). The red box indicates the sample locations and the area covered by Figure 10. The black boxes on the LIDAR scan indicate the locations of photos in panels (b)–(d). The numbers on the section diagram indicate different thrust blocks. (b) A photograph taken at ~140 m showing sharp lower contact (white dashed line) between a thrust block above and the deformed silt and sand below. (c) A photograph taken at ~220 m showing faults dissecting the intrabedded silt and sand and the thrust block above. The large normal fault seen in the middle part of the photo is infilled by massive sand. (d) A close-up photograph of the sediment-filled normal fault (hydrofracture) in panel (c). The yellow scale is about 30 cm. (For interpretation of the references to colour in this figure legend, the reader is referred to the web version of this article.)

number of normal (extensional) faults with a dominant dip toward the southeast (Fig. 9), although some dip toward the northwest. The relative complexity of deformation and intensity of faulting/thrusting decreases to the southwest (ice-distal part). This probably reflects a decrease in strain away from the ice front during the thrust stacking (Sigfúsdóttir et al., 2018).

The moraine is overlain by an up to 2-m-thick unit of coarse gravel (unit F in Fig. 9a). This unit is interpreted as having been deposited under high pressure in a subglacial setting, which indicates that the moraine was overridden by the glacier. However, it is unclear if it was overridden by the same or a younger advance (Sigfúsdóttir et al., 2018). The original structure of the moraine is preserved indicating that it did not undergo extensive subglacial deformation during the overriding. However, some of the normal faults that crosscut (postdate) the thrusts-bound blocks were possibly developed in response to extensional deformation as the glacier overrode the moraine (Sigfúsdóttir et al., 2018).

Macroscale description of the basal detachment

This study focuses on a more than 150-m-long detachment in the southernmost part of the thrust stack (~100–250 m; Fig. 9a). The base of the thrust block is very sharp, and the deposits in the footwall (both units E and A) are variably deformed. The relative intensity of this deformation decreases southward toward the leading edge of the thrust-block moraine. In the northern part, between ~100 and 180 m, the sediments are deformed by numerous folds and boudins, which are crosscut by normal and reverse faults bounded by subhorizontal shears (Fig. 9b). The geometry of these faults suggests that they developed as subhorizontal Reidel shears

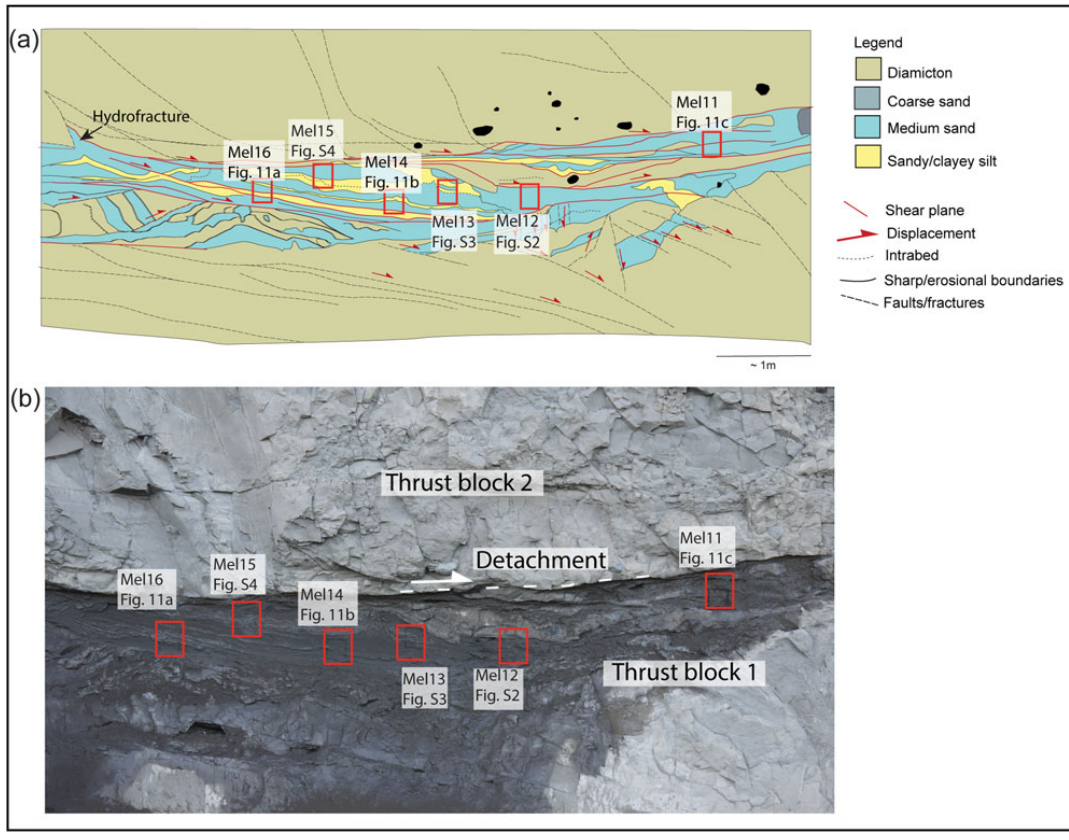

Figure 10. (colour online) (a) A diagram showing the part of the basal detachment where samples Mel 11–16 were collected. The location is marked in Figure 9a. (b) A photograph of the sampling location.

(Y shears) within the footwall of the basal detachment confining a zone of normal and reverse faults (R and P shears) developed at an angle to the main direction of transport (Phillips and Lee, 2011). The majority of the normal and reverse faults do not crosscut the main detachment, indicating that they predated or were developed at the same time as this larger-scale structure. Closer to the leading edge of the thrust-block moraine (between ~180 and 300 m; Fig. 9a), the bedded silts and sands have undergone less penetrative deformation. For example, the bedded unit E sediments are relatively intact, although crosscut by a large number of well-defined, southeast- and northwest-dipping normal faults (Fig. 9c). Based on the observed crosscutting relationships, these faults are interpreted as both predating and postdating the thrust detachment. A small number of the faults are infilled/lined by massive and stratified sand indicating deposition by running water and therefore suggesting that these faults were exploited as fluid pathways/hydrofractures. These hydrofractures are relatively thin (up to ~3 cm), and usually, they crosscut other structures indicating that they were formed during the late stage of the deformation (Fig. 9d).

Microscale deformation structures

Six thin sections were taken from samples collected at ~110 m (Fig. 9a), from the glaciomarine interbedded silt, sand, and diamictons of unit E located immediately below the southernmost thrust detachment (Fig. 10). Three of them are described subsequently (Mel 11, 14, and 16; Fig. 11), and the remaining three (Mel 12, 13, and 15) are available as Supplementary Material (Supplementary Fig. 2). The Mel 11 to 16 thin sections contain moderately to well-sorted, open-packed, fine- to medium-grained sand (Fig. 11; Supplementary Fig. 2). The sand grains are usually subrounded to angular in shape and mainly consist of basaltic rock (lithic) fragments. Fresh, angular fragments of volcanic glass are also common. The sand layers are interbedded with thinner layers of silt and silty clay. The contacts between well-sorted silt and sand layers are commonly diffusive, and locally they appear interdigitate, which could indicate local liquefaction and subsequent mixing of these sediments. The more rigid, clay-rich layers have undergone brecciation and extension (boudinage), most likely in response to/

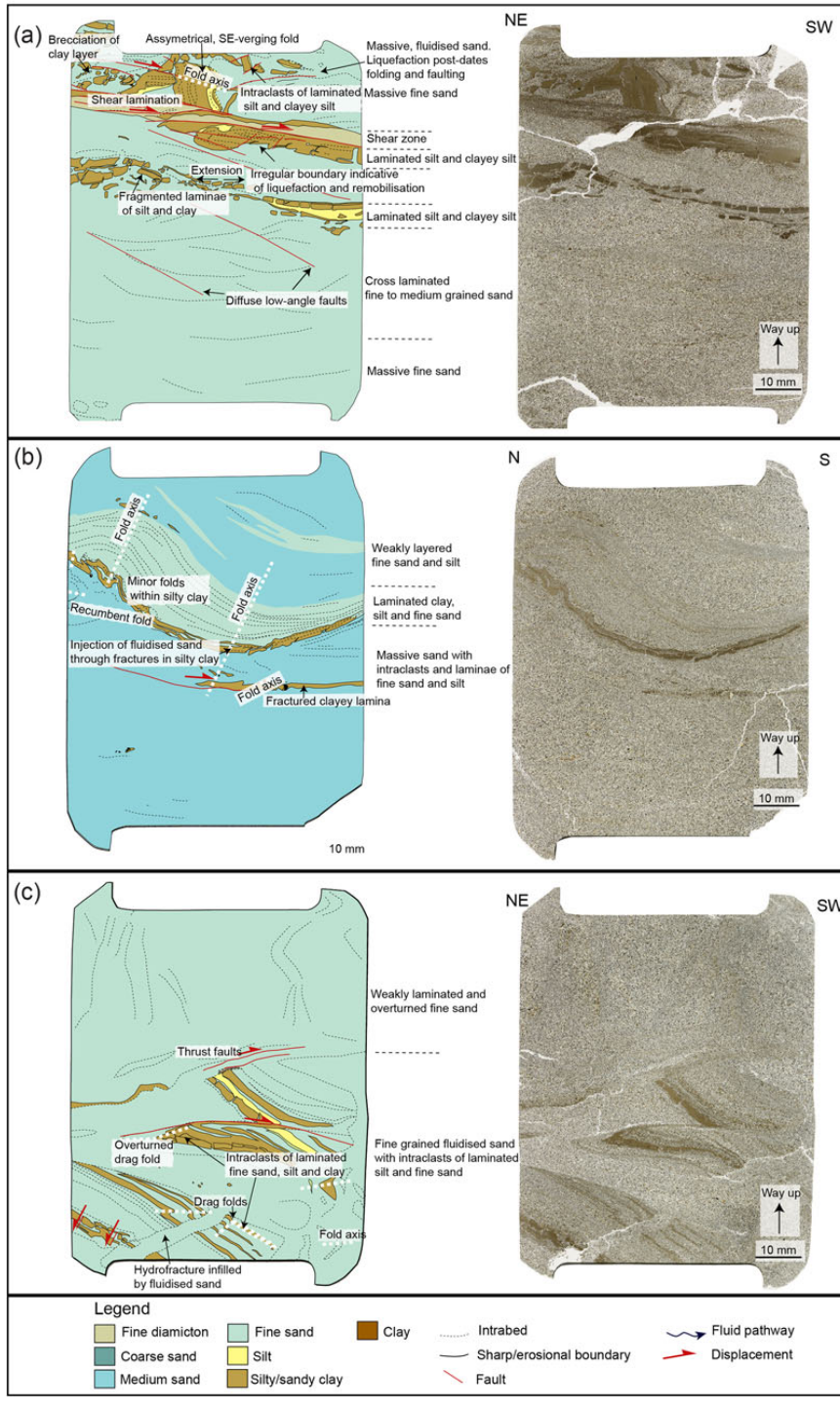

Figure 11. (colour online) Interpretation diagram of samples Mel 16 (a), Mel 14 (b), and Mel 11 (c). The samples were collected from bedded/laminated glaciomarine sand and silt/clay located below the thrust-block detachment. The sampling locations are marked in Figure 10. These thin sections reveal that the folded interlaminated sediments are crosscut by hydrofractures and faults/shears.

accompanying the liquefaction of the adjacent sand (Fig. 11). Locally, the clayey intraclasts are dispersed within the fluidised silt and sand (see upper part in sample Mel 16; Fig. 11a), although they usually have sharp edges and are often aligned and partly preserve the primary layering indicating a short transport pathway. The bedded/laminated clays, silts, and sands are locally folded with the vergence of folds recording an apparent sense of shear toward the southwest (see Mel 14; Fig. 11b). In the lower half of thin section Mel 11 (Fig. 11c), the folded, bedded/laminated clay, silt, and sand are crosscut by a vein infilled by open-packed fine sand. Within this sand layer, there are intraclasts of laminated sand, silt, and clay with smooth edges. This relationship suggests that the sand layer was injected into the preexisting interlaminated sediment resulting in hydrofracturing and brecciation of the host sediments. Intraclasts from the host sediments would then be incorporated into the sediments being injected into the developing hydrofracture. As described previously, the deformed unit E sediments are crosscut by a number of shears and faults, some of which are clearly visible in thin section (e.g., Mel 16; Fig. 11a).

DEVELOPMENT OF THE ÁSGIL AND MELALEITI THRUST-BLOCK MORAINES: A SEQUENTIAL MODEL AND DISCUSSION

The detailed macro- and microscale study of the detachments within the Ásgil and Melaleiti thrust moraines shows that their development was accompanied by repeated phases of sediment liquefaction, injection, and hydrofracturing. The observed microstructural relationships indicate that these processes occurred during the transport and emplacement of the autochthonous sediment blocks. This sequence of events associated with the detachment, transport, and emplacement of thrust blocks in the moraines can be explained in terms of a detailed four-stage model (Fig. 12).

Stage 1: detachment

The structural architecture of the moraines exposed in Melabakkar-Ásbakkar indicates that they formed in response to south/southeastward-directed ice push by a glacier advancing from Borgarfjörður (Fig. 1b) (Ingólfsson, 1987, 1988; Sigfúsdóttir et al., 2018). Thus, the thrust blocks comprising the moraines at Ásgil and Melaleiti can be assumed to be derived offshore, north/northwest of the study site. As the moraines were formed in a submarine setting (Ingólfsson, 1987, 1988; Sigfúsdóttir et al., 2018), the sediment blocks that were detached, displaced, and stacked to form the thrust-block moraines were presumably unfrozen and water saturated during glaciotectonism.

The earliest phase of deformation recorded by the thrust-block sediments at Ásgil is the liquefaction of the silt and fine-grained sand layers toward the base of the thrust block, indicative of increasing porewater pressures within the sediments as they are being deformed. Although it is uncertain if the liquefaction occurred during detachment or at a later stage during thrust-stack development, it would have dramatically lowered the shear strength of the sediment facilitating deformation and enabling low-frictional detachments to form within the substratum (Moran et al., 1980; Bluemle and Clayton, 1984; Phillips et al., 2007; Phillips and Merritt, 2008; Burke et al., 2009; Vaughan-Hirsch et al., 2013) (Fig. 12, stage 1). Detachments typically develop within weak, sorted sand and silt layers contained (sealed) between more impermeable layers (clay, diamicton, bedrock) enabling porewater pressures to build up within the silts and sands (Bluemle and Clayton, 1984; van der Wateren, 1985; Croot, 1987; Boulton and Caban, 1995; Phillips and Merritt, 2008; Vaughan-Hirsch and Phillips, 2017) (Fig. 12, stage 1). Consequently, laterally extensive, subhorizontal beds of silt/sand within the glaciomarine deposits at Melasveit are considered to have provided a focus for initial deformation, leading to thrust propagation and the detachment of the slablike sediment blocks.

Elevated porewater pressures within ice-marginal/proglacial sediments are likely to occur because of ice load, tectonic thickening, and basal shear stress applied by the advancing glacier (van der Wateren, 1985; Boulton and Caban, 1995). Also, it is likely that preferential flow of subglacial meltwater toward the ice margin from compressed subglacial deposits farther upglacier and/or external sources (i.e., surface melting) might have contributed to further elevating the water content/pressures within the deforming sequence (Boulton et al., 2001, Vaughan-Hirsch and Phillips, 2017). Syntectonic subaquatic outwash sediments forming lenticular aprons/fans along the leading edge of some of the moraines in Melasveit (i.e., Ásgil) indicate that the large-scale glaciotectonism at Melasveit was associated with high meltwater fluxes (Sigfúsdóttir et al., 2018). This relationship, as well as evidence for sustained pressurised water flow along the developing detachments (see Stage 2 and 3), may even be used to support that the advances that resulted in the formation of the moraines were a result of accelerated ice flow or possibly surging. This is because a rapid application of glaciotectonic stress would have favoured overpressurisation of the subglacial meltwater and, thus, formation of thrust-block moraines (e.g., Kamb et al., 1985; Kamb, 1987; Piotrowski and Tulaczyk, 1999; Fischer and Clarke, 2001; Kjær et al., 2006; Phillips et al., 2013, 2018).

Stage 2: proglacial/ice-marginal thrusting and movement along the décollements

Because of gravity spreading and compression from the rear caused by the weight gradient at the ice margins and the ice flow, respectively (Fig. 12, stage 2) (Rotnicki, 1976; Pedersen, 1987; Aber et al., 1989; van der Wateren, 1995; Bennett, 2001; Pedersen, 2005; Aber and Ber, 2007; Sigfúsdóttir et al., 2018), the detached sediment blocks were "pushed"/"displaced" forward by the advancing glacier (Fig. 12, stage 2). The transport of the allochthonous sdiment blocks was most likely aided by continued elevated porewater pressures and fluid flow being maintained along the earlier formed detachments. Evidence for this is provided by the repeated phases

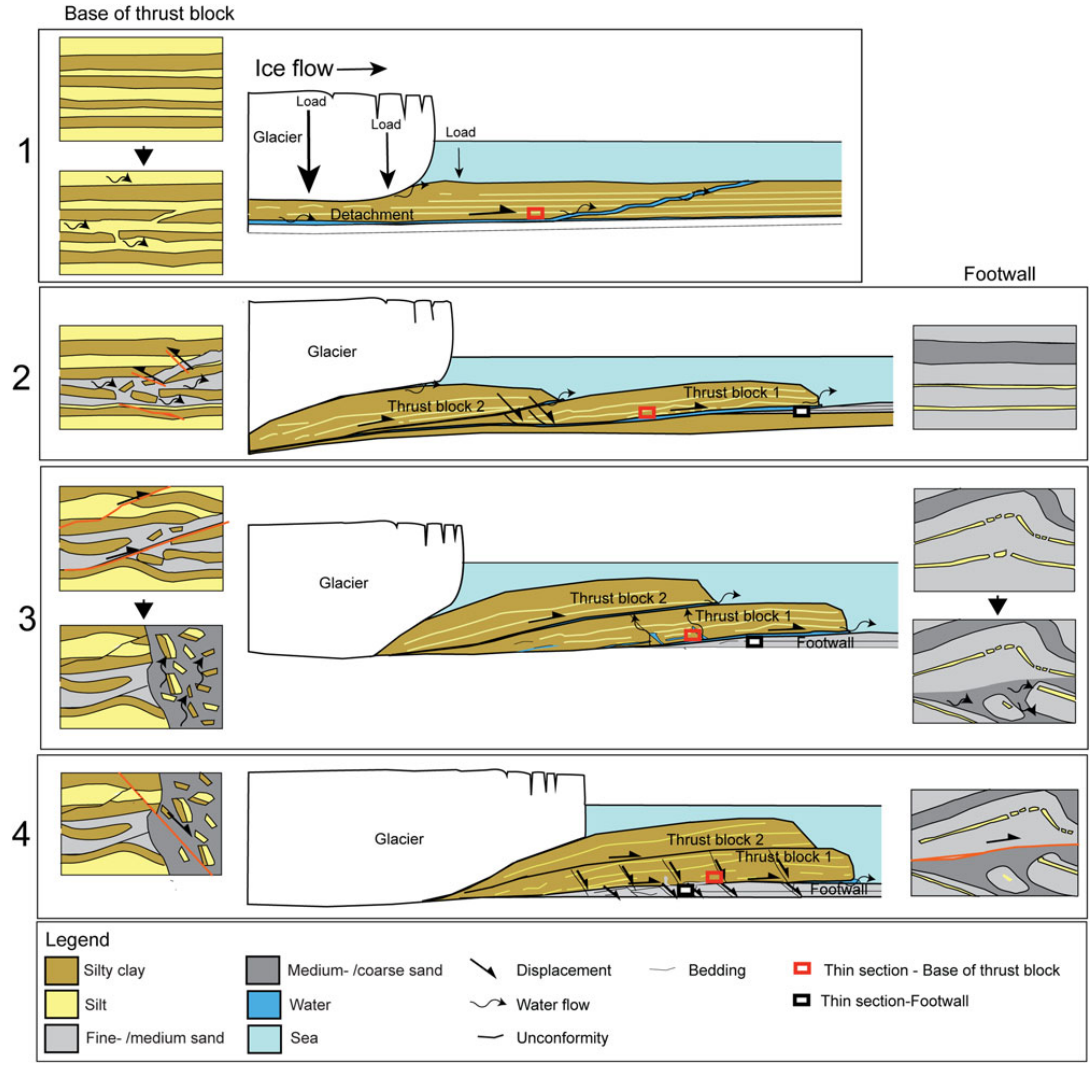

Figure 12. (colour online) A sequential model explaining the formation of the moraines. See text for detailed description. Stage 1: As the glacier advanced across the seafloor, water pressures rose within the glaciomarine sediments. Porewater pressures build up within silt and sand layers sealed between less permeable deposits. This caused liquefaction of the silt and sand enabling large sediment blocks to decouple from the underling sediments/or bedrock. Stage 2: The sediment blocks were transported forward because of gravity spreading and ice push. Repeated phases of sediment liquefaction and injection occurred along the earlier developed detachment resulting in formation of a complex hydrofracture system along the base of the sediment blocks. The deformation associated with the transport was focused within this relative thin, water-lubricated zone. Stage 3: The dislocated thrust blocks were stacked at the ice margins to form thrust-block moraines. The thrust blocks were accreted on top of highly permeable deposits of sands and gravels. Initially, the thrust blocks slid over the water-saturated sands and gravels without much internal deformation, but with increased sediment draining and elevated overburden pressures, the friction increased. This resulted in folding and faulting separated by events of hydrofracturing and water escape. Stage 4: Further draining of the sediments led to brittle deformation (faulting) and lockup of the thrust blocks. The Melaleiti moraine was subsequently overridden, but the Ásgil moraine was not (Sigfúsdóttir et al., 2018).

of liquefaction and injection along these décollement surfaces, thereby minimising the amount of shear being transmitted into the adjacent sediments and facilitating the displacement of the large slabs of unconsolidated sediments by the advancing ice. The detachments would have acted as fluid pathways, focusing water escape within the relatively clay-rich glaciomarine sequence and facilitating the southward migration of water through the deforming sediment pile.

At Ásgil, the complex, crosscutting sets of hydrofractures and associated brecciation of the sediments within a relatively thin "deformation zone" at the base of the thrust block clearly indicate that water pressures within the deforming sediment pile repeatedly exceeded the cohesive strength of these deposits. Crosscutting relationships between different generations of hydrofractures observed in the thin sections imply that the grain size of the sediments infilling this evolving hydrofracture system generally increased (Fig. 12, stage 2). This may be explained by increasing water pressures, widening of the hydrofractures, or simply the increased availability of coarse-grained sediments as the thrust block overrode the subaquatic fan deposited in front of the evolving moraine (see stage 3). Well-defined, sharp, erosive contacts between the hydrofractures show that they were probably formed in response to several phases of injection and fragmentation of the sediments between periods of partial solidification of the deposits rather than gradual changes in flow regime during a single event (Fig. 12, stage 2). These variations could either be because of fluctuations in the submarginal hydrology (water input) or release of hydrostatic pressure because of periodic water escape toward the front of the evolving imbricate thrust stack. This potentially resulted in a stick-slip type of movement along water-lubricated surfaces (subhorizontal hydrofractures) developed along the base of the thrust blocks (Boulton et al., 2001; Phillips and Merritt, 2008). The movement was largely focused along those water-lubricated surfaces that were active at a particular moment but may then have switched following local drainage and activation of new water-lubricated thrusts.

Stage 3: development of the thrust-block moraines

The dislocated thrust blocks were accreted at the ice margin leading to the formation of the glaciotectonic thrust-block moraines (Fig. 12, stage 3). At Melaleiti, the thrust blocks were emplaced on a less compact and permeable sequence of interbedded silt, sand, and gravel of the underlying thrust blocks. Similarly, at Ásgil, the detached thrust blocks were emplaced on a sequence of ice-marginal sands and gravels, which were deposited at an earlier stage during the readvance. Despite the high permeability of these underlying deposits, which would have facilitated drainage of the proposed water-lubricated basal detachments, the lowermost block is thought to have been transported across the coarser-grained sediments in the footwall resulting in little disturbance of these sediments below the leading edge of the thrusts (Fig. 12, stage 2). This is thought to indicate that, initially, the leading edges of the thrust blocks were in effect "decoupled" from the underlying sediments, possibly indicating that the rate of subglacial meltwater being transmitted through the basal detachment temporarily exceeded the rate at which water was dissipated through the footwall sediments. The subaquatic setting may have aided this process because of the water-saturated sediments and relatively low hydraulic gradient at the margins, which may have led to slower meltwater release. Furthermore, consistently high subglacial water pressures are maintained below water-terminating glaciers as the minimum value is determined by the pressure exerted by the proglacial water column (Benn et al., 2007; Sugiyama et al., 2011). All this may have contributed to low effective pressures and facilitated low frictional sliding of the glacier and the thrust blocks.

Eventually, however, the presence/introduction of highly permeable sand and gravel within the footwall of the thrust, possibly coupled with increasing overburden pressures below the evolving thrust-block moraine, resulted in the partial dewatering of this basal detachment and increased effective pressures. This led to an increased cohesive strength of the sediments and frictional drag between the allochthonous thrust block (hanging wall) and the underlying footwall. This process resulted in the locking up of the basal décollement and possibly contributed to further accretion of the thrust block onto the up-ice side of the evolving glaciotectonic landform (Fig. 12, stage 3).

The northward increase in the relative intensity of deformation (folding, faulting) within the up-ice sections of both the Ásgil and Melaleiti (Figs. 2 and 9) moraines is consistent with increased amount of shearing within the structurally deeper parts of the evolving glaciotectonic landforms (Fig. 12, stage 3). Detailed analysis of the thin sections taken from the base of the thrust blocks and the footwall sediments within the structurally deeper parts of the moraines reveal that this deformation involved a complex interplay between ductile shearing (folding and faulting) and sediment liquefaction, injection, hydrofracturing, and brecciation (Fig. 12, stage 3).

Large hydrofractures formed within the Ásgil moraine during this phase of thrust stacking, extending from the sands and gravels in the footwall, and cutting upward into the overlying, rigid thrust block. The upward infilling is consistent with potential formation of these hydrofractures in a submarginal/proglacial setting where the pressurised water at depth is able to escape up toward the surface because of the decrease in overburden pressures (Boulton and Caban, 1995; van der Meer et al., 2009; Phillips et al., 2012; Ravier et al. 2015). Although, the Melasveit moraines were formed in a subaquatic setting, which would have affected the stress gradient at the margins, the development of the hydrofractures most likely followed a similar pattern as recorded in terrestrial settings because of lower overburden pressures toward and in front of the grounded ice margins (Benediktsson et al., 2008, 2010; Phillips et al., 2013; Ravier et al., 2015). The large hydrofractures suggest that the pressures within the subglacial hydrogeologic system temporarily increased during the late stage of the glaciotectonism, possibly because of increasing overburden pressures during the displacement and accretion of the thrust blocks onto the up-ice side of the evolving glaciotectonic landform. Additionally/alternatively, the impermeable sediment within the thrust blocks, coupled with the deposition of an ice-marginal fan/apron, may have impeded the escape of meltwater from beneath the ice margin, resulting in an increased hydrostatic pressure within the subglacial hydrogeologic system. The hydrofracturing led to increased permeability of the thrust

stack and possibly facilitated a decrease in water pressures below the evolving thrust-block moraine (Phillips et al., 2012).

Stage 4: emplacement

The fall in water pressures within the deforming sediments coupled with hydrofracturing and fluid escape toward the leading edge of the evolving thrust stack resulted in dewatering of the deforming sediment pile (Fig. 12, stage 4). This, in turn, led to progressive increase in friction between the base of the thrust blocks and the underlying deposits (Phillips et al., 2007; Benediktsson et al., 2008, 2010) contributing to the cessation of displacement of the allochthonous blocks and their accretion onto the up-ice side of the evolving thrust-block moraine. Field evidence from both Ásgil and Melaleiti indicates that the initial ductile deformation structures (i.e., folds) and hydrofractures are postdated by discrete faulting and thrusting, recording a switch from ductile to brittle deformation associated with the dewatering of the deforming sequence. The crosscutting relationship between the faults and the detachments at the base of the thrust blocks clearly indicates that these moderate to high-angle brittle structures developed both prior to and after the final emplacement of the thrust blocks. At Ásgil, most of the faults are small and only record minor displacement (up to a few decimetres). However, at Melaleiti, a high number of larger-scale faults and subhorizontal shears were observed crosscutting the earlier developed ductile structures within the high-strain zone at the base of the thrust blocks. Most of the faults dip toward the southeast (down-ice) and probably formed initially as down-ice dipping Reidel shears in response to simple shear (cf. Phillips and Lee, 2011) related to the riding of the structurally higher thrust block over the underlying thrust block, which had already been emplaced.

CONCLUSIONS

Based on a microscale study of detachments within two ice-marginal thrust-block moraines in Melasveit, western Iceland, we propose a detailed structural model for processes occurring during glaciotectonic thrusting, including the detachment, transport, and accretion of large, rigid sediment blocks.

The initial detachment of the sediment blocks most likely took place in response to ice push and gravity spreading at the margins of the advancing glacier. Overpressurised submarginal/proglacial groundwater led to fluidisation of bedded/laminated glaciomarine sediments and detachment along water-lubricated layers.

The transport of the sediment blocks was aided by elevated porewater pressures along the detachments. This minimised the amount of shear transmitted into the large, unconsolidated, and unfrozen sediment blocks allowing them to be transported by the glacier. Water pressures within the deforming sediment pile repeatedly exceeded the cohesive strength of these blocks during emplacement and accretion resulting in hydrofracturing and fluid escape toward the front of the thrust blocks.

The leading edges of the thrust blocks were in effect "decoupled" from the underlying sediments resulting in only minor disturbance of the footwall. However, the relative intensity of deformation (folding, faulting) increased up-ice, as well as the amount of shearing within the structurally deeper parts of the evolving glaciotectonic landforms.

During the final stages of the formation of the thrust-block moraines, a switch from ductile to brittle deformation was associated with partial dewatering and fall in water pressures. This resulted in the cessation of displacement of the blocks and their accretion onto the up-ice side of the evolving thrust-block moraine.

This study stresses the role of overpressurised porewater within submarginal/pro-glacial sediments in the transport of unfrozen and unlithified thrust blocks during large-scale glaciotectonism. The hydrogeology along with the lithologic characteristics of the deforming sediments were the key factors in controlling the changing style of deformation during the detachment, transport, and accretion of the thrust blocks.

SUPPLEMENTARY MATERIAL

The supplementary material for this article can be found at https://doi.org/10.1017/qua.2019.48.

ACKNOWLEDGMENTS

This project was funded by the Icelandic Research Fund (grant no. 141002-051 to Í. Ö. Benediktsson) and the Royal Physiographic Society in Lund (grants to T. Sigfúsdóttir and Í. Ö. Benediktsson). Additional support was provided by the British Geological Survey (to E. Phillips). We would like to thank Heimir Ingimarsson, Sandrine Roy, and Kim Teilmann for their assistance in the field. Thanks are also due to Rob Storrar and an anonymous referee for constructive reviews that improved this paper. E. Phillips publishes with permission of the executive director of the British Geological Survey.

REFERENCES

Aber, J.S., 1988. Ice-shoved hills of Saskatchewan compared with Mississippi Delta mudlumps: implications for glaciotectonic models. In: Croot, D.G. (Ed.), Glaciotectonic *Forms and Processes*. Balkema, Rotterdam, the Netherlands, pp. 1–9.

Aber, J.S., Ber, A. 2007. *Glaciotectonism. Developments in Quaternary Science 6*. Elsevier, Amsterdam.

Aber, J.S., Croot, D.G., Fenton, M.M., 1989. *Glaciotectonic Landforms and Structures*. Springer, Dordrecht, the Netherlands.

Alley, R., 1989. Water-pressure coupling of sliding and bed deformation: I. Water system. *Journal of Glaciology* 35, 108–118.

Banham, P.H., 1975. *Glaciotectonic Structures: A General Discussion with Particular Reference to Contorted Drift of Norfolk*. Seal House Press, Liverpool, UK.

Baroni, C., Fasano, F., 2006. Micromorphological evidence of warm-based glacier deposition from the Ricker Hills Tillite (Victoria Land, Antarctica). *Quaternary Science Reviews* 25, 976–992.

Benediktsson, Í.Ö., Möller, P., Ingólfsson, Ó., van der Meer, J.J.M., Kjær, K.H., Krüger, J., 2008. Instantaneous end moraine and

sediment wedge formation during the 1890 glacier surge of Brúarjökull, Iceland. *Quaternary Science Reviews* 27, 209–234.

Benediktsson, Í.Ö., Schomacker, A., Johnson, M.D., Geiger, A.J., Ingólfsson, Ó., Guðmundsdóttir, E.R., 2015. Architecture and structural evolution of an early Little Ice Age terminal moraine at the surge-type glacier Múlajökull, Iceland. *Journal of Geophysical Research: Earth Surface* 120, 1895–1910.

Benediktsson, Í.Ö., Schomacker, A., Lokrantz, H., Ingólfsson, Ó., 2010. The 1890 surge end moraine at Eyjabakkajökull, Iceland: a re-assessment of a classic glaciotectonic locality. *Quaternary Science Reviews* 29, 484–506.

Benn, D.I., Evans, D.J.A., 2010. *Glaciers and Glaciation*. Hodder Education, London.

Benn, D.I., Warren, C.R., Mottram, R.H., 2007. Calving processes and the dynamics of calving glaciers. *Earth-Science Reviews* 82, 143–179.

Bennett, M.R., 2001. The morphology, structural evolution and significance of push moraines. *Earth-Science Reviews* 53, 197–236.

Bluemle, J.P., Clayton, L., 1984. Large-scale glacial thrusting and related processes in North Dakota. *Boreas* 13, 279–299.

Boulton, G.S., Caban, P., 1995. Groundwater flow beneath ice sheets: part II— its impact on glacier tectonic structures and moraine formation. *Quaternary Science Reviews* 14, 563–587.

Boulton, G.S., Dent, D.L., Morris, E.M., 1974. Subglacial shearing and crushing, and the role of water pressures in tills from southeast Iceland. *Geografiska Annaler: Series A, Physical Geography* 56, 135–145.

Boulton, G.S., Dobbie, K.E., Zatsepin, S., 2001. Sediment deformation beneath glaciers and its coupling to the subglacial hydraulic system. *Quaternary International* 86, 3–28.

Boulton, G.S., Van der Meer, J.J.M., Beets, D.J., Hart, J.K., Ruegg, G.H.J., 1999. The sedimentary and structural evolution of a recent push moraine complex, Holmstrombreen, Spitsbergen. *Quaternary Science Reviews* 18, 339–371.

Broster, B.E., Seaman, A.A., 1991. Glacigenic rafting of weathered granite. *Canadian Journal of Earth Sciences* 28, 649–654.

Burke, H., Phillips, E.R., Lee, J.R., Wilkinson, I.P., 2009. Imbricate thrust stack model for the formation of glaciotectonic rafts: an example from the Middle Pleistocene of north Norfolk, UK. *Boreas* 38, 620–637.

Clayton, L., Moran, S.R., 1974. A glacial process-form model. In: Coates, D.R. (Ed.), *Glacial geomorphology*. Binghampton State University of New York Publications in Geomorphology, 89–119.

Croot, D.G., 1987. Glacio-tectonic structures: a mesoscale model of thin-skinned thrust sheets? *Journal of Structural Geology* 9, 797–808.

Evans, D.J.A., 2018. *Till: A Glacial Process Sedimentology*. Wiley-Blackwell, Chichester, West Sussex, UK.

Evans, D.J.A., England, J., 1991. High Arctic thrust block moraines. *Canadian Geographer/Le Géographe canadien* 35, 93–97.

Fischer, U.H., Clarke, G.K.C., 2001. Review of subglacial hydro-mechanical coupling: Trapridge Glacier, Yukon Territory, Canada. *Quaternary International* 86, 29–43.

Franzson, H., 1978. Structure and Petrochemistry of the Hafnarfjall-Skarðsheiði Central Volcano and the Surrounding Basalt Succession, W-Iceland. *University of Edinburgh*, Edinburgh, UK.

Hart, J.K., 1994. Proglacial glaciotectonic deformation at Melabakkar-Ásbakkar, west Iceland. *Boreas* 23, 112–121.

Hart, J.K., Roberts, D.H., 1994. Criteria to distinguish between subglacial glaciotectonic and glaciomarine sedimentation, I. Deformation styles and sedimentology. *Sedimentary Geology* 91, 191–213.

Hiemstra, J., van der Meer, J., 1997. Pore-water controlled grain fracturing as an indicator for subglacial shearing in tills. *Journal of Glaciology* 43, 446–454.

Huddart, D., Hambrey, M.J., 1996. Sedimentary and tectonic development of a high-arctic, thrust-moraine complex: Comfortlessbreen, Svalbard. *Boreas* 25, 227–243.

Ingólfsson, Ó., 1987. The Late Weichselian glacial geology of the Melabakkar-Asbakkar coastal cliffs, Borgarfjörður, W-Iceland. *Jökull* 37, 57–81.

Ingólfsson, Ó., 1988. Glacial history of the lower Borgarfjördur area, western Iceland. *Geologiska Föreningens i Stockholm Förhandlingar* 110, 293–309.

Ingólfsson, Ó., Norddahl, H., 2001. High relative sea level during the Bolling Interstadial in western Iceland: a reflection of ice-sheet collapse and extremely rapid glacial unloading. *Arctic, Antarctic, and Alpine Research* 33, 231–243.

Ingólfsson, Ó., Norddahl, H., Schomacker, A., 2010. 4 Deglaciation and Holocene glacial history of Iceland. In: Schomacker, A., Krüger, J., Kjær, K.H. (Eds.), *Developments in Quaternary Sciences*. Vol. 13, The Mýrdalsjökull Ice Cap, Iceland: Glacial Processes, Sediments and Landforms on an Active Volcano. Elsevier, Amsterdam, pp. 51–68.

Jennings, A., Syvitski, J., Gerson, L., Grönvold, K., Geirsdóttir, Á., Hardardóttir, J., Andrews, J., Hagen, S., 2000. Chronology and paleoenvironments during the late Weichselian deglaciation of the southwest Iceland shelf. *Boreas* 29, 163–183.

Kamb, B., 1987. Glacier surge mechanism based on linked cavity configuration of the basal water conduit system. *Journal of Geophysical Research: Solid Earth* 92, 9083–9100.

Kamb, B., Raymond, C.F., Harrison, W.D., Engelhardt, H., Echelmeyer, K.A., Humphrey, N., Brugman, M.M., Pfeffer, T., 1985. Glacier surge mechanism: 1982–1983 surge of Variegated Glacier, Alaska. *Science* 227, 469–479.

Khatwa, A., Tulaczyk, S., 2001. Microstructural interpretations of modern and Pleistocene subglacially deformed sediments: the relative role of parent material and subglacial processes. *Journal of Quaternary Science* 16, 507–517.

Kjær, K.H., Larsen, E., van der Meer, J., Ingólfsson, Ó., Krüger, J., Benediktsson, Í. Ö., Knudsen, C.G., Schomacker, A., 2006. Subglacial decoupling at the sediment/bedrock interface: a new mechanism for rapid flowing ice. *Quaternary Science Reviews* 25, 2704–2712.

Menzies, J., 2000. Micromorphological analyses of microfabrics and microstructures indicative of deformation processes in glacial sediments. *Geological Society, London, Special Publications* 176, 245–257.

Moon, T., Joughin, I., Smith, B., Broeke, M.R., Berg, W.J., Noël, B., Usher, M., 2014. Distinct patterns of seasonal Greenland glacier velocity. *Geophysical Research Letters* 41, 7209–7216.

Moran, S.R., Clayton, L., Hooke, R.L., Fenton, M.M., Andriashek, L.D., 1980. Glacier-bed landforms of the prairie region of North America. *Journal of Glaciology* 25, 457–476.

Neudorf, C.M., Brennand, T.A., Lian, O.B., 2013. Till-forming processes beneath parts of the Cordilleran Ice Sheet, British Columbia, Canada: macroscale and microscale evidence and a new statistical technique for analysing microstructure data. *Boreas* 42, 848–875.

Norddahl, H., Ingólfsson, Ó., 2015. Collapse of the Icelandic ice sheet controlled by sea-level rise? *Arktos* 1, 13.

Norddahl, H., Ingólfsson, Ó., Pétursson, H.G., Hallsdóttir, M., 2008. Late Weichselian and Holocene environmental history of Iceland. *Jökull* 58, 343–364.

Patton, H., Hubbard, A., Bradwell, T., Schomacker, A., 2017. The configuration, sensitivity and rapid retreat of the Late Weichselian Icelandic ice sheet. *Earth-Science Reviews* 166, 223–245.

Pedersen, S.A.S., 1987. Comparative studies of gravity tectonics in Quaternary sediments and sedimentary rocks related to fold belts. In: Jones, M.E., Preston, R.M.F. (Eds.), *Deformation of Sediments and Sedmentary Rocks*. Geological Society, London, Special Publications 29, 165–179.

Pedersen, S.A.S., 2005. Structural Analysis of the Rubjerg Knude Glaciotectonic Complex, Vendsyssel, Northern Denmark. Geological Survey of Denmark and Greenland Bulletin 8. Geological Survey of Denmark and Greenland, Danish Ministry of the Environment, Copenhagen.

Phillips, E., Cotterill, C., Johnson, K., Crombie, K., James, L., Carr, S., Ruiter, A., 2018. Large-scale glacitectonic deformation in response to active ice sheet retreat across Dogger Bank (southern central North Sea) during the Last Glacial Maximum. *Quaternary Science Reviews* 179, 24–47.

Phillips, E., Everest, J., Evans, D.J.A., Finlayson, A., Ewertowski, M., Guild, A., Jones, L., 2017. Concentrated, 'pulsed' axial glacier flow: structural glaciological evidence from Kvíárjökull in SE Iceland. *Earth Surface Processes and Landforms* 42, 1901–1922.

Phillips, E., Everest, J., Reeves, H., 2012. Micromorphological evidence for subglacial multiphase sedimentation and deformation during overpressurized fluid flow associated with hydrofracturing. *Boreas* 42, 395–427.

Phillips, E., Lipka, E., van der Meer, J.J.M., 2013. Micromorphological evidence of liquefaction, injection and sediment deposition during basal sliding of glaciers. *Quaternary Science Reviews* 81, 114–137.

Phillips, E., Merritt, J., 2008. Evidence for multiphase water-escape during rafting of shelly marine sediments at Clava, Inverness-shire, NE Scotland. *Quaternary Science Reviews* 27, 988–1011.

Phillips, E., Merritt, J., Auton, C., Golledge, N., 2007. Microstructures in subglacial and proglacial sediments: understanding faults, folds and fabrics, and the influence of water on the style of deformation. *Quaternary Science Reviews* 26, 1499–1528.

Phillips, E.R., Auton, C.A., 2000. Micromorphological evidence for polyphase deformation of glaciolacustrine sediments from Strathspey, Scotland. *Geological Society, London, Special Publications* 176, 279–292.

Phillips, E.R., Lee, J.R., 2011. Description measurement and analysis of glacitectonically deformed sequences. In: Phillips, E.R., Lee, J.R., Evans, H.M. (Eds.), *Glacitectonics: Field Guide*. Quaternary Research Association, London, pp. 5–31.

Phillips, E.R., van der Meer, J.J.M., Ferguson, A. 2010. A new 'microstructural mapping' methodology for the identification and analysis of microfabrics within glacial sediments. *Quaternary Science Reviews* 30, 2570–2596.

Piotrowski, J.A., Tulaczyk, S., 1999. Subglacial conditions under the last ice sheet in northwest Germany: ice-bed separation and enhanced basal sliding? *Quaternary Science Reviews* 18, 737–751.

Ravier, E., Buoncristiani, J.-F., Menzies, J., Guiraud, M., Portier, E., 2015. Clastic injection dynamics during ice front oscillations: a case example from Sólheimajökull (Iceland). *Sedimentary Geology* 323, 92–109.

Rijsdijk, K.F., Owen, G., Warren, W.P., McCarroll, D., van der Meer, J.J.M., 1999. Clastic dykes in over-consolidated tills: evidence for subglacial hydrofracturing at Killiney Bay, eastern Ireland. *Sedimentary Geology* 129, 111–126.

Rotnicki, K., 1976. The theoretical basis for and a model of the origin of glaciotectonic deformations. *Quaestiones Geographicae* 3, 103–139.

Ruszczynska-Szenajch, H., 1987. The origin of glacial rafts: detachment, transport, deposition. *Boreas* 16, 101–112.

Rüther, D.C., Andreassen, K., Spagnolo, M., 2013. Aligned glaciotectonic rafts on the central Barents Sea seafloor revealing extensive glacitectonic erosion during the last deglaciation. *Geophysical Research Letters* 40, 6351–6355.

Sigfúsdóttir, T., Benediktsson, Í.Ö., Phillips, E., 2018. Active retreat of a Late Weichselian marine-terminating glacier: an example from Melasveit, western Iceland. *Boreas* 47, 813–836.

Sole, A.J., Mair, D.W.F., Nienow, P.W., Bartholomew, I.D., King, M.A., Burke, M.J., Joughin, I., 2011. Seasonal speedup of a Greenland marine-terminating outlet glacier forced by surface melt–induced changes in subglacial hydrology. *Journal of Geophysical Research: Earth Surface* 116, F03014.

Sugiyama, S., Skvarca, P., Naito, N., Enomoto, H., Tsutaki, S., Tone, K., Marinsek, S., Aniya, M., 2011. Ice speed of a calving glacier modulated by small fluctuations in basal water pressure. *Nature Geoscience* 4, 597–600.

Syvitski, J.P., Jennings, A.E., Andrews, J.T., 1999. High-resolution seismic evidence for multiple glaciation across the southwest Iceland shelf. *Arctic, Antarctic, and Alpine Research* 31, 50–57.

van der Meer, J.J.M., 1987. Micromorphology of glacial sediments as a tool in distinguishing genetic varieties of till. *Geological Survey of Finland, Special Paper* 3, 77–89.

van der Meer, J.J.M., 1993. Microscopic evidence of subglacial deformation. *Quaternary Science Reviews* 12, 553–587.

van der Meer, J.J.M., Kjær, K.H., Krüger, J., Rabassa, J., Kilfeather, A.A., 2009. Under pressure: clastic dykes in glacial settings. *Quaternary Science Reviews* 28, 708–720.

van der Wateren, D.F.M., 1985. A model of glacial tectonics, applied to the ice-pushed ridges in the Central Netherlands. *Bulletin of the Geological Society of Denmark* 34, 55–74.

van der Wateren, F.M., 1995. Structural Geology and Sedimentology of Push Moraines: Processes of Soft Sediment Deformation in a Glacial Environment and the Distribution of Glaciotectonic Styles. Medelingen Rijks Geologische Dienst 54. Rijks Geologische Dienst, Haarlem, the Netherlands.

Vaughan-Hirsch, D.P., Phillips, E., Lee, J.R., Hart, J.K., 2013. Micromorphological analysis of poly-phase deformation associated with the transport and emplacement of glaciotectonic rafts at West Runton, north Norfolk, UK. *Boreas* 42, 376–394.

Vaughan-Hirsch, D.P., Phillips, E.R., 2017. Mid-Pleistocene thin-skinned glaciotectonic thrusting of the Aberdeen Ground Formation, Central Graben region, central North Sea. *Journal of Quaternary Science* 32, 196–212.

Paper III

Refining the history of Younger Dryas and Early Holocene glacier oscillations in the Borgarfjörður region, western Iceland

Thorbjörg Sigfúsdóttir and Ívar Örn Benediktsson

Thorbjörg Sigfúsdóttir (thorbjorg.sigfusdottir@geol.lu.se), Department of Geology, Lund University, Sölvegatan 12, 223 62 Lund, Sweden and Institute of Earth Sciences, University of Iceland, Sturlugata 7, 101 Reykjavík, Iceland; Ívar Örn Benediktsson, Institute of Earth Sciences, University of Iceland, Sturlugata 7, 101 Reykjavík, Iceland.

Abstract

The lower Borgarfjörður region, western Iceland, has been central to the reconstructions of the dynamics and collapse of the Icelandic Ice Sheet during the deglaciation. Here, extensive stratigraphic sections and landforms provide a rare opportunity to study past glacier dynamics in this part of Iceland. Previous studies reveal that a large outlet glacier in Borgarfjörður advanced during the Late Weichselian resulting in large-scale deformation of glaciomarine sediments and the formation of a series of ice-marginal moraines. However, the events recorded by these sediments and landforms are poorly constrained in time. We present and discuss 22 new radiocarbon dates in the context of recent reconstructions of the regional glacier dynamics in order to constrain the timing of the glacier oscillations. The results show that a dynamic, marine-terminating glacier advanced out of Borgarfjörður sometime after c. 13.0 cal. ka BP, resulting in the formation of an extensive moraine complex. The timing indicates that the advance occurred during climate cooling and widespread glacier expansions within the Younger Dryas (YD). Followed by the first initial advance, the glacier exhibited at least five readvances punctuated by phases of retreat. Each re-advance terminated proximal (within 5 km) to the outermost moraine complex although the extent of periodic retreat and the exact timing of these oscillations are unknown. All these phases of re-advance occurred prior to the onset of the Holocene (around 11.7 cal. ka BP), during which marine fauna re-colonized the area and the Borgarfjörður glacier retreated from the moraines. During the Early Holocene (sometime after c. 11.3 cal. ka BP), the Borgarfjörður glacier readvanced to a position within ~5 km of the YD ice limit. This is the first recorded Early Holocene large-scale glacier advance in western Iceland and suggests that glacier expansion in this region coincided with widespread advances elsewhere in Iceland.

Iceland is situated in a sensitive location in the North Atlantic where Arctic waters transported with the East Greenland Current and East Icelandic Current meet the relatively warm and saline Atlantic waters of the Irminger Current (Malmberg 1985; Björck et al. 1997; Eiríksson et al. 2000, 2004; Moffa-Sánchez et al. 2019). Variations in the strength of these currents therefore directly impact the climate in Iceland (Geirsdóttir et al. 2009; Ólafsdóttir et al. 2010). Numerous studies have indicated that glacier advances and retreats in Iceland during the Holocene were generally synchronous with fluctuations in climate (Hubbard et al. 2006; Geirsdóttir et al. 2009; Ingólfsson et al. 2010; Patton et al. 2017; Harning et al. 2018), although complex responses of individual glaciers show that this relationship is not straightforward (Kirkbride & Dugmore 2006; Brynjólfsson et al. 2015; Ingólfsson et al. 2016). In spite of improved knowledge of the Late Weichselian deglaciation history of Iceland in recent decades the records are still sporadic and often poorly constrained in time (Geirsdóttir et al. 2009; Norðdahl & Ingólfsson 2015). This hampers correlation between glacial and climate records and therefore our ability to understand the relationships between glacier dynamics and climate/oceanographic changes.

The lower Borgarfjörður region, western Iceland (Fig. 1), holds several key locations for studies of Late Weichselian glacier and environmental history in this part of Iceland and has been crucial for reconstructions of the collapse of the Icelandic Ice Sheet (IIS) during the deglaciation (Ingólfsson 1987, 1988; Ingólfsson & Norðdahl 2001; Ingólfsson et al. 2010; Sigfúsdóttir et al. 2018). The area accommodates well preserved glacial sediments

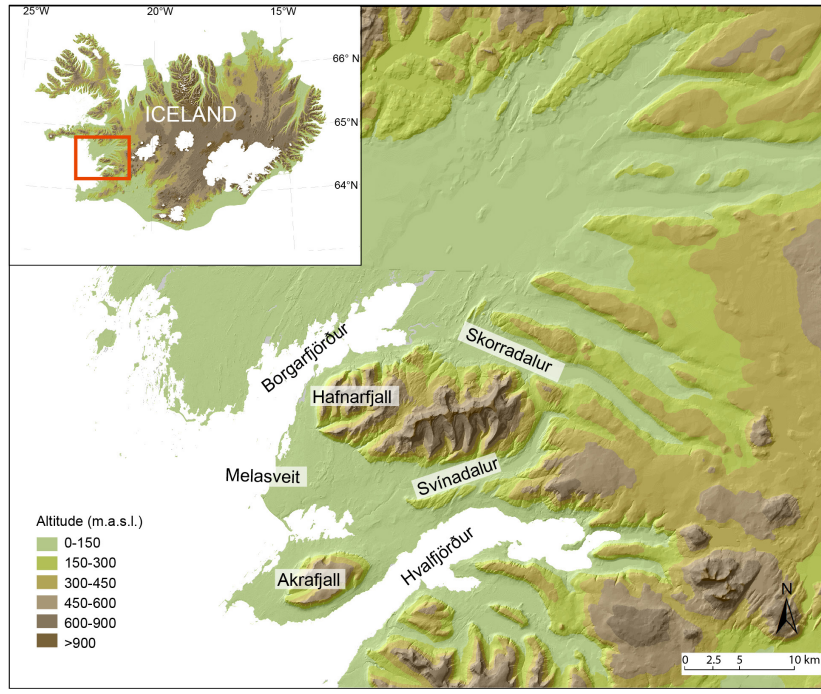

Figure 1. A topographic map of the lower-Borgarfjörður region based on a digital elevation model from the National Land Survey of Iceland (Landmælingar Íslands). Fjords, valleys and mountains mentioned in the text are labelled on the map.

and landforms from the deglaciation that record glacier fluctuations and sea level changes during that time. These sediments and landforms are exposed in extensive coastal and river sections providing insights into the glacial and environmental history.

Although the region has been studied by a number of researchers in the past (Bárðarson 1923, 1927; Ashwell 1975; Ingólfsson 1984, 1987, 1988; Hart 1994; Hart & Roberts 1994; Magnúsdóttir & Norðdahl 2000; Ingólfsson & Norðdahl 2001; Sigfúsdóttir et al. 2018), there are many stratigraphical and chronological problems left unsolved. Previous studies have also revealed contrasting results regarding the glacier dynamics and the timing of glacier advances and retreats, partly because of the shortage of data on the temporal and spatial extent of glaciers in western Iceland (Norðdahl & Pétursson 2005). In this paper, we present 22 new radiocarbon ages from marine molluscs retrieved from four sections in lower Borgarfjörður. These new data and earlier published ages from the region (Ingólfsson 1987, 1988; Ingólfsson & Norðdahl 2001) are merged in order to reassess the regional glacier history.

Regional setting

Borgarfjörður is a northeast-southwest trending fjord (Fig. 1) that was carved during Pleistocene glaciations into bedrock dominated by basalt lava flows of Neogene age (Franzson 1978; Ingólfsson 1984, 1988). The fjord and the associated valley is about 45 km long and up to 20 km wide and the bedrock in the lowland areas is largely covered by stratified, shell-bearing, glaciomarine sediments indicating extensive shallow marine/coastal waters in the Late Weichselian (Ashwell 1975; Ingólfsson 1988). A number of tributary valleys occur on the eastern side of Borgarfjörður, the southernmost of which is Skorradalur (Fig. 1). Skorradalur, as well as some of the other tributary valleys, is separated from the main fjord-valley system by a bedrock threshold. At the mouth of some of these valleys, deltas are found at around 65-80 m a.s.l., capping the threshold and recording meltwater outflow from tributary catchments (Ashwell 1967, 1975).

The southern part of Borgarfjörður is dominated by the steep slopes of the over 1000 m high Hafnarfjall-Skarðsheiði mountain massif (Franzson 1978). Southwest of Mt. Hafnarfjall, at the mouth of Borgarfjörður, is the lowland district of Melasveit and Leirársveit (Fig. 1). At some point during the Pleistocene ice streamed from the north-east along Borgarfjörður as well as from Hvalfjörður and Svínadalur and coalesced in the Leirársveit/Melasveit area (Fig. 1), as indicated by striations on bedrock (Ingólfsson 1988). The Melasveit area contains thick succession of Late Weichselian glacial and glaciomarine deposits that have largely undergone deformation by an outlet glacier from Borgarfjörður and possibly other outlet glaciers during the Late Weichselian

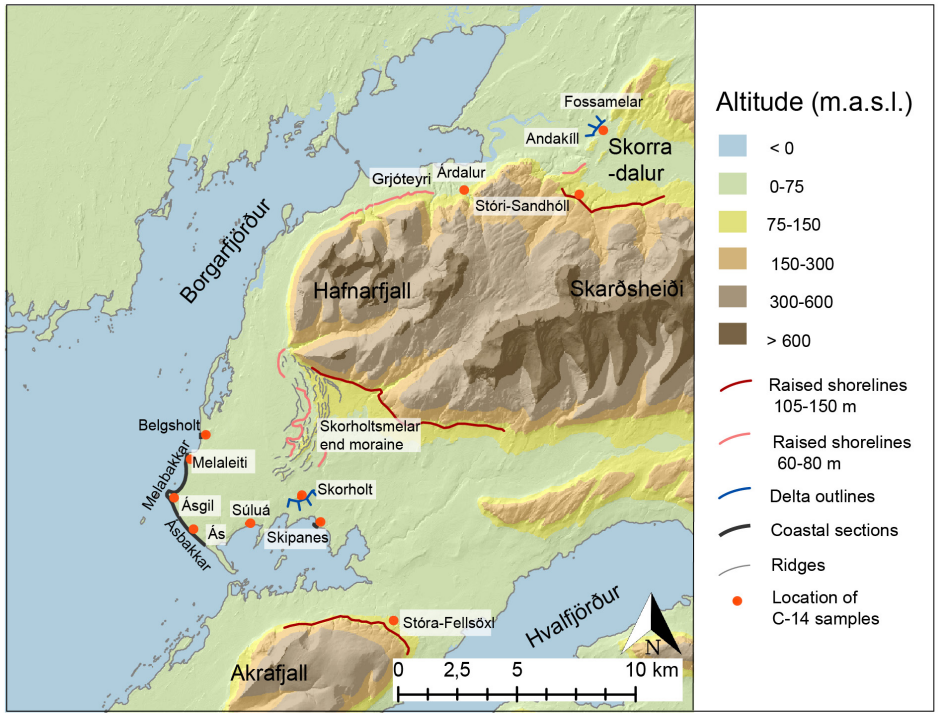

Figure 2. A topographic map of the Borgarfjörður region, including the Melasveit area, showing localities and the main geological features referred to in the text. The 60-70 m raised shorelines are drawn according to a reconstruction in Ingólfsson (1988), the 105-150 m shor-lines are drawn according to Magnúsdóttir and Norðdhal (2000) and Ingólfsson & Norðdahl (2001). The map excludes younger shorelines at lower levels. Base map from the National Land Survey of Iceland (Landmælingar Íslands)

(Ingólfsson 1988; Hart & Roberts 1994; Sigfúsdóttir et al. 2018). These deposits are mostly overlain by coarse littoral sand and gravel deposited during the isostatic readjustment of the area in the Early Holocene (Ingólfsson 1988). The most prominent glacial landform in Melasveit-Leirársveit is the multi-crested Skorholtsmelar moraine complex that is over 2 km long and rises more than 40 m above its surroundings (Fig. 2). Sets of marine shorelines that occur at different altitudes have been mapped in the area reflecting the complex interplay between the isostatic adjustments and eustatic sea levels changes (Ingólfsson 1988; Ingólfsson & Norðdahl 2001).

Review of previous research on the deglaciation history of the Lower-Borgarfjörður region

Deglaciation and Early-Bølling ice-sheet collapse

During the Last Glacial Maximum (LGM), the western part of the Icelandic Ice Sheet most likely extended to the shelf break around 200 km offshore (Hubbard et al. 2006; Norðdahl et al. 2008; Ingólfsson et al. 2010). It has been estimated that around 60% of the IIS was marine-based and thus highly vulnerable to changes in sea level and ocean temperatures (Ingólfsson & Norðdahl 2001; Hubbard et al. 2006; Norðdahl & Ingólfsson 2015; Patton et al. 2017). Around 15.0 cal. ka BP, at the start of Bølling, the western sector of the IIS experienced a rapid retreat, perhaps as a result of rising sea level due to degradation of the large Laurentide and Eurasian ice sheets in the Northern Hemisphere around that time (Syvitski et al. 1999, Andrews et al. 2000, Ingólfsson & Norðdahl 2001; Norðdahl & Ingólfsson 2015; Hughes et al. 2016; Patton et al. 2017; Margold et al. 2018). Evidence from

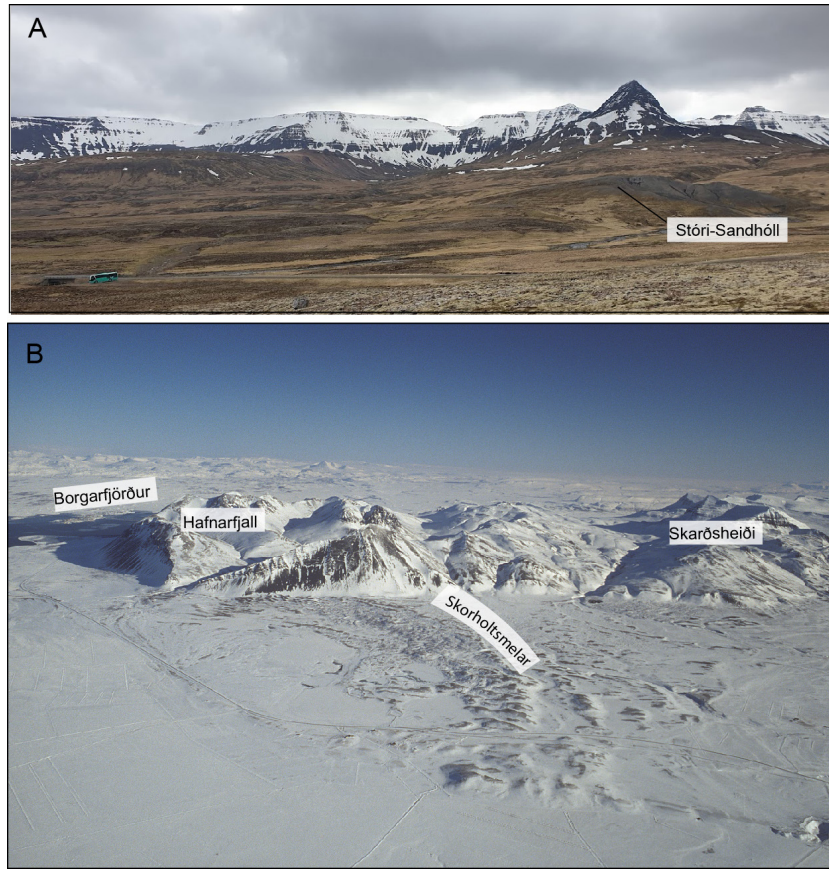

Figure 3. A: Photo of Early Bølling shoreline the Stóri-Sandhóll hillock, at 120-150 m altitude in the Skorradalur tributary valley. B: Oblique aerial photograph of the Skorholtsmelar end moraines. Photography by Ágúst Guðmundsson. The locations of these landforms can be seen on Fig. 2.

marine cores retrieved from the shelf off south-western Iceland indicate that the retreat was synchronous with the strengthening of the Irminger Current that caused relatively warm waters to be transported northwards to the western coast of Iceland (Jennings et al. 2000).

Bølling-Allerød high relative sea-level and glaciomarine deposition

Due to isostatic depression, the lowland areas of Borgarfjörður were submerged upon glacier retreat. The highest recorded marine levels in the region occur in Skorradalur (Fig. 1) where a series of marine terraces reaches up to about 148 m a.s.l. at Stóri-Sandhóll (Figs 2, 3A). Investigated terraces consist of up to 20 m thick, stratified glaciomarine diamicton capped with gravel, which Ingólfsson & Norðdahl (2001) interpreted as a littoral deposit. Whole shells and shell fragments retrieved from the glaciomarine diamicton have yielded radiocarbon ages around 14.7 cal. ka BP (Ingólfsson & Norðdahl 2001; Norðdahl & Ingólfsson 2015). These shells provide the earliest ages of ice-free coastal areas after the LGM in Iceland (Norðdahl & Pétursson 2005). Additionally, Ashwell (1967) radiocarbon dated shell fragments to 13.7 cal. ka BP of the same diamicton. Raised marine shorelines are also found at 115-125 m a.s.l. flanking the southern slope of Mt. Hafnarfjall-Skarðsheiði (Fig. 2) and a littoral delta is situated at 105 m a.s.l. at Stóra-Fellsöxl at the northern side of Mt. Akrafjall (Fig. 2) (Ingólfsson 1988; Magnúsdóttir & Norðdahl 2000). A whalebone retrieved from the delta gravel at Akrafjall yielded an age of 14.7 cal. ka BP (Magnúsdóttir & Norðdahl 2000). The high altitude of these shorelines, coupled with the fact that the Icelandic crust responds immediately to glacier loading/unloading, has been used as further evidence for the rapid glacier retreat from the western shelf during the early-Bølling (Ingólfsson & Norðdahl 2001).

During the Bølling-Allerød (c. 14.9-12.7 cal. ka BP), glaciomarine sediments accumulated in the lowland area of Melasveit (Ingólfsson 1987, 1988) and can now be seen in a number of sections (Fig. 2). The lowermost glaciomarine sediments were defined by Ingólfsson (1987, 1988) as a single unit that was informally named

Table 1: List of previously published ^{14}C ages from the Borgarfjörður area and surrounding regions. The ^{14}C ages are calibrated with the Marine13 dataset (Reimer et al. 2013) with the Calib 7.1 program (Stuiver et al. 2019). The ^{14}C ages are presented in the table without a reservoir correction but the calibrated ages are reservoir corrected using ΔR of 24±23 (Håkansson 1983; Norðdahl & Ingólfsson 2015).

Lab no.	Age ^{14}C BP	Calibrated age range (2 sigma) (cal. BP)	Calibrated median probability (cal. BP)	Location	Unit/Type of sediment	Reference
Lu- 2197	10370 ± 90	11162-11802	11.4	Skipanes	Unit G	Ingólfsson (1988)
Lu- 2378	10520 ± 150	11192-12255	11.7	Skipanes	Unit G	Ingólfsson (1988)
Lu-2056	11330 ± 80	12620-12963	12.8	Súluá	Glaciomarine	Ingólfsson (1988)
Lu-2376	11830 ± 100	13077-13482	13.3	Melabakkar-Ásbakkar	Unit C	Ingólfsson (1987)
Lu-2373	11910 ± 140	13075-13679	13.4	Melabakkar-Ásbakkar (Ásgil north)	Unit D	Ingólfsson (1987)
Lu-2196	11980 ± 130	13164-13717	13.4	Melabakkar-Ásbakkar (Ásgil north)	Unit D	Ingólfsson (1987)
Lu-2372	12080 ± 120	13278-13791	13.5	Melabakkar-Ásbakkar (Ásgil north)	Unit D	Ingólfsson (1987)
Lu - 2374	12250 ± 100	13438-13925	13.7	Skipanes	Unit A	Ingólfsson (1988)
I- 1825	12240 ± 200	13276-14124	13.7	Andakíll	Glaciomarine	Ashwell (1967)
I-1824	12270 ± 150	13386-14043	13.7	Stóri Sandhóll	Glaciomarine	Ashwell (1967)
Lu-2377	12310 ± 110	13473-14011	13.7	Melabakkar-Ásbakkar (Ás)	Unit A	Ingólfsson (1987)
Lu-2375	12350 ± 120	13493-14071	13.8	Melabakkar-Ásbakkar	Unit G	Ingólfsson (1987)
AAR-3654	12370 ± 95	13557-14058	13.8	Skorholt	Delta gravel	Magnúsdóttir and Norðdahl (2000)
Lu-2379	12380 ± 110	13539-14090	13.8	Melabakkar-Ásbakkar (Ás)	Unit A	Ingólfsson (1987)
Lu-2192	12460 ± 120	13590-14206	13.9	Melabakkar-Ásbakkar (Melaleiti)	Unit A	Ingólfsson (1987)
Lu-2371	12510 ± 140	13576-14495	14.0	Árdalur	Glaciomarine	Ingólfsson (1985)
Lu-2193	12830 ± 110	14096-15032	14.5	Melabakkar-Ásbakkar (Melaleiti)	Unit A	Ingólfsson (1987)
Lu-2194	12830 ± 110	14095-15031	14.5	Grjóteyri	Glaciomarine	Ingólfsson (1988)
Lu-2195	12870 ± 110	14139-15073	14.6	Melabakkar-Ásbakkar (Ás)	Unit A	Ingólfsson (1987)
Ua-12021	12880 ± 85	14181-15042	14.6	Stóri Sandhóll	Glaciomarine	Ingólfsson and Norðdahl (2001)
AAR-3734	12940 ± 80	14268-15.111	14.7	Stóra Fellsöxl	Delta gravel	Magnúsdóttir and Norðdahl (2000)
Ua-11773	12975 ±105	14252-15185	14.8	Stóri Sandhóll	Glaciomarine	Ingólfsson and Norðdahl (2001)

'the Ásbakkar diamicton' but is referred to as 'Unit A' in Sigfúsdóttir et al. (2018) and in this paper. Previously, shells and shell fragments identified to the Macoma calcarea community have been radiocarbon dated revealing ages between 14.6 and 13.7 cal. ka BP in Unit A (Ingólfsson 1987, 1988). Together, the fauna and isotope composition indicate a low salinity, fjord environment with sea surface temperatures similar to present (Ingólfsson 1987, 1988; Ingólfsson et al. 2010). The relative sea level fell during the Bølling-Allerød due to isostatic rebound but rose again in response to glacier readvances and associated isostatic depression around the Allerød - Younger Dryas boundary (Norðdahl & Pétursson 2005; Norðdahl et al. 2008). Shell fragments of Allerød ages have been found in the glaciomarine units in Melasveit, i.e. in the Melabakkar-Ásbakkar coastal cliffs and at Súluá (Fig. 2; Table 1). They contain a larger number of high-Arctic species (Portlandia arctica and Buccinum groenlandicum) (In-

gólfsson 1988) compared to the Bølling aged samples, indicating that the influence of Arctic waters increased in Allerød (Norðdahl & Pétursson 2005; Pétursson et al. 2015).

Glacier readvances and the formation of the Skorholtsmelar, Melabakkar-Ásbakkar, and Belgsholt moraines

The extensively deformed marine sediments in Melasveit have provided clear indication that glacier(s) readvanced into the lowland areas of Borgarfjörður during the Late Weichselian (Ingólfsson 1987, 1988; Sigfúsdóttir et al. 2018). Furthermore, the configuration of the Skorholtsmelar moraine ridge, distribution of erratic boulders and lithology of surface deposits indicate that the moraine formed by a glacier advancing southwards from Borgarfjörður (Figs 2, 3B) (Ingólfsson 1987, 1988; Sigfúsdóttir et al. 2018). The eastern side (ice-distal) is partly flanked by the Skorholt delta possibly formed by subglacial outwash when the glacier was standing at the moraine ridge (Fig. 2) (Ingólfsson 1988). The delta is truncated with a gravel horizon at 52 m a.s.l. indicating the minimum sea level during the deposition of the delta and therefore, most likely also the moraine. A radiocarbon age of a reworked shell fragment obtained from the delta yielded a maximum age of 13.7 cal. ka BP for the deposition of the delta (Magnúsdóttir & Norðdahl 2000). The Skorholtsmelar end moraine is attached to Mt. Hafnarfjall on one end but can be traced 5 km to the west where the moraine is abruptly eroded (Figs 2, 3) and thus, cannot be traced further west as a morphological feature on the surface. However, a trace of erratics on the surface indicates the westward continuation of the end moraine, the remains of which may thus be largely buried at this place. At least six buried glaciotectonic moraines are exposed in the >5 km long coastal sections of Melabakkar-Ásbakkar in Melasveit (Fig. 2) (Sigfúsdóttir et al. 2018). Based on sedimentology, glaciotectonics, geomorphology and their relative position, Sigfúsdóttir et al. (2018) suggested the buried moraines to represent at least six glacier advances from the north. The southernmost and largest buried moraine, Ás, is over 1.5 km wide in the cliff section and is considered to be an extension of the Skorholtsmelar moraine complex further inland (Fig. 2). Generally, the moraines become smaller and younger towards the north most likely reflecting readvances during an active retreat from the maximum position at Ás-Skorholtsmelar. Valley/outlet glaciers may have advanced into the area from the east as well. Ingólfsson (1988) tentatively suggested that glaciers emanating from Hvalfjörður and Svínadalur may have extended into the lowland area of Leirársveit during the Late Weichselian (Fig. 2). It has also been suggested that the southernmost part of Melabakkar-Ásbakkar may record proglacial deformation by ice advancing from the east and that the Skorholtsmelar moraine may therefore represent a confluence zone between glaciers from the north and the south, at least during the early stages of its development (Hart 1994; Hart & Roberts 1994). There is, however, no clear evidence in the stratigraphical and geomorphological record supporting the idea that Late Weichselian glaciers extended that far into the region from the south (Ingólfsson 1988; Sigfúsdóttir et al. 2018).

Timing of glacier readvances: Stratigraphical and chronological problems

Uncertainties exist regarding the timing of glacier readvances in the region and there is a mismatch between different landform/sediment records. Based on detailed stratigraphical studies, Ingólfsson (1987, 1988) suggested two glacier advances into the Melasveit area during the Late Weichselian. The first and the larger advance occurred in late Bølling (shortly after c. 14 cal. ka BP) resulting in the deformation of the Ásbakkar diamicton (Unit A) and the construction of the Skorholtsmelar end moraine. The second advance occurred after c. 13.0 cal. ka BP and terminated approximately half way across the Melabakkar-Ásbakkar cliffs (Fig. 2) resulting in the deformation of glaciomarine sediments containing shell fragments of Allerød age (13.4-13.5 cal. ka BP). As discussed in Magnúsdóttir & Norðdahl (2000) and Norðdahl & Pétursson (2005), this sequence of events is challenged by the presence of the 120-150 m high Bølling shorelines in Skorradalur, and the 60-80 m high shorelines, correlated to YD, extending from Skorholtsmelar to the mouth of Skorradalur (Fig. 2). Magnúsdóttir & Norðdahl (2000) and Norðdahl & Pétursson (2005) argue that the shorelines would not have been preserved if a glacier advanced from the north after their formation.

The current general view is that the Skorholtsmelar moraine complex and the glaciotectonics seen in the coastal cliffs in Melasveit were formed by a glacier advance in late-Bølling (around 14.0 cal. ka BP) (Norðdahl et al. 2008; Ingólfsson et al. 2010; Pétursson et al. 2015). Such a large-scale advance at this time would have been out of phase with other suggested glacier advances in Iceland. Therefore, it has been hypothesised that it was a result of a glaciodynamic instability induced by the collapse of the marine-based part of the ice sheet in the early-Bølling (Ingólfsson & Norðdahl 2001; Norðdahl et al. 2008).

The question still remains why younger shell fragments are found within the deformed sediments in Melabakkar-Ásbakkar and other sections in Melasveit. It has been hypothesised that processes other than glaciotectonism could have been responsible for the deformation of the shell-bearing sediments (Norðdahl & Pétursson 2005). However, recent detailed studies of the stratigraphy and structures in the coastal cliffs clearly show that

the sediments were primarily deformed by a glacier advancing from the north (Sigfúsdóttir et al. 2018, 2019). This agrees with previous studies of the glaciotectonics of the cliffs (Ingólfsson 1987; Hart 1994; Hart & Roberts 1994). The present study complements these reconstructions with new radiocarbon ages providing better time constraints on these events.

Methods

Twenty-two mollusc samples were collected from glaciomarine and deltaic sediments exposed in the coastal cliffs of Melabakkar-Ásbakkar, Belgsholt and Skipanes as well as from a raised sea cliff at Fossamelar at the mouth of Skorradalur (Fig. 2). Sampled shells have been radiocarbon dated to constrain the timeline of glacier oscillations in the area. This study builds on a detailed documentation by Sigfúsdóttir et al. (2018) of the stratigraphy and glaciotectonics exposed in the coastal cliffs of Melabakkar-Ásbakkar and Belgsholt, which are thus only briefly described in this paper. Descriptions of sediment characteristics and deformation structures is according to Evans & Benn (2004) and Phillips & Lee (2011). The geometry of folds, faults and thrusts was measured in the field and the orientation of these structures was plotted on a Schmidt equal area lower hemisphere projection and analysed with Stereonet 9 software (Allmendinger et al. 2012; Cardozo & Allmendinger 2013).

The marine molluscs were radiocarbon dated at the Radiocarbon Dating Laboratory in Lund, Sweden. All the 14C ages in the text are calibrated with the Marine13 dataset (Reimer et al. 2013) with the Calib 7.1 program (Stuiver et al. 2019) and reservoir corrected by using ΔR of 24±23 to accommodate local variability in the reservoir age (Håkansson 1983; Norðdahl & Ingólfsson 2015). The reservoir age is known to have fluctuated in the past and due to more influence of arctic water masses during the Late Weichselian and Early Holocene, the reservoir ages were most likely higher than today (Larsen et al. 2002; Eiríksson et al. 2004; Ólafsdóttir et al. 2010). However, as the variability in ocean water reservoir age off western Iceland has not been established, this paper uses the modern reservoir age. This correction procedure is consistent with other published research from sites in the Borgarfjörður region (Ingólfsson 1987, 1988; Ingólfsson & Norðdahl 2001; Norðdahl & Ingólfsson 2015). The ages presented in the text and figures are calibrated median probability ages, rounded to the nearest 100 cal. years. The new radiocarbon ages as well as previously published dates referred to in the text are presented in Table 1 and 2, where the 2 sigma cal. BP age range is also given.

Results

Sigfúsdóttir *et al.* (2018) provided a detailed description of the stratigraphy and glaciotectonics exposed in the Melabakkar-Ásbakkar and Belgsholt cliffs. This paper follows their stratigraphic framework and interpretations and adopts their division of the sediments into eight units (A-H) (Fig. 4). In addition, this paper briefly describes two smaller sections at Skipanes and Fossamelar in Skorradalur (Fig. 2). Here radiocarbon ages of marine macrofossils from these sections are presented and their stratigraphic location described.

Melabakkar-Ásbakkar

Melabakkar-Ásbakkar are over 5 km long and up to 30 m high, subvertical coastal cliffs that are well-exposed and largely clean due to wave erosion (Figs 2, 4). Their stratigraphy is dominated by thick units of glaciomarine sediments separated by beds of sand and gravel. The lower units in the cliffs (units A-E) have undergone glaciotectonic deformation and form large ridges that can be seen in the cliffs (Figs 4, 5). Sigfúsdóttir et al. (2018), designated these ridges the following names; Ás, Ásgil (north and south), Fúla, and Melaleiti. These names will be used in this paper as well (locations marked with red boxes on Fig. 4). Based on the internal architecture of these ridges, they are interpreted as a series of moraines formed through glaciotectonic deformation and ice-marginal deposition by a glacier advancing from the north (Sigfúsdóttir et al. 2018). Stratigraphic and geomorphological relationship show that the southernmost and largest moraine, Ás, represents the maximum ice extent into the area and generally the other moraines in the series represent readvances during an overall northward retreat from the maximum position (Sigfúsdóttir et al. 2018). The moraine ridges are overlain and separated by an up to 25 m thick undeformed glaciomarine sediment (Unit G) grading upwards into littoral deposits (Unit H) (Figs 4, 5). These sediments cover the ridges, which consequently have poor morphological expression on the surface.

Thirteen new radiocarbon dates from samples collected in the Melabakkar-Ásbakkar cliffs together with ten previously published dates (Ingólfsson 1987) were used to provide maximum ages for the deposition of the sediment units and the formation of the moraines.

The moraine forming sediments (sediment units A-E) -

The lowermost and the most extensive sediment unit exposed in Melabakkar-Ásbakkar is a fossil –bearing, glaciomarine diamicton Unit A (Fig. 4) (named 'Ásbakkar diamicton' by Ingólfsson (1987, 1988)). Based on its stratigraphic location, sedimentology, fossil fauna and radiocarbon ages, Unit A has previously been interpret-

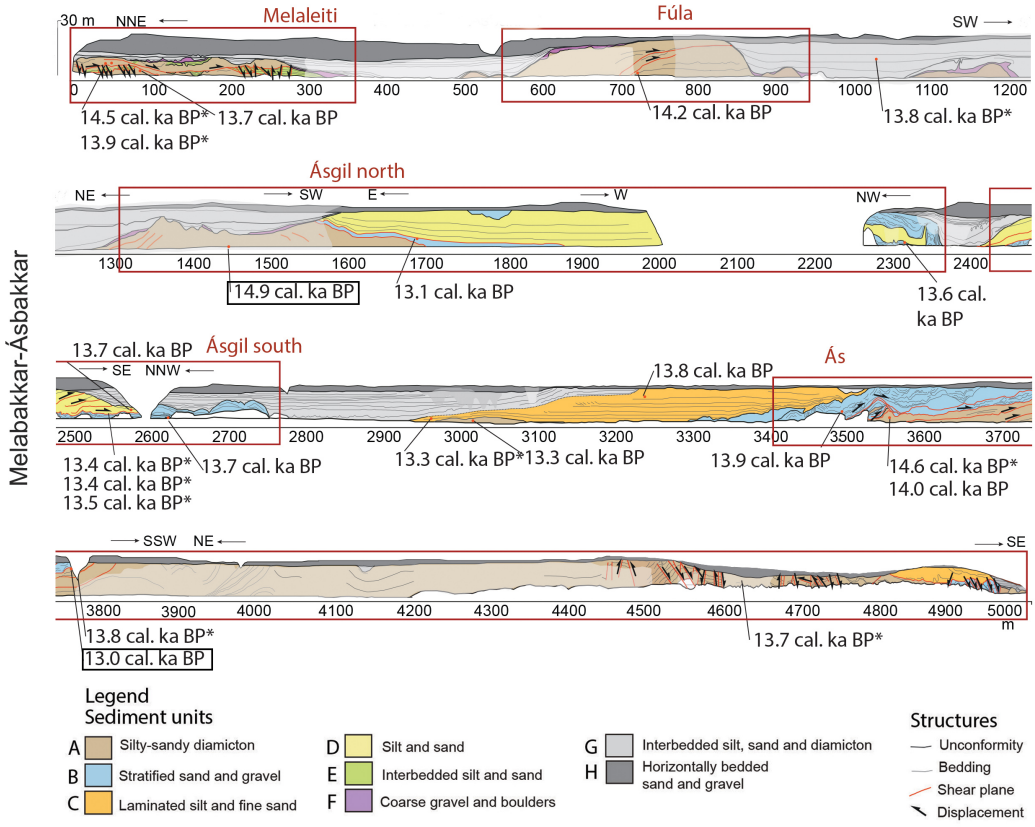

Figure. 4. A section diagram of the Melabakkar-Ásbakkar coastal cliffs. Glaciotectonic stress was from left to right. The red boxes circumscribe the buried glaciotectonic end moraines exposed in the cliffs. Sampling locations and the calibrated radiocarbon ages of shells from the Melabakkar-Ásbakkar coastal cliffs are included. Ages marked with an asterisk are from Ingólfsson (1987). Black boxes denote the oldest and youngest measured age. The oldest age (14.9 cal. ka BP) marks the minimum timing for glaciomarine deposition in the area while the youngest age (13.0 cal. ka BP) can be used to indicate the maximum timing of the re-advance that deformed the glaciomarine sediments. Note that none of the shells obtained from these deposits are *in situ*. Units B-G only contain shell fragments, interpreted as reworked material. Unit A contained nearly complete valves, which are interpreted to reflect the true age of the deposit (see Table 2).

ed to have been deposited during the deglaciation after the LGM (Ingólfsson 1987, 1988). The concentration of fossils is locally high and both shell fragments as well as nearly complete shells of marine molluscs are found. Although the shells are not in situ they are often unbroken, or just slightly damaged, possibly during post-depositional deformation of the unit, indicating only minimal transport, (Ingólfsson et al. 2010; Sigfúsdóttir et al. 2018). Therefore, they are interpreted to represent the true age of the sediment and a maximum age of the deformation. Six new dates of fossil molluscs from this unit yielded ages between 14.9 cal. ka BP and 13.0 cal. ka (Table 2). The five previously published ages from this unit (at Melabakkar-Ásbakkar) ranged between 14.6 and 13.7 cal. ka BP (Ingólfsson 1987) (Table 1). Unit A is widely exposed and heavily deformed along the entire section, exhibiting a variety of ductile deformation structures (e.g. folds, boudins) and forming a substantial part of most of the moraines exposed in the cliffs (Fig. 4). The youngest shell retrieved from Unit A (no. LuS 11253, 13.0 cal. ka BP; Table 2) was enclosed within the southernmost and oldest moraine and serves, therefore, as a maximum constraining age for the deposition of the Unit A and the formation of the end moraine.

Sediment Unit B stratigraphically overlies Unit A and consists of stratified sand and gravel between thinner beds of diamictons. Unit B is discontinuous but can be identified within and/or on the distal sides of the ridges (Figs 4, 5A). Based on its sedimentary texture- and structures, and its stratigraphic position, it has been interpreted as subaquatic fans and meltwater sediments deposited in association with the advance that deformed the underlying Unit A (Sigfúsdóttir et al. 2018). The unit is most likely time-transgressive (generally younger towards

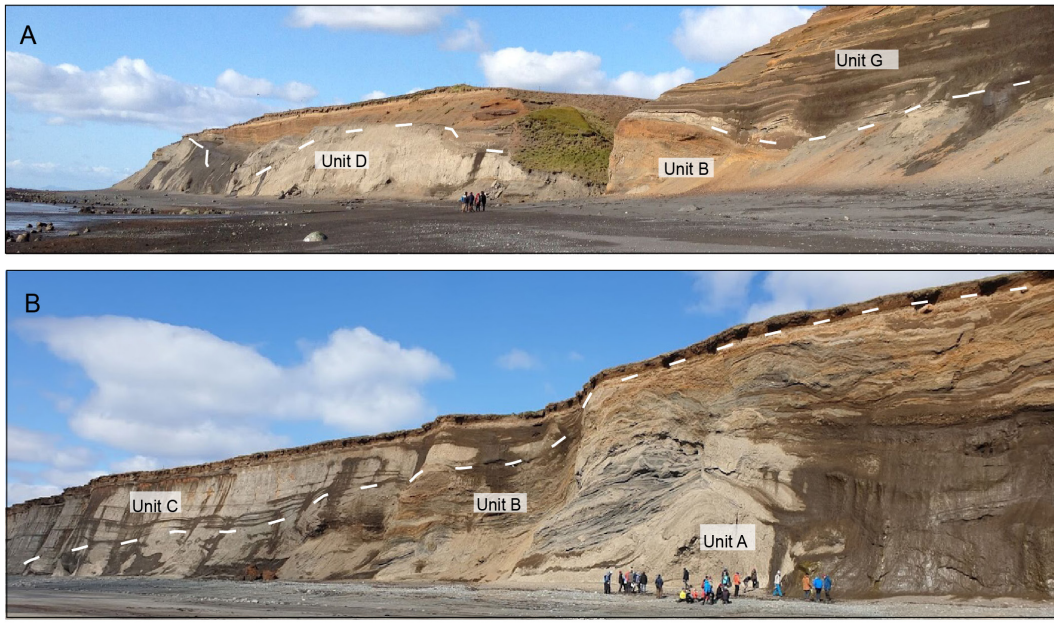

Figure 5. A. The buried Ásgil moraines and subaquatic fan. The photograph covers approximately 2300-2700m on Fig. 4. B. The northernmost part of the buried Ás moraine, exposed in the Melabakkar-Ásbakkar coastal cliffs. The photograph covers approximately 3200-3600 m on Fig. 4. The dashed lines on both photographs indicate the boundaries between the moraines and the overlying, undisturbed glaciomarine deposits.

the north) and deposited during the stepwise retreat of the ice margin (Sigfúsdóttir et al. 2018). Locally, the unit contains a high amount of broken and abraded shells but no whole shells were found. Two shell fragments were radiocarbon dated to 13.6 and 13.9 cal. ka BP (LuS 112-48 and 51; Table 2). As the shell fragments are obviously reworked, they can only be assumed to reflect the maximum age of the unit and its stratigraphic position shows that it is younger than Unit A; hence, indicating deposition after 13.0 cal. ka BP.

Units C-E are up to 25 m thick successions of bedded and laminated silt, sand and diamicton stratigraphically overlying the glaciomarine Unit A (and usually also Unit B). Units C-E are interpreted to be time-transgressive and become generally younger towards the north. The units are interpreted to have been deposited in an ice-proximal environment during the stepwise retreat of the glacier and subsequently deformed by repeated advances of the ice margin (Sigfúsdóttir et al. 2018). Apparently, these units do not seem to contain any in situ macrofossils but small shell fragments found in the sediments were sampled and radiocarbon dated in an attempt to further constrain the maximum age of units C-E.

The lower part of Unit C appears mostly undeformed and is draped over the southernmost end moraine (Ás; 3300-3500 m on Figs 4, 5B). The upper contact of the unit is erosional and deformation in the uppermost layers probably indicates overriding by a glacier (Sigfúsdóttir et al. 2018). One shell fragment from a diamicton in the uppermost part of Unit C gave an age of 13.8 cal. ka BP (LuS11252; Table 2). Previously, one marine mollusc had been sampled for dating from a similar stratigraphic location in the unit giving an age of 13.3 cal. ka BP (Lu-2376; Table 1) (Ingólfsson 1987).

Unit D occurs in the northern to central parts of the cliffs where it displays glaciotectonic thrusting and folding and, together with units A and B, constitutes the buried moraines in that part of the cliffs. Two samples from Unit D, collected from poorly sorted silt/sand beds gave ages of 13.1 cal. ka BP (LuS 11260; Table 2) and 13.7 cal. ka BP (LuS 11247; Table 2). These ages are similar to previously published ages of 13.4 - 13.5 cal. ka BP from this unit (Lu-2196, Lu-2372, Lu-2373; Table 1) (Ingólfsson 1987).

Despite the fact that the ages of the shell fragments in units C - E fall within a relatively narrow time span, the shell fragments are all reworked and thus do not represent the depositional age of the hosting units. Therefore, these ages must be regarded as maximum ages of units C - E. As these units stratigraphically overlie Unit A, they are younger than 13.0 cal. ka BP.

Undeformed sediments (sediment units F-H) -

Between the glaciotectonic moraines, there is an up to 25 m thick fining-upward bedded diamicton, sand and silt (Fig. 4) (Unit G). This unit is undeformed and has therefore been interpreted to have been deposited in an ice-proximal to ice-distal environment after the glacier re-

Table 2: ^{14}C ages of marine shells sampled in this study. The ^{14}C ages are calibrated with the Marine13 dataset (Reimer et al. 2013) with the Calib 7.1 program. The ^{14}C ages are presented in the table without a reservoir correction but the calibrated ages are reservoir corrected using ΔR of 24±23 (Håkansson 1983; Norðdahl & Ingólfsson 2015).

Lab no.	Age ^{14}C BP	Calibrated age range (2σ) (cal. BP)	Calibrated median probability (cal. ka BP)	Material	Location	Unit	*In situ*	Latitude-longitude
LuS 11255	10330 ± 55	11159-11634	11.3	*Hiatella arctica* One complete valve	Belgsholt	Unit E	No	N64.25.678 W022.00.828
LuS 11265	10410 ± 55	11229-11761	11.5	Unidentified shell fragment	Skipanes	Unit G	No	N64.23.774 W021.54.667
LuS 11266	10415 ± 55	11233-11768	11.5	*Chlamys islandica* Nearly complete bivalve	Skipanes	Unit G	Yes	N64.23.774 W021.54.667
LuS 11254	10410 ± 60	11231-11786	11.5	*Hiatella arctica* One complete valve	Belgsholt	Unit E	No	N64.25.678 W022.00.828
LuS 11256	10540 ± 55	11377-11991	11.7	*Balanus balanus* Complete shell	Belgsholt	Unit E	No	N64.25.678 W022.00.828
LuS 11669	10550 ± 60	11378-12013	11.7	*Balanus balanus* Complete shell	Skorradalur, Fossamelar	Cliff	Yes	N64.32.764 W021.40.450
LuS 11257	11285 ± 55	12617-12881	12.7	Unidentified shell fragment	Belgsholt	Unit E	No	N64.25.678 W022.00.828
LuS 11253	11535 ± 55	12798-13147	13.0	*Chlamys islandica* Large fragment	Melabakkar-Ásbakkar (Ás)	Unit A	No	N64.23.598 W022.01.344
LuS 11260	11600 ± 60	12867-13229	13.1	Unidentified shell fragment	Melabakkar-Ásbakkar (Ásgil north)	Unit D	No	N64.24.389 W022.01.862
LuS 11249	11840 ± 65	13144-13430	13.3	*Hiatella arctica* One nearly complete valve	Melabakkar-Ásbakkar	Unit A	No	N64.23.906 W22.01.880
LuS 11248	12200 ± 60	13452-13806	13.6	Unidentified shell fragment	Melabakkar-Ásbakkar (Ásgil north)	Unit B	No	N64.24.254 W022.02.382
LuS 11245	12260 ± 60	13496-13866	13.7	*Chlamys islandica* One nearly complete valve	Melabakkar-Ásbakkar (Melaleiti)	Unit A	No	N64.25.160 W022.01.507
LuS 11247	12275 ± 60	13509-13886	13.7	Unidentified shell fragment	Melabakkar-Ásbakkar (Ásgil south)	Unit D	No	N64.24.132 W022.02.164
LuS 11246	12300 ± 65	13527-13927	13.7	Unidentified shell fragment	Melabakkar-Ásbakkar (Ásgil south)	Unit A	No	N64.24.111 W022.02.119

LuS 11252	12385 ± 65	13647-14030	13.8	Unidentified shell fragment	Melabakkar-Ásbakkar	Unit C	No	N64.23.833 W022.01.742
LuS 11251	12455 ± 60	13747-14087	13.9	Unidentified shell fragment	Melabakkar-Ásbakkar (Ás)	Unit B	No	N64.23.703 W022.01.555
LuS 11264	12565 ± 65	13839-14198	14.0	Unidentified shell fragment	Skipanes	Unit A	No	N64.23.774 W021.54.667
LuS 11250	12580 ± 60	13855-14209	14.0	*Chlamys islandica* One nearly complete valve	Melabakkar-Ásbakkar (Ás)	Unit A	No	N64.23.687 W022.01.525
LuS 11262	12715 ± 60	14009-14645	14.2	Unidentified shell fragment	Melabakkar-Ásbakkar (Fúla)	Unit A	No	N64.24.826 W022.01.501
LuS 11263	12740 ± 70	14025-14727	14.3	Unidentified shell fragment	Skipanes	Unit A	No	N64.23.774 W021.54.667
LuS 11258	12760 ± 70	14050-14763	14.3	Unidentified shell fragment	Belgsholt	Unit A	No	N64.25.607 W022.00.812
LuS 11259	12980 ± 60	14406-15147	14.9	*Chlamys islandica* One nearly complete valve	Melabakkar-Ásbakkar (Ásgil north)	Unit A	No	N64.24.448 W022.01.756

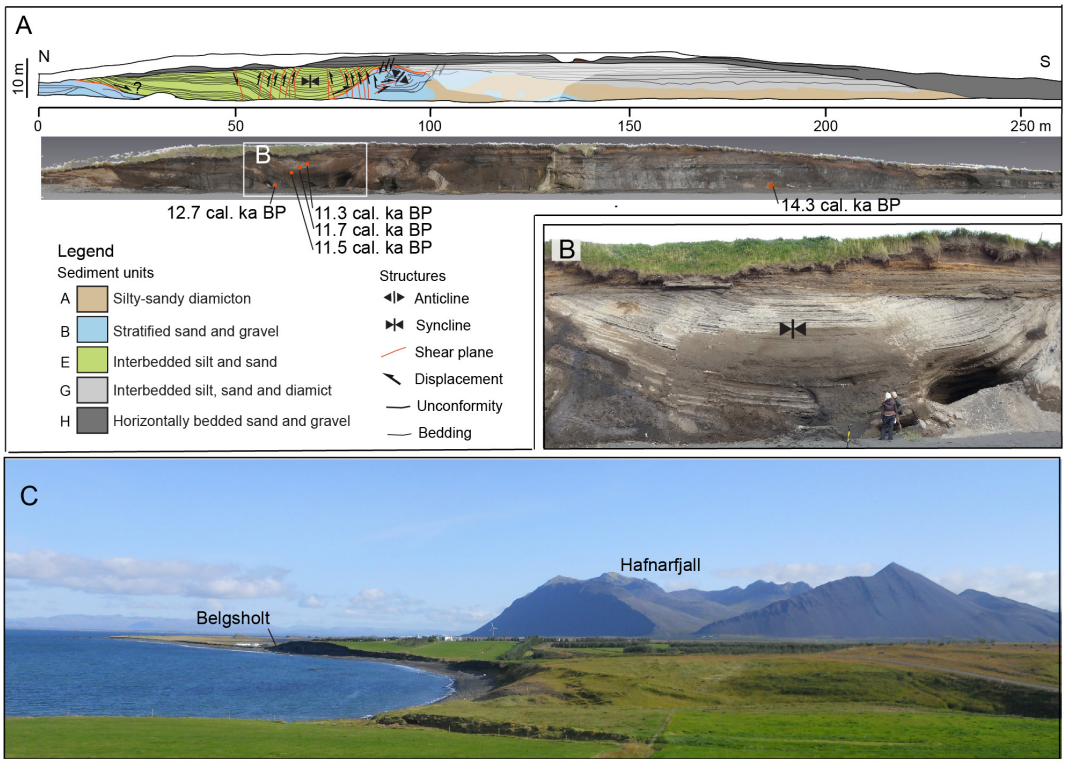

Figure 6. A section diagram and LiDAR image of the Belgsholt coastal cliff (from Sigfúsdóttir et al. 2018), showing the location of radiocarbon dated shells. The maximum confining age provided by the radiocarbon dated shells indicate that the glaciotectonic moraine was formed after about 11.3 cal. ka BP. B. A large syncline in bedded/laminated glaciomarine sediments containing abundant whole shells of marine molluscs. Glaciotectonic stress was from left to right. C. An overview of the Belgsholt moraine and -coastal cliff. Mt. Hafnarfjall in the background. View to the northeast.

treated from the nearest ridge to the south (Sigfúsdóttir et al. 2018). No whole shells were found in situ within this unit and shell fragments appeared to be nearly absent. One radiocarbon date of shell fragments has previously been published yielding an age of 13.8 cal. ka BP (Lu-2375; Table 1) (Ingólfsson 1987). The shell fragments were reworked and, because they gave an older age than the deformed, stratigraphically underlying sediment, they only indicate the maximum age of deposition and cannot be used as a minimum age constraint for the deformation of the underlying ridges. The uppermost unit exposed in the cliffs is an up to 10 m thick unit of subhorizontally stratified sand and gravel that has previously been interpreted as littoral sediment deposited during the isostatic rebound of the area during Early Holocene (Fig. 4) (Unit H; Fig. 4) (Ingólfsson 1987, 1988).

Belgsholt

Belgsholt is a W-E trending ridge that is transected by coastal erosion approximately transverse to the ridge trend (Figs 6). The internal architecture of the Belgsholt ridge is well-exposed in the coastal cliffs showing that the ridge is primarily composed of marine sediments deformed by thrusting and folding from a northerly direction. Based on this, Belgsholt is interpreted as an ice-marginal moraine formed by a glacier advancing from Borgarfjörður (Sigfúsdóttir et al. 2018). The Belgsholt ridge shows no signs of having been overridden and has been interpreted as younger than the Melabakkar-Ásbakkar moraines. The Belgsholt ridge is overlain by undeformed bedded glaciomarine sediments (Unit H) which indicate a sea level at least 12 m above present at some point after the moraine was formed (Sigfúsdóttir et al. 2018).

At the base of the moraine, there is an extensively deformed, heterogeneous, silty-sandy, clast poor diamicton (Fig. 6A). The diamicton contains shell fragments but no whole shells were found. A shell fragment from this unit gave the age of c. 14.3 cal. ka BP (LuS 11258; Table 2), which indicates the maximum age of the unit. Due to its stratigraphic position, the diamicton is correlated to Unit A, which is widely exposed in the area, i.e. in Melabakkar-Ásbakkar and Skipanes (Ingólfsson 1987, 1988). The Unit A diamicton is overlain by sand and gravel (Unit B) and these two units appear intermixed. The stratigraphically uppermost unit in the deformed succession is Unit E (Fig. 6A). It consists of interbedded diamicton, silt

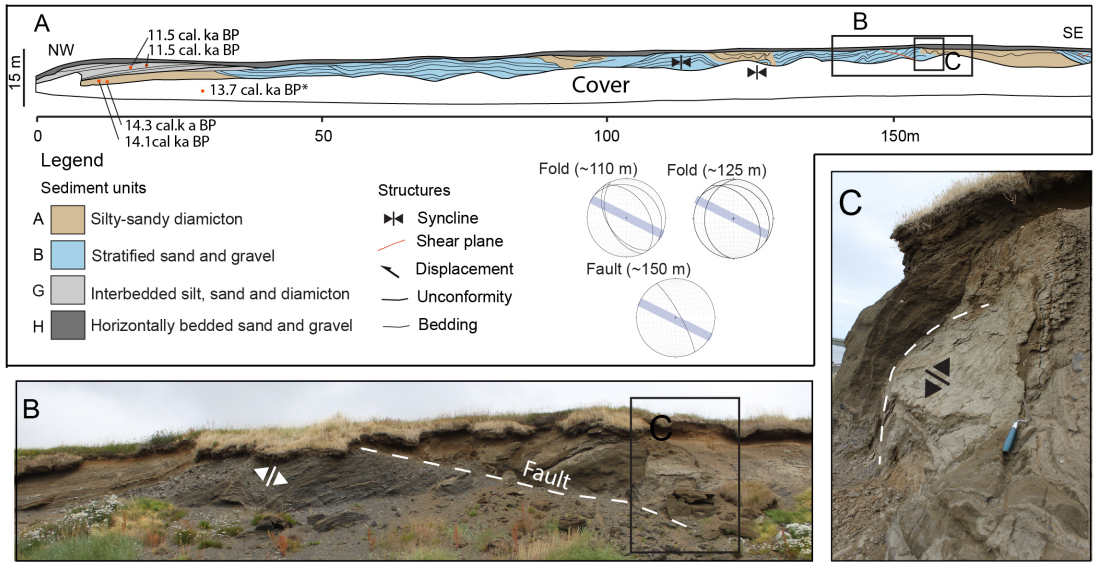

Figure 7. A diagram of the Skipanes coastal section including structural data. The glaciotectonised sediments that form the main part of the ridge are overlain by undeformed bedded/laminated marine sediments (Unit G). Sampling locations of radiocarbon dated shells are marked on the diagram and ages from Ingólfsson 1988 are marked with an asterisk. Radiocarbon dated shell fragments from the glaciotectonised unit A and an in situ paired bivalve from the undeformed, overlying unit G show that the Skipanes ridge was formed sometime between c. 13.7 and 11.5 cal. ka BP.

and sand, abundant in intact marine molluscs, which are not in situ but are sitting in an original position relative to the sediment unit they are enclosed in. Internally, Unit E has undergone minor deformation and thus, original bedding and sediment structures (i.e. cross-bedding and lamination) are preserved. The lower boundary of Unit E is sharp and is marked by shear faults and folds, and the whole unit is folded into a large syncline, which is cross-cut by multiple reverse faults radiating from the syncline core (Fig. 6B). Unit E has been interpreted as a thrust block that was detached and transported southwards by a glacier prior to the final deposition at its present location (Sigfúsdóttir et al. 2018). Four mollusc samples were collected from this unit (Unit E; Fig. 6A). A reworked shell fragment collected from a diamicton at the base of Unit E gave an age of 12.7 cal. ka BP indicating maximum age. Three samples of well-preserved shells of Balanus balanus and Hiatella arctica collected from the finely laminated, uppermost part of the unit ranged in age between 11.3 and 11.7 cal. ka BP (LuS 11254-56; Table 2). Despite the glaciotectonic deformation of the unit, they are clearly sitting in the original position relative to the sediments they are enclosed in and can consequently be assumed to represent the depositional age of the sediment. These ages do overlap within one standard deviation (Table 2) and are therefore statistically of the same age. These ages serve as a maximum constraining age for the formation of the Belgsholt moraine.

Skipanes

Skipanes is an over 15 m high coastal section located approximately 2 km east of the Skorholtsmelar end moraine (Fig. 2). The section is over 300 m long, oriented approximately NW-SE. Most of the cliff is covered by thick debris and vegetation, which prevented a holistic documentation and reconstruction of the large-scale architecture of the ridge (Fig. 7).

Presently the uppermost part (around 3 m) of the section is exposed. It consists of two main units; mollusc bearing marine diamicton, lithologically similar to the sediment Unit A in Melabakkar-Ásbakkar, and stratified sand and gravel lithologically similar to Unit B in Melabakkar-Ásbakkar (Fig. 4). The boundaries between these units are in some places sharp while in others the diamicton forms diapirs and flame structures, possibly as a result of being squeezed upwards through the more rigid sand and gravel.

Both units (A and B) form large, open folds and analysis of the deformation structures showed that they are mainly characterized by open folds that are most noticeable in the middle part of the section at 100-150 m (Fig. 7). At around 110 m, the stratified sand and gravel (Unit A) is folded into an open anticline (trend and plunge of fold axis: 339°/12°) followed by an open syncline at ~ 130 m (trend and plunge of fold axis: 327°/5°). A small overturned fold with vergence towards the southeast (axial plane ~ 236°/60°) is visible at ~ 125 m (Fig. 7). At about 150 m, there is a northeast dipping shear plane, above which the layers are folded. The fold-axis is

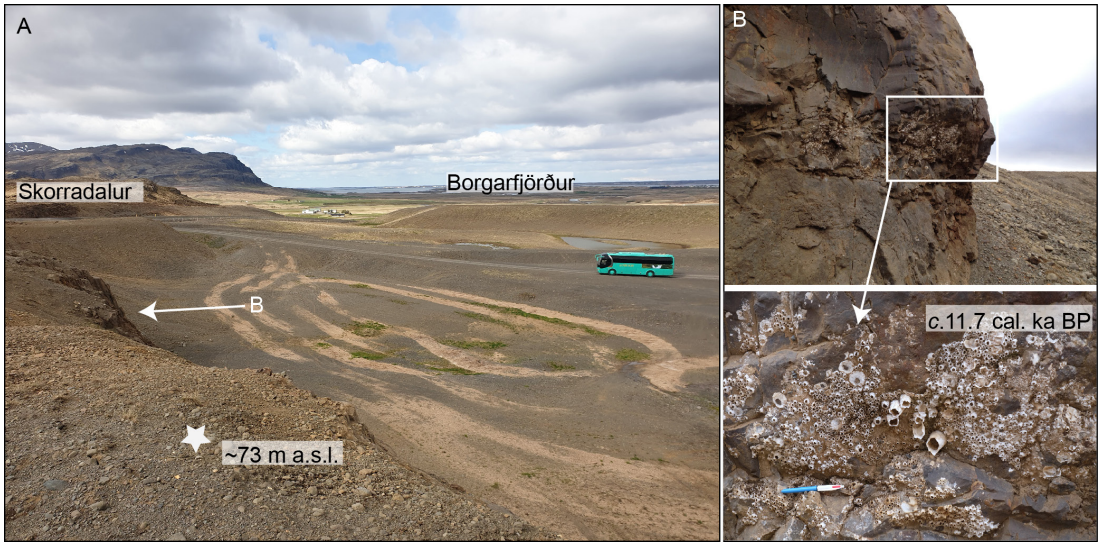

Figure 8. A: An overview photograph taken from a cliff at Fossamelar in the mouth of Skorradalur with a view to the west down the Borgarfjörður fjord/valley. B. Intact shells of Balanus balanus attached to the cliff at 69 m.a.s.l.. Radiocarbon dating of the shells yielded 11.7 cal. ka BP.

sub-parallel to the trend of the section (NW-SE). Overall, the directional features indicate ice-push from a north-easterly direction. Previous documentation of the cliff section, carried out when the section was much better exposed, showed that sediments in the lower part of the section were also folded and faulted (Ingólfsson 1988).

Two radiocarbon dates of shell fragments sampled from the deformed diamicton (Unit A) yielded ages of 14.1 and 14.3 cal. ka BP (Fig. 7) (LuS 11263-64; Table 2). Previously, Ingólfsson (1988) published one sample from folded diamicton at the base of the cliff sections (now covered in debris) giving an age of 13.7 cal. ka BP (Fig. 7) (Lu-2374; Table 1).

The glaciotectonic units are truncated by an erosional surface above which there is a unit of bedded sand and silt (Fig. 7). This bedded unit does not show any clear indications of deformation and therefore it most likely post-dates the deformation of the lower sediment units. Within the sand layers, both whole shells and shell fragments are abundant. Radiocarbon dating of two samples from this unit, one of which was a whole paired bivalve of Chlamys islandica, yielded the age of 11.5 cal. ka BP for both (LuS 11265-66; Table 2). Previously published radiocarbon dated samples collected from the same unit gave similar ages; 11.7 and 11.4 cal. ka BP (Lu-2197 and Lu-2378; Table 1; Ingólfsson 1988).The age of the paired bivalve (11.5 cal. ka BP), most likely reflects the true depositional age and consequently the minimum age for the deformation of the sediment units below.

Fossamelar-Skorradalur

One shell of a Balanus balanus barnacle was collected at Fossamelar in the mouth of Skorradalur (Fig. 2). The shell was found in a group of other Balanus balanus shells attached to a rock cliff facing the Borgarfjörður valley at 69 m a.s.l. (Fig. 8). The cliff is covered by a delta that has built up by water flowing from Skorholtsmelar into Borgarfjörður when the relative sea level in that part of the fjord was around 73 m above the present. The cliffs where the shells are found have become exposed due to quarrying (Fig. 8). Although no clean sections are found in the immediate surroundings of the cliffs, exposures in the quarry around 100-200 m to the east of the sampling location show that the delta consists of two generations of foresets. The lower one dips northwestwards to Borgarfjörður while the upper one dips towards the northeast. Radiocarbon dating of the Balanus balanus shell gave the age of 11.7 cal. ka BP (LuS 11669; Table 2).

The age of the shell, coupled with the altitude of the sampling location, indicate that the minimum sea level was 69 m above the present level when the barnacle was living there. Furthermore, the altitude of the topsets of the delta, overlying the cliff, shows that the relative sea-level was at least 73 m above the present level sometime after 11.7 cal. ka BP.

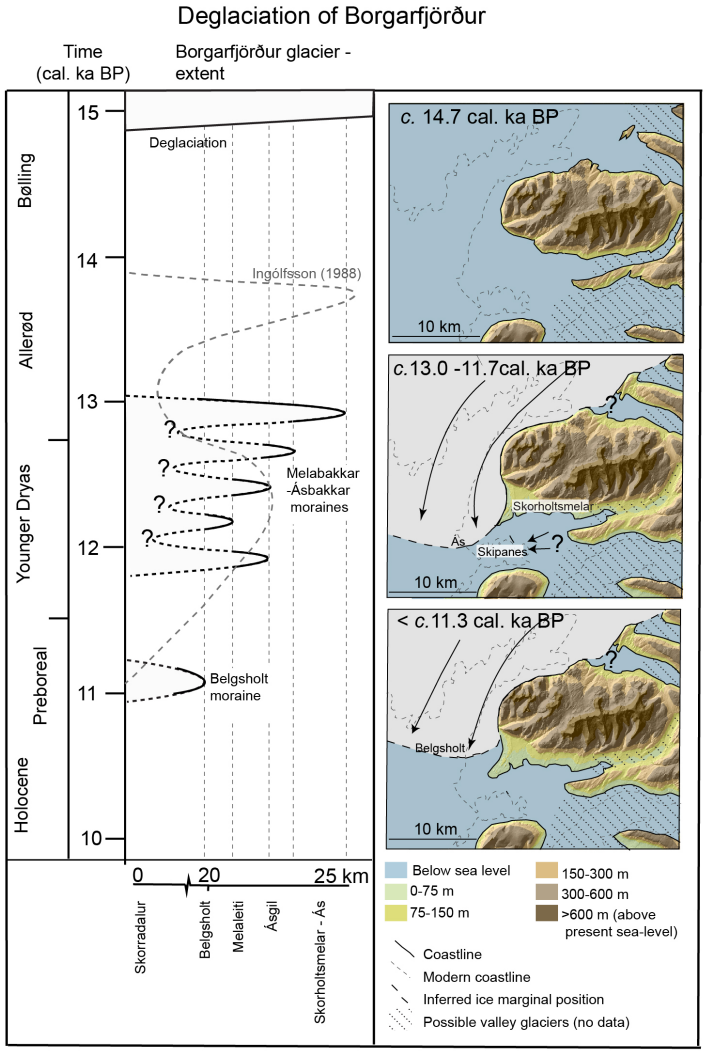

Figure 9. A time-distance model of the advances and retreats of the Borgarfjörður glacier. The grey dashed line shows the reconstruction of Ingólfsson (1988). The schematic time slices show the hypothesized aerial extent of the glacier and sea level position during three different time intervals. The reconstructions are based on radiocarbon ages, altitude of raised shorelines, geomorphology, and stratigraphic and glaciotectonic studies. It should be noted that the potential lateral ice margins along the mouth of the tributary valleys on the eastern side of Borgarfjörður during the Younger Dryas and Early Holocene (central and lower time slices) are speculative but serve to indicate a possible scenario that could explain the preservation of the Stóri-Sandhóll Bølling shoreline at 148 m a.s.l. in the outer part of Skorradalur. It is also noteworthy that mountain glaciers are likely to have been present during this time but are not drawn as their size is unknown.

Revised Late-Weichselian glaciation history of the lower-Borgarfjörður area

Bølling – Allerød: Open marine conditions

The age range of radiocarbon dated marine molluscs implies ice-free glaciomarine conditions in lower Borgarfjörður during the Bølling-Allerød interstadial between c. 14.7 and 13.0 cal. ka (Fig. 9). Ice-marginal positions of the Borgarfjörður glacier during this time are unknown but the age of mollusc-bearing glaciomarine sediments at Stóri-Sandhóll, Skorradalur, and elsewhere in Borgarfjörður, i.e. at Andakíll, Árdalur and Grjóteyri (Fig. 2) (Table 1), suggest that the glacier had retreated at least inside the mouth of the tributary valley in the early part of the interstadial (Fig. 9) (Ashwell 1967, 1975; Ingólfsson & Norðdahl 2001).

Overall, little is known about how far inland the western part of the IIS retreated during the Bølling – Allerød, largely because subsequent glacier advances removed most the of the evidence for earlier retreat. However, widespread raised shorelines and marine sediments indicate that the coastal areas were ice-free around this time (Ingólfsson 1988; Magnúsdóttir & Norðdahl 2000; Norðdahl & Pétursson 2005; Lloyd et al. 2009). Evidence from other parts of Iceland are also sparse although subaerial lava flows in northern Iceland at Mývatn, around 50 km inside the present coastline, indeed indicate that glaciers retreated far inland during this time (Sæmundsson 1991; Norðdahl et al. 2012).

Previous reconstructions of glacier dynamics in the Borgarfjörður region indicated a large advance during Late-Bølling, shortly after 14.0 cal. ka BP (Ingólfsson 1988), that constructed the large Skorholtsmelar terminal moraine complex in Melasveit (Fig. 2). This was suggested to have been possibly caused by the destabilisation of the ice sheet following the early-Bølling rapid retreat (Ingólfsson & Norðdahl 2001). This hypothesis was mainly based on the ages of radiocarbon dated shells from the lowermost, subglacially deformed unit (Unit A in this paper). However, the present study yields ages of 13.0 cal. ka BP as the lowest confining age for Unit A as well as for the construction of the large terminal moraine at Ás, which we correlate to the Skorholtsmelar moraine complex (Figs 2, 4; Sigfúsdóttir et al. 2018). Therefore, the glacier advance that constructed the terminal moraine in Melasveit (Skorholtsmelar and Ás moraine) must have occurred after 13.0 cal. ka BP and is most likely coeval with other recorded glacier advances in Iceland (Norðdahl & Pétursson 2005; Geirsdóttir et al. 2009; Ingólfsson et al. 2010). Consequently, this implies that the Bølling-Allerød interstadial in the lower Borgarfjörður region was dominated by ice-free coastlines and open marine conditions, similar to other areas in Iceland.

Younger Dryas: Advance of the Borgarfjörður glacier and active retreat

Following an ice-free period characterised by the deposition of the glaciomarine sediments (Unit A) between c. 14.9 and 13.0 cal. ka BP, a glacier emanating from Borgarfjörður readvanced into the Melasveit-Leirársveit area (Fig. 2 and 9). This is indicated by an extensive glaciotectonic deformation of the lowermost glaciomarine sediments (Unit A) and the distinct erosional/tectonic unconformity that defines its upper contact (Fig. 4) (Ingólfsson 1988; Sigfúsdóttir *et al.* 2018). The southernmost and largest moraine exposed in the Melabakkar-Ásbakkar cliffs (Ás; Fig. 4) and the Skorholtsmelar moraine ridge inland are correlated as being the same terminal moraine complex that delimits the maximum extent of this advance (Ingólfsson 1987, 1988). The youngest measured radiocarbon ages from Unit A, notably from within the terminal moraine (Ás), indicate that the advance of the Borgarfjörður glacier and the formation of the end moraine occurred after c. 13.0 cal. ka BP.

After the Borgarfjörður glacier retreated northwards from its maximum position at Skorholtsmelar and Ás, it formed the series of thrust moraines now exposed in the Melabakkar-Ásbakkar coastal cliffs (Fig. 4) (Sigfúsdóttir *et al.* 2018). Stratigraphic and glaciotectonic relationships show that the moraines become overall younger towards the north, indicating that they were formed during advances of the ice margin as it generally retreated northwards (Sigfúsdóttir *et al.* 2018). During this time, up to 25 m thick units of intrabedded ice-proximal glaciomarine sediments (units C-E) accumulated in front of the ice margin and were largely deformed by ice push during subsequent advances. In summary, units B-E at Melabakkar-Ásbakkar are interpreted to reflect a variable proximity of the glacier and high sea-level positions (at least 25 m higher than present).

As these units do not contain any whole, *in situ* fossils their absolute age cannot be determined by radiocarbon dating. Shell fragments collected from these units ranged in age between 13.1 and 13.9 cal. ka BP (Tables 1 and 2). These ages overlap with ages from the stratigraphically underlying Unit A, suggesting that shell fragments within these units are reworked from older units. Thus, they do not provide any tighter time constraints for the formation of these units or the timing of the glacier oscillations. However, reconstructions of sea levels changes in Iceland imply that the glaciomarine sediments forming the 25 m thick units during and after the moraine formation could potentially have been formed during the Younger Dryas or Early Holocene when the relative sea levels rose as a result of re-expansion of the IIS after having reached present day levels during the Allerød (Norðdahl & Pétursson 2005; Norðdahl *et al.* 2008). Stratigraphical relationships show that the Melabakkar-Ásbakkar moraines most likely predate the glaciomarine sediments in Belgsholt, which are dated to 11.7-11.3 cal. ka BP; thus, implying that the Melabakkar-Ásbakkar moraines were formed before *c*. 11.7 cal. ka BP. Additionally, no shells of Early Holocene age have been radiocarbon dated from the Melabakkar-Ásbakkar coastal cliffs further supporting that the deformed glaciomarine sediments there pre-date the Holocene. By combining all available evidence, from this and previous studies, the most likely time-frame for the formation of the Skorholtsmelar terminal moraine as well as the Melabakkar-Ásbakkar moraine series is between *c*. 13.0 -11.7 cal. ka BP, which roughly corresponds to the Younger Dryas (Fig. 9).

The exact timing of moraine formation and punctuated retreat is unknown for the series of moraines exposed in Melabakkar-Ásbakkar other than they formed sometime between c. 13.0 -11.7 cal. ka BP.. The model in Figure 9 is likely to overestimate the time span for

the formation of the Melabakkar-Ásbakkar moraines as it uses the entire time frame given by the radiocarbon ages. Large, glaciotectonic moraines of similar size as each of the Melabakkar-Ásbakkar moraines are known to form during single large-scale advances/surges (Boulton *et al.* 1999a; Benediktsson *et al.* 2010; Lovell & Boston 2017) given that there is enough material available for the moraine construction. The time between the series of Melasveit readvances is reflected in the inter-advance accumulation of rhythmically bedded/laminated glaciomarine sediments (Units C-E), which are deformed by subsequent readvances. For example, the ~25 m thick Unit C lies stratigraphically between the southernmost moraine Ás and the Ásgil moraine (c. 2500-3500 m on Fig. 4). Sediment rates in ice-proximal marine setting can be very high; for example, annually laminated fine diamicton, silt and sand in Glacier Bay in Alaska was recorded as 48 cm/ year (Cowan *et al.* 1997) and 74 cm/ year in an ice-proximal position at Muir Glacier in Alaska (Cowan *et al.* 1999). This implies that only a few decades would be sufficient amount of time to allow the deposition of Unit C and the construction of these two moraines. High rates of glaciomarine sedimentation during or in between the advances, may be supported by the lack of living fauna, the absence of bioturbation as well as widespread load structures (Ó Cofaigh & Dowdeswell 2001; Sigfúsdóttir *et al.* 2018). Given the thickness of syntectonic sediments and the maximum time span indicated by the radiocarbon dates, a few hundred years, would be a realistic time frame for the formation of the entire Melabakkar-Ásbakkar moraine series.

Borgarfjörður glacier dynamics

These advances of the Borgarfjörður glacier were likely coeval with other post-LGM glacier advances in Iceland, which generally commenced around the Allerød-Younger Dryas transition and have been associated with increased mass balance of the IIS around that time (around 12.9 cal. ka BP) (Geirsdóttir & Eiríksson 1994; Norðdahl & Pétursson 2005; Geirsdóttir et al. 2009). This growth of glaciers has been linked with a weakening of the Irminger Current and increased influence of cold Arctic waters in coastal and offshore areas of Iceland as well as a rapid cooling of air temperature (Rundgren 1995; Jennings et al. 2000; Norðdahl & Pétursson 2005; Norðdahl et al. 2008; Geirsdóttir et al. 2009; Ingólfsson et al. 2010).

Although the large-scale readvance of the Borgarfjörður glacier was most likely driven by deteriorating climate in the YD, it is, however, still unclear whether the moraine series inside this limit represents shorter-term climate fluctuations within the YD or some glaciodynamic response. Climate records from lake- and marine cores spanning the YD have indicated rapid fluctuations in atmospheric and sea surface temperatures (Bakke et al. 2009). However, it is well-known that once a retreat of marine-terminating glaciers is initiated, i.e. due to long-term (multi-century) climate/ocean warming, following advances and retreats are often out of phase with climate forcing (Pfeffer 2007; Post et al. 2011; McNabb & Hock 2014). Although some marine-terminating glaciers respond to short-term climate fluctuations (Joughin et al. 2008; Carr et al. 2013), others show regionally asynchronous behaviour with climate, especially on decadal to annual time scales (Post et al. 2011; Moon et al. 2012).

The lower Borgarfjörður region does not exhibit a complete sediment-landform assemblage diagnostic of surge-type glacier behaviour (Ottesen et al. 2008; Flink et al. 2015). However, large moraines exhibiting heavily tectonised sediments associated with elevated water pressures and meltwater runoff, like those seen in the moraine series in Melasveit, are usually associated with glacier surges due to rapid application of glacial stress (Huddart & Hambrey 1996; Boulton et al. 1999; Evans & Rea 1999; Bennett et al. 2004; Benediktsson et al. 2008; 2010; 2015; Ingólfsson et al. 2016; Lovell & Boston 2017; Sigfúsdóttir et al. 2019). A comparable retreat pattern as seen in the Melabakkar-Ásbakkar cliffs is common in front of terrestrial surge-type glaciers in Iceland that had their greatest surges during the Little Ice Age maximum but have since then had successively smaller surges due to an overall warming climate (Bennett et al. 2004; Benediktsson et al. 2008; 2009; 2010, 2015; Striberger et al. 2011). Such patterns are also common in front of modern retreating, surge-type, marine-terminating glaciers, e.g. on Svalbard (Ottesen & Dowdeswell 2006; Ottesen et al. 2008; Flink et al. 2015; Larsen et al. 2018). Therefore, we surmise that the oscillations recorded in the Melabakkar-Ásbakkar cliffs in Melasveit represent successively smaller advances/surges of the Borgarfjörður glacier due to gradually decreasing mass balance during the Younger Dryas.

Early Holocene: Open marine conditions and a readvance of the Borgarfjörður glacier

Around 11.7 cal. ka BP, open marine conditions dominated the lower Borgarfjörður region as indicated by marine molluscs in ice-distal glaciomarine sediments (Unit E) in Belgsholt and Skipanes, and a Balanus balanus shell at 69 m a.s.l. at Fossamelar (Figs 2, 9). The presence of the shells as well as their radiocarbon ages between 11.3-11.7 cal. ka BP, firmly imply ice-free conditions in the Early Holocene. The age of the deformed, shell-bearing, glaciomarine sediments within the ice-marginal moraine at Belgsholt (Fig. 2) indicates a glacier readvance into the Melasveit area after c. 11.3 cal. ka BP (Fig. 9). The location of Belgsholt only about 5 km inside the Younger Dryas limit (defined by the Skorholtsmelar/Ás moraine) shows that the Borgarfjörður glacier was nearly as ex-

tensive during the Early Holocene as it was during the Younger Dryas. Since no shells were found in the glaciomarine sediments capping the moraine it is difficult to constrain its minimum age. However, the thickness of these sediments suggests that sea level was at least 12 m higher than present during or after the formation of the moraine. Given that relative sea-level dropped below the present sea level around 10.7 cal. ka BP (Norðdahl et al. 2008; Pétursson et al. 2015), this suggest that the Belgsholt moraine was formed in the Early Holocene between around 11.3 and 10.7 cal. ka BP. These results indicate a more extensive glacial advance in the lower Borgarfjörður region during the Early Holocene than previously thought. Based on the altitude of the dated Balanus shells coupled with the altitude of the overlying delta at Fossamelar, Skorradalur (Fig. 2), the relative sea level must have been over 70 m in this area after c. 11.7 cal. ka BP. The ages of these shells could indicate that the advance to Belgsholt occurred after the glacier retreated to Fossamelar (over 20 km from Belgsholt). This would require the preservation of the Balanus shells throughout the advance to Belgsholt. However, because of the statistical overlap in calibrated age ranges of shells sampled from these two places (Table 2), it cannot be excluded that the glacier advanced to Belgsholt but then retreated rapidly to a position inside Fossamelar to allow the habitation of the Balanus balanus shells there.

The altitude of the delta at Fossamelar and the age of the underlying shells suggest that the 70-80 m shorelines in the inner parts of Borgarfjörður are not of Younger Dryas age, as previously proposed (Ingólfsson 1988; Norðdahl et al. 2008) but rather of Early Holocene age formed during a stepwise retreat from the Belgsholt moraine (the youngest one in the moraine series), which therefore explains their good preservation. The problem, however, still remains why the 120-150 m high Bølling aged shorelines in the tributary valley of Skorradalur are preserved despite subsequent YD glacier advances down the main valley of Borgarfjörður. The simplest explanation is that the outer parts of Skorradalur were ice-free while the Borgarfjörður glacier advanced through its main valley (Fig. 9).

Although evidence for Early Holocene glacier advances in the coastal regions of western Iceland has hitherto been scarce (Norðdahl et al. 2008; Ingólfsson et al. 2010), studies from other parts of Iceland have reported glacier readvances or halts in retreat around this time (Geirsdóttir et al. 2009; Ingólfsson et al. 2010; Pétursson et al. 2015). One of the most prominent examples is the Búði moraine system that can be traced over 25 km across most of the south Icelandic lowland (Geirsdóttir et al. 1997, 2000). The Búði moraine system includes two sets of end moraines; the outer part correlated to the Younger Dryas and the inner part radiocarbon dated to 11.2 cal. ka BP (Geirsdóttir et al. 1997, 2000, 2009; Norðdahl & Pétursson 2005). In eastern Iceland, glaciers readvanced around 11.2 cal. ka BP, commonly reaching the inner parts of fjords (Norðdahl & Einarsson 2001; Norðdahl & Pétursson 2005; Norðdahl et al. 2019), and glaciers in the northern part of Iceland are also known to have advanced in the Early Holocene although they were considerably smaller than during the Younger Dryas (Andrés et al. 2019). Because of this widespread evidence of Early Holocene glacier readvances, it is possible that glaciers in western Iceland followed the same pattern.

These Early Holocene readvances across Iceland have been described as short-lived (Ingólfsson et al. 2010) and have been correlated with the Preboreal oscillation (Björck et al. 1997; Geirsdóttir et al. 2000). The Preboreal oscillation was a brief period of cooling climate recorded around 11.2- 11.5 ka BP in Greenland ice cores (Rasmussen et al. 2007) and has been linked with deteriorating climate and glacier advances/still-stands in northern Europe (Björck et al. 1997; Bakke et al. 2005; Mangerud et al. 2019). However, due to uncertainty in the age of the Early Holocene advance of the Borgarfjörður glacier, this correlation to other climate and glacier records remains tentative. Alternatively, the advance may have been driven by glaciodynamic response, possibly caused by an internal instability following the YD retreat. That would be in agreement with glacier records in Svalbard, which show widespread readvances during the Early Holocene (Lønne 2005; Farnsworth et al. 2018; Larsen et al. 2018) that appear to be asynchronous and most likely result from dynamic instability during the deglaciation (Farnsworth et al. 2018).

Other regional Younger Dryas- Early Holocene glacier advances?

It has previously been hypothesized that outlet/valley glaciers from Svínadalur or Hvalfjörður (Fig. 1) may have expanded from the east into the Leirársveit area, south and east of the Skorholtsmelar moraine, at some point during the Late Weichselian (Ingólfsson 1988; Hart 1994; Hart & Roberts 1994). This is possibly supported by our structural measurements in the Skipanes ridge that indicate ice-flow direction from the east. This also suggests that Late Weichselian - Early Holocene glacier advances were not only confined to Borgarfjörður but may also have occurred in other valleys and fjords in this region. However, it should be noted that the section was poorly exposed and the number of structural measurements is thus limited. Also, earlier investigations had considered Skipanes as potentially a proglacial ridge associated with the glaciotectonics in Melabakkar-Ásbakkar (Ingólfsson 1988). Whether the Skipanes ridge was formed by glacier advances from Svínadalur or Hvalfjörður in the east, or from Borgarfjörður in the north, the radiocarbon dates suggest that it formed between c. 13.7 and 11.5 cal. ka BP.

Conclusions

This study provides a revised reconstruction of glacier advances and retreats in the lower-Borgarfjörður region, western Iceland, based on 22 new radiocarbon ages of marine molluscs, recent detailed stratigraphic and glaciotectonic investigations, as well as a re-evaluation of pre-existing data. The main conclusions are as follows:

- The stratigraphy and glaciotectonic architecture of coastal cliffs in Melasveit, alongside new and pre-existing radiocarbon dates, suggest ice-free, open marine conditions in the Lower-Borgarfjörður region between c. 14.9-13.0 cal. ka BP, corresponding to the Bølling–Allerød interstadial.
- New radiocarbon dates suggest that a large marine-terminating outlet glacier in Borgarfjörður advanced after *c*. 13.0 cal. ka BP and formed the Skorholtsmelar-Ás terminal moraine. This advance was coeval with a widespread climate cooling and glacier advances in Iceland and the North Atlantic region during the Early Younger Dryas.
- Between c. 13.0 and 11.7 cal. ka BP, the Borgarfjörður glacier oscillated resulting in the formation of a series of glaciotectonic end moraines, which are exposed in the Melabakkar-Ásbakkar coastal cliffs. These oscillations may signify a dynamic instability within the glacier, such as surges or speed-ups, that resulted in recurrent readvances of the ice-margin during an overall retreat.
- The coastal areas of Melasveit, lower-Borgarfjörður once again became ice free during the Early Holocene (between *c*. 11.7-11.3 cal. ka BP), as indicated by radiocarbon ages of marine molluscs of that age sampled within glaciomarine sediments at a number of locations in the area.
- After 11.3 cal. ka BP, the Borgarfjörður glacier readvanced to Belgsholt at least 5 km within the Younger Dryas ice-limit. This is the first recorded major Early Holocene advance in western Iceland but coincides with findings from several other parts of Iceland that indicate general readvances in the Preboreal around c. 11.2 cal. ka BP.
- Radiocarbon dated mollusc shells at Skipanes yield ages between c. 13.7 – 11.5 cal. ka BP as a possible time frame for the formation of the glaciotectonics induced from the east. This suggests glacier advance also from Svínadalur and/or Hvalfjörður into the Melasveit area either during Younger Dryas or Early Holocene. This implies that glacier advances in this region of western Iceland were not restricted to the Borgarfjörður glacier.
- Our results imply that the timing of glacier advances in the Borgarfjörður region coincides with the timing of Younger Dryas and Early Holocene glacier advances in other parts of Iceland and the North Atlantic Region.

Acknowledgements

This project was funded by the Icelandic Research Fund (grant no. 141002-051 to Í. Ö. Benediktsson) and the Royal Physiographic Society in Lund (grants to T. Sigfúsdóttir and Í. Ö. Benediktsson). Ólafur Ingólfsson, Hreggviður Norðdahl and Jón Eiríksson are thanked for valuable discussions about the deglaciation history of Iceland and Ágúst Guðmundsson is thanked for providing us with photographs of the area. We would also like to thank Heimir Ingimarsson, Sandrine Roy and Kim Teilmann for their assistance in the field. Thanks are due to Iestyn Barr and an anonymous reviewer for constructive reviews that improved this paper.

References

Allmendinger, R. W., Cardozo, N. C. & Fischer, D. M. 2012: Structural Geology Algorithms: Vectors and Tensors. 302 pp. Cambridge University Press, Cambridge.

Andrés, N., Palacios, D., Sæmundsson, Þ., Brynjólfsson, S. & Fernández-Fernández, J. M. 2019: The rapid deglaciation of the Skagafjörður fjord, northern Iceland. Boreas 48, 92-106.

Andrews, J. T., Hardardóttir, J., Helgadóttir, G., E. Jennings, A., Geirsdóttir, Á., Sveinbjörnsdóttir, Á. E., Schoolfield, S., Kristjánsdóttir, G. B., Micaela Smith, L., Thors, K. & Syvitski, J. P. M. 2000: The N and W Iceland Shelf: insights into Last Glacial Maximum ice extent and deglaciation based on acoustic stratigraphy and basal radiocarbon AMS dates. Quaternary Science Reviews 19, 619-631.

Ashwell, I. Y. 1967: Radiocarbon ages of shells in the glaciomarine deposits in western Iceland. The Geographical Journal 133, 48-50.

Ashwell, I. Y. 1975: Glacial and Late Glacial processes in western Iceland. Geografiska Annaler: Series A, Physical Geography 57, 225-245.

Bakke, J., Dahl, S. O. & Nesje, A. 2005: Lateglacial and early Holocene palaeoclimatic reconstruc-

tion based on glacier fluctuations and equilibrium-line altitudes at northern Folgefonna, Hardanger, western Norway. Journal of Quaternary Science 20, 179-198.

Bakke, J., Lie, Ø., Heegaard, E., Dokken, T., Haug, G. H., Birks, H. H., Dulski, P. & Nilsen, T. 2009: Rapid oceanic and atmospheric changes during the Younger Dryas cold period. Nature Geoscience 2, 202-205.

Bárðarson, G. G. 1923: Fornar sjávarminjar við Borgarfjörð og Hvalfjörð. 116 p. Vísindafélag Íslands, Reykjavík.

Bárðarson, G. G. 1927: Ágrip af jarðfræði. 192 pp. Bókaverslun Sigfúsar Eymundssonar, Reykjavík.

Benediktsson, Í. Ö., Ingólfsson, Ó., Schomacker, A. & Kjær, K. H. 2009: Formation of submarginal and proglacial end moraines: implications of ice-flow mechanism during the 1963–64 surge of Brúarjökull, Iceland. Boreas 38, 440-457.

Benediktsson, Í. Ö., Möller, P., Ingólfsson, Ó., van der Meer, J. J. M., Kjær, K. H. & Krüger, J. 2008: Instantaneous end moraine and sediment wedge formation during the 1890 glacier surge of Brúarjökull, Iceland. Quaternary Science Reviews 27, 209-234.

Benediktsson, Í. Ö., Schomacker, A., Johnson, M. D., Geiger, A. J., Ingólfsson, Ó. & Guðmundsdóttir, E. R. 2015: Architecture and structural evolution of an early Little Ice Age terminal moraine at the surge-type glacier Múlajökull, Iceland. Journal of Geophysical Research: Earth Surface 120, 1895-1910.

Benediktsson, Í. Ö., Schomacker, A., Lokrantz, H. & Ingólfsson, Ó. 2010: The 1890 surge end moraine at Eyjabakkajökull, Iceland: a re-assessment of a classic glaciotectonic locality. Quaternary Science Reviews 29, 484-506.

Bennett, M. R., Huddart, D., Waller, R. I., Cassidy, N., Tomio, A., Zukowskyj, P., Midgley, N. G., Cook, S. J., Gonzalez, S. & Glasser, N. F. 2004: Sedimentary and tectonic architecture of a large push moraine: a case study from Hagafellsjökull-Eystri, Iceland. Sedimentary Geology 172, 269-292.

Björck, S., Rundgren, M., Ingólfsson, Ó. & Funder, S. 1997: The Preboreal oscillation around the Nordic Seas: terrestrial and lacustrine responses. Journal of Quaternary Science 12, 455-465.

Boulton, G. S., Van der Meer, J. J. M., Beets, D. J., Hart, J. K. & Ruegg, G. H. J. 1999: The sedimentary and structural evolution of a recent push moraine complex, Holmstrombreen, Spitsbergen. Quaternary Science Reviews 18, 339-371.

Brynjólfsson, S., Schomacker, A., Ingólfsson, Ó. & Keiding, J. K. 2015: Cosmogenic 36Cl exposure ages reveal a 9.3 ka BP glacier advance and the Late Weichselian-Early Holocene glacial history of the Drangajökull region, northwest Iceland. Quaternary Science Reviews 126, 140-157.

Cardozo, N. & Allmendinger, R. W. 2013: Spherical projections with OSXStereonet. Computers & Geosciences 51, 193-205.

Carr, J. R., Stokes, C. R. & Vieli, A. 2013: Recent progress in understanding marine-terminating Arctic outlet glacier response to climatic and oceanic forcing: Twenty years of rapid change. Progress in Physical Geography: Earth and Environment 37, 436-467.

Cowan, E. A., Cai, J., Powell, R. D., Clark, J. D. & Pitcher, J. N. 1997: Temperate glacimarine varves; an example from Disenchantment Bay, Southern Alaska. Journal of Sedimentary Research 67, 536-549.

Cowan, E. A., Seramur, K. C., Cai, J. & Powell, R. D. 1999: Cyclic sedimentation produced by fluctuations in meltwater discharge, tides and marine productivity in an Alaskan fjord. Sedimentology 46, 1109-1126.

Eiríksson, J., Knudsen, K. L., Haflidason, H. & Henriksen, P. 2000: Late-glacial and Holocene palaeoceanography of the North Icelandic shelf. Journal of Quaternary Science 15, 23-42.

Eiríksson, J., Larsen, G., Knudsen, K. L., Heinemeier, J. & Símonarson, L. A. 2004: Marine reservoir age variability and water mass distribution in the Iceland Sea. Quaternary Science Reviews 23, 2247-2268.

Evans, D. J. A. & Benn, D. I. 2004: A Practical Guide to the Study of Glacial Sediments. 266 pp. Arnold, London.

Evans, D. J. A. & Rea, B. R. 1999: Geomorphology and sedimentology of surging glaciers: a land-system approach. Annals of Glaciology 28, 75-82.

Farnsworth, W. R., Ingólfsson, Ó., Retelle, M., Allaart, L., Håkansson, L. M. & Schomacker, A. 2018: Svalbard glaciers re-advanced during the Pleistocene–Holocene transition. Boreas 47, 1022-1032.

Flink, A. E., Noormets, R., Kirchner, N., Benn, D. I., Luckman, A. & Lovell, H. 2015: The evolution of a submarine landform record following recent and multiple surges of Tunabreen glacier, Svalbard. Quaternary Science Reviews 108, 37-50.

Franzson, H. 1978: Structure and Petrochemistry of the Hafnarfjall-Skarðsheiði Central Volcano and the Surrounding Basalt Succession, W-Iceland. 264 pp. The University of Edinburgh, Edinburgh.

Geirsdóttir, Á. & Eiríksson, J. 1994: Sedimentary facies and environmental history of the Late-glacial glaciomarine Fossvogur sediments in Reykjavík, Iceland. Boreas 23, 164-176.

Geirsdóttir, Á., Hardardóttir, J. & Eiríksson, J. 1997: The Depositional History of the Younger Dryas-Preboreal Búdi Moraines in South-Central Iceland. Arctic and Alpine Research 29, 13-23.

Geirsdóttir, Á., Hardardóttir, J. & Sveinbjörnsdóttir, Á. E. 2000: Glacial extent and catastrophic meltwater events during the deglaciation of Southern Iceland. Quaternary Science Reviews 19, 1749-1761.

Geirsdóttir, Á., Miller, G. H., Axford, Y. & Sædís, Ó. 2009: Holocene and latest Pleistocene climate and glacier fluctuations in Iceland. Quaternary Science Reviews 28, 2107-2118.

Håkansson, S. 1983: A reservoir age for the coastal waters of Iceland. Geologiska Föreningens i Stockholm Förhandlingar 105, 65-68.

Harning, D. J., Geirsdóttir, Á. & Miller, G. H. 2018: Punctuated Holocene climate of Vestfirðir, Iceland, linked to internal/external variables and oceanographic conditions. Quaternary Science Reviews 189, 31-42.

Hart, J. K. 1994: Proglacial glaciotectonic deformation at Melabakkar-Ásbakkar, west Iceland. Boreas 23, 112-121.

Hart, J. K. & Roberts, D. H. 1994: Criteria to distinguish between subglacial glaciotectonic and glaciomarine sedimentation, I. Deformation styles and sedimentology. Sedimentary Geology 91, 191-213.

Hubbard, A., Sugden, D., Dugmore, A., Norddahl, H. & Pétursson, H. G. 2006: A modelling insight into the Icelandic Last Glacial Maximum ice sheet. Quaternary Science Reviews 25, 2283-2296.

Huddart, D. & Hambrey, M. J. 1996: Sedimentary and tectonic development of a high-arctic, thrust-moraine complex: Comfortlessbreen, Svalbard. Boreas 25, 227-243.

Hughes, A. L. C., Gyllencreutz, R., Lohne, Ø. S., Mangerud, J. & Svendsen, J. I. 2016: The last Eurasian ice sheets – a chronological database and time-slice reconstruction, DATED-1. Boreas 45, 1-45.

Ingólfsson, Ó. 1984: A review of Late Weichselian Studies in the lower Part of the Borgarfjörður region, western Iceland. Jökull 34, 117-130.

Ingólfsson, Ó. 1987: The Late Weichselian glacial geology of the Melabakkar-Asbakkar coastal cliffs, Borgarfjörður, W-Iceland. Jökull 37, 57-81.

Ingólfsson, Ó. 1988: Glacial history of the lower Borgarfjördur area, western Iceland. Geologiska Föreningens i Stockholm Förhandlingar 110, 293-309.

Ingólfsson, Ó., Benediktsson, Í. Ö., Schomacker, A., Kjær, K. H., Brynjólfsson, S., Jónsson, S. A., Korsgaard, N. J. & Johnson, M. D. 2016: Glacial geological studies of surge-type glaciers in Iceland — Research status and future challenges. Earth-Science Reviews 152, 37-69.

Ingólfsson, Ó. & Norðdahl, H. 2001: High Relative Sea Level during the Bolling Interstadial in Western Iceland: A Reflection of Ice-sheet Collapse and Extremely Rapid Glacial Unloading. Arctic, Antarctic, and Alpine Research 33, 231-243.

Ingólfsson, Ó., Norðdahl, H. & Schomacker, A. 2010: 4 Deglaciation and Holocene Glacial History of Iceland. In Schomacker, A., Krüger, J. & Kjær, K. H. (eds.): Developments in Quaternary Sciences, 51-68 pp. Elsevier, Amsterdam.

Jennings, A., Syvitski, J., Gerson, L., Grönvold, K., Geirsdóttir, Á., Hardardóttir, J., Andrews, J. & Hagen, S. 2000: Chronology and paleoenvi-

ronments during the late Weichselian deglaciation of the southwest Iceland shelf. Boreas 29, 163-183.

Joughin, I., Howat, I. M., Fahnestock, M., Smith, B., Krabill, W., Alley, R. B., Stern, H. & Truffer, M. 2008: Continued evolution of Jakobshavn Isbrae following its rapid speedup. Journal of Geophysical Research: Earth Surface 113. DOI:10.1029/2008JF001023

Kirkbride, M. P. & Dugmore, A. J. 2006: Responses of mountain ice caps in central Iceland to Holocene climate change. Quaternary Science Reviews 25, 1692-1707.

Larsen, E., Lyså, A., Rubensdotter, L., Farnsworth, W. R., Jensen, M., Nadeau, M. J. & Ottesen, D. 2018: Lateglacial and Holocene glacier activity in the Van Mijenfjorden area, western Svalbard. arktos 4. DOI: 10.1007/s41063-018-0042-2

Larsen, G., Eiríksson, J., Knudsen, K. L. & Heinemeier, J. 2002: Correlation of late Holocene terrestrial and marine tephra markers, north Iceland: implications for reservoir age changes. Polar Research 21, 283-290.

Lloyd, J. M., Norðdahl, H., Bentley, M. J., Newton, A. J., Tucker, O. & Zong, Y. 2009: Lateglacial to Holocene relative sea-level changes in the Bjarkarlundur area near Reykhólar, North West Iceland. Journal of Quaternary Science 24, 816-831.

Lønne, I. 2005: Faint traces of high Arctic glaciations: an early Holocene ice-front fluctuation in Bolterdalen, Svalbard. Boreas 34, 308-323.

Lovell, H. & Boston, C. M. 2017: Glacitectonic composite ridge systems and surge-type glaciers: an updated correlation based on Svalbard, Norway. arktos 3. .DOI: 10.1007/s41063-017-0028-5.

Magnúsdóttir, B. & Norðdahl, H. 2000: Aldur hvalbeins og efstu fjörumarka í Akrafjalli (English summary: Re-examination of the deglaciation history of the area around Akrafjall in South-western Iceland). Náttúrufræðingurinn 69, 177-188.

Malmberg, S.-A. 1985: The water masses between Iceland and Greenland. Journal of the Marine Research Institute 9, 127-140.

Mangerud, J., Hughes, A. L. C., Sæle, T. H. & Svendsen, J. I. 2019: Ice-flow patterns and precise timing of ice sheet retreat across a dissected fjord landscape in western Norway. Quaternary Science Reviews 214, 139-163.

Margold, M., Stokes, C. R. & Clark, C. D. 2018: Reconciling records of ice streaming and ice margin retreat to produce a palaeogeographic reconstruction of the deglaciation of the Laurentide Ice Sheet. Quaternary Science Reviews 189, 1-30.

McNabb, R. W. & Hock, R. 2014: Alaska tidewater glacier terminus positions, 1948–2012. Journal of Geophysical Research: Earth Surface 119, 153-167.

Moffa-Sánchez, P., Moreno-Chamarro, E., Reynolds, D. J., Ortega, P., Cunningham, L., Swingedouw, D., Amrhein, D. E., Halfar, J., Jonkers, L., Jungclaus, J. H., Perner, K., Wanamaker, A. & Yeager, S. 2019: Variability in the northern North Atlantic and Arctic oceans across the last two millennia: A review. Paleoceanography and Paleoclimatology 34, pp. 1399-1436.

Moon, T., Joughin, I., Smith, B., Howat, I. 2012: 21st-Century Evolution of Greenland Outlet Glaciers. Science 336, 576-578.æ

Norðdahl, H. & Einarsson, T. 2001: Concurrent changes of relative sea-level and glacier extent at the Weichselian–Holocene boundary in Berufjordur, Eastern Iceland. Quaternary Science Reviews 20, 1607-1622.

Norðdahl, H. & Ingólfsson, Ó. 2015: Collapse of the Icelandic ice sheet controlled by sea-level rise? arktos 1, DOI: 10.1007/s41063-015-0020-x .

Norðdahl, H., Ingólfsson, Ó., Pétursson, H., G. & Hallsdóttir, M. 2008: Late Weichselian and Holocene environmental history of Iceland. Jökull 58, 343-364.

Norðdahl, H., Ingólfsson, Ó. & Pétursson, H. G. 2012: Ísaldarlok á Íslandi. Tímarit hins íslenska náttúrufræðifélags 82, 73-86.

Norðdahl, H., Ingólfsson, Ó., Vogler, E. D., Steingrímsson, B. Ó. & Hjartarson, Á. 2019: Glacio-isostatic age modelling and Late Weichselian deglaciation of the Lögurinn basin, East Iceland. Boreas 48, 563-580.

Norðdahl, H. & Pétursson, H., G. 2005: Relative sea-level changes in Iceland: new aspects of the

Weichselian deglaciation of Iceland. In Caseldine, C., Russell, J., Hardardóttir, J. & Knudsen, O. (eds.): Iceland-Modern Processes and Past Environments, 25-78 pp. Elsevier, Amsterdam.

Ó Cofaigh, C. & Dowdeswell, J. A. 2001: Laminated sediments in glacimarine environments: diagnostic criteria for their interpretation. Quaternary Science Reviews 20, 1411-1436.

Ólafsdóttir, S., Jennings, A. E., Geirsdóttir, Á., Andrews, J. & Miller, G. H. 2010: Holocene variability of the North Atlantic Irminger current on the south- and northwest shelf of Iceland. Marine Micropaleontology 77, 101-118.

Ottesen, D. & Dowdeswell, J. A. 2006: Assemblages of submarine landforms produced by tidewater glaciers in Svalbard. Journal of Geophysical Research: Earth Surface 111. DOI: 10.1029/2005JF000330.

Ottesen, D., Dowdeswell, J. A., Benn, D. I., Kristensen, L., Christiansen, H. H., Christensen, O., Hansen, L., Lebesbye, E., Forwick, M. & Vorren, T. O. 2008: Submarine landforms characteristic of glacier surges in two Spitsbergen fjords. Quaternary Science Reviews 27, 1583-1599.

Patton, H., Hubbard, A., Bradwell, T. & Schomacker, A. 2017: The configuration, sensitivity and rapid retreat of the Late Weichselian Icelandic ice sheet. Earth-Science Reviews 166, 223-245.

Pétursson, H. G., Norddahl, H. & Ingólfsson, Ó. 2015: Late Weichselian history of relative sea level changes in Iceland during a collapse and subsequent retreat of marine based ice sheet. Cuadernos de Investigación Geográfica 41, 261-277.

Pfeffer, W. T. 2007: A simple mechanism for irreversible tidewater glacier retreat. Journal of Geophysical Research: Earth Surface 112. DOI: 10.1029/2006jf000590.

Phillips, E. R. & Lee, J. R. 2011: Description, measurement and analysis of glacitectonically deformed sequences. In Phillips, E. R., Lee, J. R. & Evans, H. M. (eds.): Glacitectonics: field guide. 5-31. Quaternary Research Association.

Post, A., O'Neel, S., Motyka, R. J. & Streveler, G. 2011: A complex relationship between calving glaciers and climate. Eos, Transactions American Geophysical Union 92, 305-306.

Rasmussen, S. O., Vinther, B. M., Clausen, H. B. & Andersen, K. K. 2007: Early Holocene climate oscillations recorded in three Greenland ice cores. Quaternary Science Reviews 26, 1907-1914.

Reimer, P. J., Bard, E., Bayliss, A., Beck, J. W., Blackwell, P. G., Ramsey, C. B., Buck, C. E., Cheng, H., Edwards, R. L., Friedrich, M., Grootes, P. M., Guilderson, T. P., Haflidason, H., Hajdas, I., Hatté, C., Heaton, T. J., Hoffmann, D. L., Hogg, A. G., Hughen, K. A., Kaiser, K. F., Kromer, B., Manning, S. W., Niu, M., Reimer, R. W., Richards, D. A., Scott, E. M., Southon, J. R., Staff, R. A., Turney, C. S. M. & van der Plicht, J. 2013: IntCal13 and Marine13 Radiocarbon Age Calibration Curves 0–50,000 Years cal BP. Radiocarbon 55, 1869-1887.

Rundgren, M. 1995: Biostratigraphic Evidence of the Allerød-Younger Dryas-Preboreal Oscillation in Northern Iceland. Quaternary Research 44, 405-416.

Sæmundsson, K. 1991: Jarðfræði Kröflukerfisins. In Garðarsson, A. & Einarsson, Á. (eds.): Náttúra Mývatns, 24-95.Hið íslenska náttúrufræðifélag, Reykjavík.

Sigfúsdóttir, T., Benediktsson, Í. Ö. & Phillips, E. 2018: Active retreat of a Late Weichselian marine-terminating glacier: an example from Melasveit, western Iceland. Boreas 47, 813-836.

Sigfúsdóttir, T., Phillips, E. & Benediktsson, Í. Ö. 2019: Micromorphological evidence for the role of pressurised water in the formation of large-scale thrust-block moraines in Melasveit, western Iceland. Quaternary Research. DOI:10.1017/qua.2019.48

Striberger, J., Björck, S., Benediktsson, Í. Ö., Snowball, I., Uvo, C. B., Ingólfsson, Ó. & Kjær, K. H. 2011: Climatic control of the surge periodicity of an Icelandic outlet glacier. Journal of Quaternary Science 26, 561-565.

Stuiver, M., Reimer, P. J. & Reimer, R. W. 2019: CALIB. 7.1 ed. [WWW program] at http://calib.org, accessed 2019-10-23.

Syvitski, J. P., Jennings, A. E. & Andrews, J. T. 1999: High-resolution Seismic Evidence for Multiple Glaciation across the Southwest Iceland Shelf. Arctic, Antarctic, and Alpine Research 31, 50-57.

.

Syvitski, J. P., Jennings, A. E. & Andrews, J. T. 1999: High-resolution Seismic Evidence for Multiple Glaciation across the Southwest Iceland Shelf. Arctic, Antarctic, and Alpine Research 31, 50-57.

.